Aus der Klinik und Poliklinik für Neurologie,
Universitätsmedizin Rostock
Direktor: Prof. Dr. Alexander Storch

Einfluss von Sauerstoff und Katecholaminen auf die fetale kortikale Entwicklung der Maus

Kumulative Dissertation

zur

Erlangung des akademischen Grades

Doktor der Medizinwissenschaften (Dr. rer. hum.)

der Universitätsmedizin Rostock

vorgelegt von

M. Sc. Franz Markert

geboren am 22.02.1989 in Großenhain

Rostock, 2022

https://doi.org/10.18453/rosdok_id00004342

Dekan: Prof. Dr. med. Emil C. Reisinger

Eingereicht am: 30.06.2022

Datum der öffentlichen Verteidigung: 25.04.2023

1. Gutachter:

Prof. Dr. med. Alexander Storch, Klinik und Poliklinik für Neurologie der Universitätsmedizin Rostock

2. Gutachterin:

PD Dr. rer. nat. et med. habil. Kirsten Peters, Biomedizinisches Forschungszentrum der Universitätsmedizin Rostock

3. Gutachter:

Prof. Dr. med. Björn Spittau, AG3 Anatomie und Zellbiologie der Universität Bielefeld

Inhaltsverzeichnis

1 Einleitung

1.1 Die embryonale kortikale Gehirnentwicklung der Maus

Die murine kortikale Entwicklung beginnt – wie auch beim Menschen – mit der Entstehung des Gehirns aus dem Ektoderm, welches neben Endoderm und Mesoderm eines der drei Keimblätter darstellt. Aus dem Ektoderm entwickelt sich bei Mäusen am Embryonalstadium (E) 7 die Neuralplatte, welche sich daraufhin beginnt einzustülpen und an E10,5 das Neuralrohr bildet (Stuhlmiller and García-Castro 2012, Chen et al. 2017). Am rostralen Ende des Neuralrohres beginnt an E10,5 die Ausbildung von vesikulären Strukturen, von denen die am weitesten rostral gelegene das Telencephalon darstellt (Chen et al. 2017). Dieses besteht bereits aus zwei separaten Bereichen, welche sich später zu den beiden kortikalen Hemisphären entwickeln.

Zur Entwicklung dieser Strukturen wird eine gewaltige Anzahl an Zellen benötigt. Ein Großteil dieser Zellen wird direkt an den Rändern der Ventrikeln produziert, der sogenannten ventrikulären Zone (VZ). Die dort angesiedelten neuralen Stammzellen, auch radiale Gliazellen (rGZ) genannt, teilen sich in der Expansionsphase zwischen E10 und E12 überwiegend symmetrisch, d.h. aus jeder Zellteilung gehen zwei Stammzellen hervor (siehe Abbildung 1; Caviness, Takahashi and Nowakowski 1995, Di Bella et al. 2021). Dieses Schema ändert sich zu E12/E13 und die Stammzellen beginnen nun mit asymmetrischen Teilungen, d.h. es entstehen eine Stammzelle und eine intermediäre Vorläuferzelle (iVZ) oder direkt ein Neuron (Miyata et al. 2004, Englund et al. 2005, Arnold et al. 2008). Während die radiale Gliazelle in der VZ verbleibt, wandern die neuen iVZs und Neuronen entlang der Ausläufer der radialen Gliazellen nach außen. Die Neurone wandern dabei bis an den äußersten Rand und bilden die ersten Schichten des Kortex, welcher größtenteils aus 6 Schichten aufgebaut ist. Die iVZ hingegen verbleiben oberhalb der VZ und bilden dort die subventrikuläre Zone (SVZ) (Haubensak et al. 2004). In dieser teilen sich die meisten iVZ symmetrisch zu zwei Neuronen, ein Teil jedoch erzeugt durch symmetrische Teilung weitere iVZ (Haubensak et al. 2004, Miyata et al. 2004, Noctor et al. 2004, Wu et al. 2005). Zudem finden sich in der SVZ auch basale radiale Gliazellen (brGZ), welche im Gegensatz zu RGZs nur noch einen basalen Ausläufer besitzen. Diese verhalten sich wie iVZ, können jedoch zusätzlich noch asymmetrische Teilungen vollziehen, sodass die brGZ verbleibt und ein Neuron oder iVZ produziert wird (Fietz et

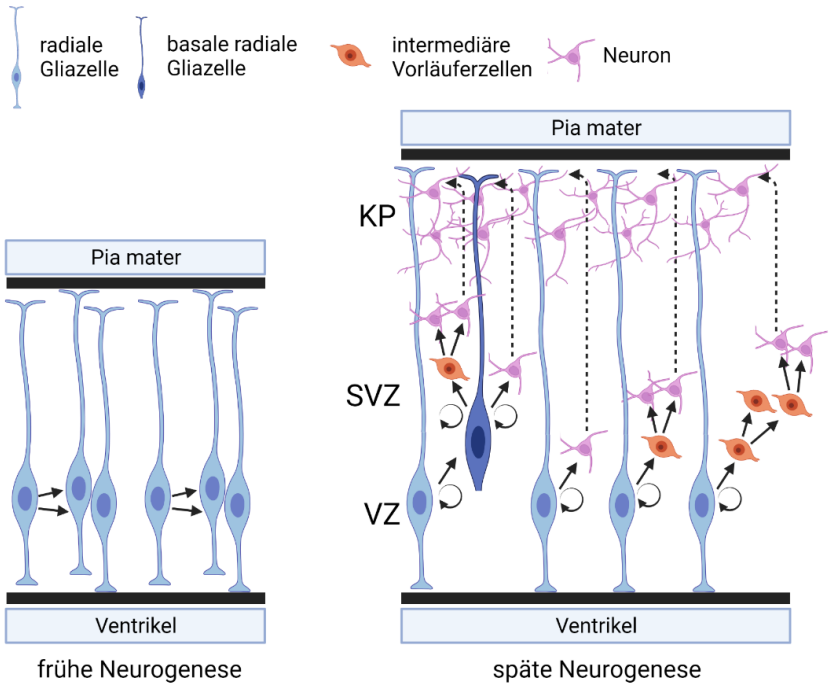

Abbildung 1: Schematische Darstellung der verschiedenen an der Neurogenese beteiligten Zellen und deren Möglichkeiten zur symmetrischen oder asymmetrischen Zellteilung während der frühen und späten Neurogenese. VZ = ventrikuläre Zone; SVZ = subventrikuläre Zone; KP = kortikale Platte. Erstellt mit BioRender.com.

al. 2010, Hansen et al. 2010). Die Art und Weise der Zellteilung innerhalb der SVZ ist dabei von entscheidender Bedeutung für die spätere Größe des jeweiligen Gehirns und stellt einen entscheidenden Unterschied in der Gehirnentwicklung zwischen Mäusen und Menschen dar (Nonaka-Kinoshita et al. 2013, Pilz et al. 2013, Florio et al. 2015).

Die in der SVZ produzierten Neurone wandern wie auch die aus der VZ kommenden entlang der basalen Ausläufer der rGZ und brGZ und siedeln sich jeweils am äußersten Rand des Kortex an. Somit entsteht das für den Kortex typische *inside-out* Schema, indem die äußersten Schichten der kortikalen Platte die chronologisch jüngsten Neurone beinhalten bzw. zuletzt entstehen. So lassen sich bereits ab E11 Neurone der inneren Schichten VI und V finden, welche zwischen E11 und E16 entstehen und zwischen E15/E16 und Postnatalstadium (P) 0 ihr Maximum an Neuronen erreichen (McKenna et al. 2011, Alsiö et al. 2013, Saurat et al. 2013). Neuronen der äußeren Schichten IV bis I dagegen sind erst ab E14/E15 sichtbar und deren Anzahl steigt bis P0 kontinuierlich an (Alsiö et al. 2013, Saurat et al. 2013, Harb et al. 2016, Stepien et al. 2020). Beispielsweise entstehen nahezu alle Neuronen der Schicht II zwischen E17 und P0 (Zgraggen et al. 2012). Neben der Entstehung von Neuronen spielen Mikroglia eine entscheidende Rolle bei der kortikalen Entwicklung (Arnò et al. 2014, Tronnes et al. 2016). Mikroglia entstehen im

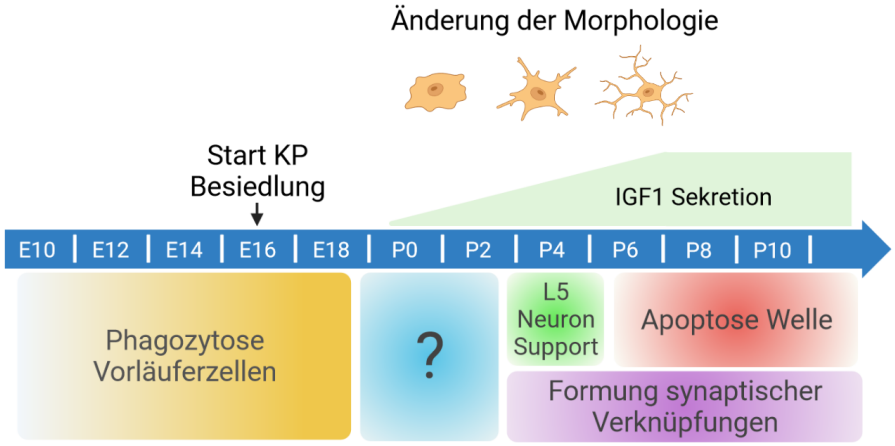

Abbildung 2: Schematische Darstellung des phänotypischen und funktionellen Umschaltens von Mikroglia im perinatalen Mauskortex. KP = kortikale Platte; IGF1 = Insulinartiger Wachstumsfaktor 1 (*Insulin like growth factor 1*). Erstellt mit BioRender.com.

Dottersack des Embryos und gelangen an ca. E11 in den sich entwickelnden Kortex, in welchem sie eine Vielzahl von Funktionen wie Phagozytose von Zellen, Förderung der Neurogenese, Erhalt spezieller Neurone und die Beeinflussung der Synapsenausbildung übernehmen (siehe Abbildung 2; (Hoshiko et al. 2012, Schafer et al. 2012, Swinnen et al. 2013, Schulz et al. 2012, Cunningham, Martínez-Cerdeño and Noctor 2013, Ueno et al. 2013, Shigemoto-Mogami et al. 2014). Chronologisch betrachtet befinden sich nahezu alle Mikroglia zunächst in den proliferierenden Zonen VZ und SVZ, in welchen sie selbst proliferieren und sowohl apoptotische als auch nicht-apoptotische Zellen phagozytieren (Alliot, Godin and Pessac 1999, Antony et al. 2011, Cunningham et al. 2013, Fricker et al. 2012). Ab P3 findet ein phänotypisches Umschalten statt, indem Mikroglia durch Sekretion von Faktoren wie Insulinartiger Wachstumsfaktor 1 (IGF1) zum Überleben von Neuronen beitragen und noch später die neuronalen Netzwerke orchestrieren (Paolicelli et al. 2011, Schafer et al. 2012, Ueno et al. 2013, Shigemoto-Mogami et al. 2014). Jedoch wird die kortikale Platte bereits ab E16 von Mikroglia besiedelt (Squarzoni et al. 2014). Deren Funktion in dieser Zeit (E16 bis P3) ist allerdings weitestgehend unbekannt und bedarf weiterer Forschung.

1.2 Sauerstoff als Einflussfaktor der Gehirnentwicklung

Eine optimale Sauerstoffversorgung stellt einen kritischen Faktor für die adäquate Entwicklung des Gehirns dar (Schneider et al. 2012, Porzionato et al. 2015). Kommt es zur

Hypoxie, etwa durch Plazentaprobleme oder Aufenthalt von Schwangeren oder Neugeborenen in großen Höhen, kann diese zu intrauteriner Wachstumsrestriktion, verringerter Neurogenese bzw. Anzahl an Neuronen sowie späteren neurologischen Einschränkungen führen (Padilla et al. 2011, Carpentier et al. 2013, Yang et al. 2013, Herrera and González-Candia 2021, Pla et al. 2020). Aber auch Hyperoxie, welche bei Frühgeburten durch iatrogene Sauerstoffbehandlung induziert wird, oder als Therapieform gegen das hypoplastische Linksherzsyndrom Anwendung findet, kann zu strukturellen Veränderungen des sich entwickelnden Gehirns führen (Felderhoff-Mueser et al. 2004, Gerstner et al. 2008, Edwards et al. 2018, Ramani et al. 2018). Problematisch daran ist, dass derartige sauerstoffbedingte Störungen im Verlauf des Lebens möglicherweise zu neurologischen Einschränkungen sowie zu Erkrankungen wie Schizophrenie oder Autismus-Spektrum-Störung führen können (Vaucher et al. 2012, Winkler-Schwartz, Garfinkle and Shevell 2014, Sola et al. 2014, Blackard et al. 2021, Wang et al. 2021).

Die Ursachen dafür könnten darin begründet liegen, dass die Wirkung von Sauerstoff nicht nur auf den Energiestoffwechsel begrenzt ist, sondern dass dieser auch als wichtiger Signalfaktor fungiert (Semenza and Wang 1992). Er wirkt dabei in verschiedensten Zelltypen über Hypoxie-induzierende Faktoren (HIF), welche unter höherem Sauerstoffpartialdruck degradiert werden, unter geringen Sauerstoffpartialdruck jedoch als Transkriptionsfaktoren aktiv sind (Maxwell, Pugh and Ratcliffe 1993, Wang and Semenza 1993, Ohh et al. 2000). Dabei können HIFs maßgeblich die Eigenschaften der Stammzellen sowie Vaskularisierungsfaktoren beeinflussen (Covello et al. 2006, Tomita et al. 2003, Milosevic et al. 2009, Forristal et al. 2010). Dieser Mechanismus spielt auch in der Gehirnentwicklung eine wichtige Rolle (Tomita et al. 2003, Wagenfuhr et al. 2015, Wagenfuhr et al. 2016, Lange et al. 2016). Obwohl noch unklar ist ob Sauerstoff ausschließlich über HIFs wirkt, wurde in Wagenführ et al. 2015 und 2016 gezeigt, dass eine 48 h lang anhaltende maternale Hyperoxie von E14,5 bis E16,5 zu einer Vergrößerung des Kortex und auch des Mittelhirns aufgrund gesteigerter Proliferation führt (siehe Abbildung 3). Insbesondere im Kortex konnten dabei vermehrt subventrikuläre Vorläuferzellen identifiziert werden, welche in großer Anzahl normalerweise nur in höher entwickelten Gehirnen vorkommen.

Die gleiche Methode hatte dagegen zu früheren Zeitpunkten der Entwicklung kaum Auswirkungen auf den Kortex (Wagenfuhr et al. 2015). Bei Verlängerung der Hyperoxie in der frühen Entwicklung auf 72 h kommt es dagegen zu einem Umschalten der kortikalen Stammzellen hin zu vermehrter Differenzierung, sodass die Dauer der Applikation eine

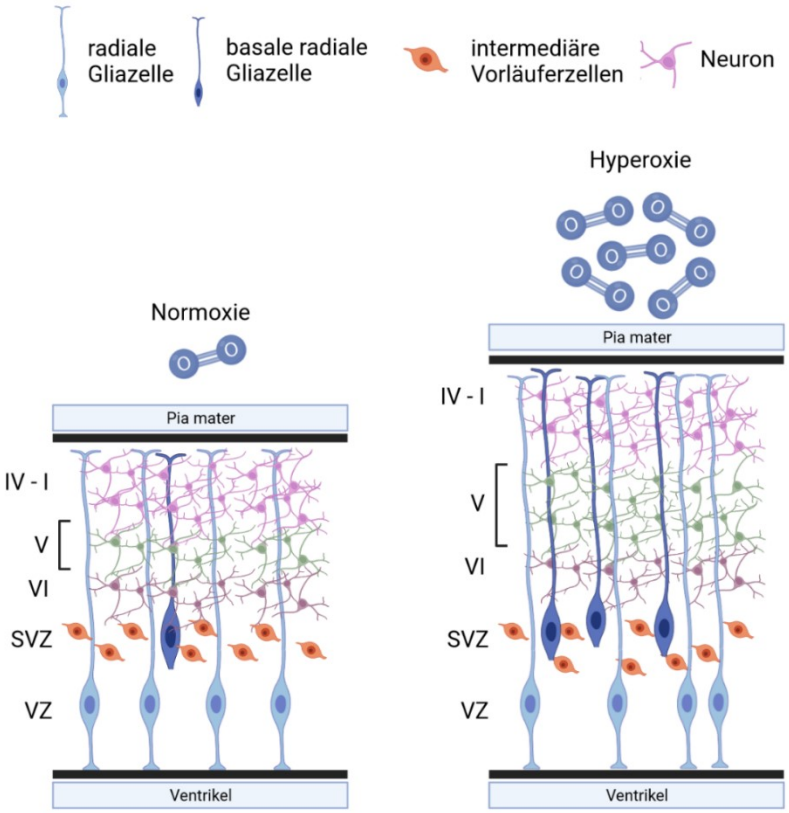

Abbildung 3: Schematische Darstellung eines expandierten E16,5 Mauskortex nach Sauerstoffbehandlung mit 75% pO_2 ab E14,5. VZ = ventrikuläre Zone; SVZ = Subventrikuläre Zone; VI = sechste kortikale Schicht; V = fünfte kortikale Schicht; IV-I = kortikale Schichten vier bis eins. Erstellt mit BioRender.com.

wichtige Rolle zu spielen scheint (Lange et al. 2016). Jedoch zeigt eine Pilotstudie mit chronischer maternaler Sauerstofftherapie gegen das hypoplastische Linksherzsyndrom, dass, trotz verringertem Kopfumfangs bei 6 Monate alten Kindern, keine neurologischen Beeinträchtigungen nachweisbar waren (Lara et al. 2016, Edwards et al. 2018). Dies lässt darauf schließen, dass morphologische Veränderungen durch Sauerstofftherapien möglicherweise durch regulatorische Prozesse normalisiert werden. Um welche Prozesse es sich dabei handelt und warum dennoch einige Kinder nach perinatalen hyperoxischen Ereignissen neurologischen Einschränkungen unterliegen, sowie welche Rolle die Dauer einer Sauerstofftherapie spielt sind noch gänzlich unbekannt. Eine Aufklärung dieser Prozesse ist für das Verständnis der Gehirnentwicklung essentiell und wird dazu beitragen, neurologische entwicklungsbiologische Beeinträchtigungen und Erkrankungen besser zu verstehen.

1.3 Katecholamine als Einflussfaktoren der Gehirnentwicklung

Katecholamine sind wichtige Neurotransmitter in einem funktionsfähigem Gehirn. Die beiden wichtigsten Katecholamine sind Dopamin (DA), welches überwiegend in Neuronen der Substantia Nigra (SN), Ventralen Tegmentalen Areal (VTA) und dem Locus Coeruleus (LC) synthetisiert wird, und Noradrenalin (NA), welches innerhalb des Gehirns ausschließlich in Neuronen des LC synthetisiert wird. Beide Populationen entwickeln sich sehr zeitig im Gehirn: dopaminerge Neurone bilden ab E10 die SN und VTA (Bayer et al. 1995, Bye, Thompson and Parish 2012); noradrenerge Neuronen entstehen bereits an E9 und bilden den LC (Pierce 1973, Steindler and Trosko 1989). Noradrenerge Neuronen projizieren in den Kortex, den Hippocampus, den Hypothalamus, das Septum und Kleinhirn (Coyle 1977, Coyle and Kuhar 1974, Gaspar et al. 1985, Gaspar et al. 1989). Dabei werden beispielsweise alle Schichten des Kortex an P5 von noradrenergen Ausläufern durchzogen und an P14 wird das Innervationsmuster einer ausgewachsenen Maus erreicht (Verney, Molliver and Grzanna 1982, Berger et al. 1983, Berger et al. 1985, Murrin, Sanders and Bylund 2007). Dopaminerge Neuronen projizieren ebenfalls in den Kortex und Hippocampus, Erreichen ihr adultes Innervationsmuster jedoch erst einige Monate nach Geburt (Kalsbeek, Matthijssen and Uylings 1989, Berger-Sweeney and Hohmann 1997). Auffällig dabei ist, dass die Entstehung der kortikalen Schichten nahezu zeitgleich mit der noradrenergen Innervation beginnt (Verney et al. 1984). Inwieweit Katecholamine die Neurogenese beeinflussen oder regulieren, ist jedoch bisher völlig unklar.

In adulten Mäusen wurde vor kurzem gezeigt, dass NA die Neurogenese im Hippocampus, der subventrikulären Zone (SVZ) und entlang des gesamten Ventrikels beeinflusst (Weselek et al. 2020). Mit Ausnahme des Hippocampus, fungiert NA dabei als Hemmstoff für die Neurogenese in der SVZ und entlang der gesamten Ventrikelachse. Dass NA je nach Bindung an verschiedene Rezeptoren fördernd oder hemmend auf die Proliferation fungiert, konnte bereits in *in vitro* Versuchen gezeigt werden (Ghiani et al. 1999, Masuda et al. 2012). Trotz dessen der Effekt von NA auf die hippokampale Neurogenese sehr gut erforscht ist gibt nur sehr wenige Studien bezüglich der periventrikulären oder embryonalen Neurogenese (Malberg et al. 2000, Kulkarni, Jha and Vaidya 2002, Jhaveri et al. 2014). Einige wenige *in vivo* Studien nutzten zudem ausschließlich toxische oder mechanische Läsionen des noradrenergen Systems, wobei nur kortikale Effekte untersucht wurden, die gegebenenfalls auf andere Einflüsse wie bestimmte Wachstumsfaktoren zurückzuführen

waren (Lidov and Molliver 1982, Murtha, Pappas and Raman 1990, Hassani et al. 2020). Zur Aufklärung der physiologischen Effekte von Katecholaminen, insbesondere von NA, auf die Gehirnentwicklung müssen daher systematisch Untersuchungen der Neurogenese in Abhängigkeit der jeweiligen Katecholaminlevel durchgeführt werden. In der aufgeführten Studie wird daher der DA und NA Gehalt zu verschiedenen Stadien der perinatalen Gehirnentwicklung von Mäusen untersucht und zum Ausmaß der Neurogenese korreliert.

2 Fragestellung

Die Entwicklung des Gehirns unterliegt einer Vielzahl von Einflussfaktoren und ist ein dynamischer, äußerst komplexer Prozess, welcher in weiten Teilen noch nicht verstanden ist. Komplikationen während der Entwicklung können verschiedenste neuronale entwicklungsbiologische Erkrankungen wie zum Beispiel Schizophrenie oder Autismus-Spektrum-Störung hervorrufen. Diese Erkrankungen sind weder heilbar, noch sind deren genaue Ursachen bisher bekannt. Zur möglichen Aufklärung und potenziellen Therapie solcher Erkrankungen ist es von großem Interesse, die Grundlagen der Entwicklung des Gehirns besser zu verstehen.

Die vorliegende Dissertation behandelt einen kleinen Ausschnitt dieses komplexen Prozesses. Dabei werden sowohl Sauerstoff, welcher bekanntermaßen die Neurogenese beeinflussen kann, als auch Katecholamine als Parameter der Gehirnentwicklung, insbesondere des Kortex, zu bestimmten Zeitpunkten untersucht. Die konkreten Fragestellungen untergliedern sich wie folgt:

- Führt kurzzeitige maternale Hyperoxie zur dauerhaften Vergrößerung des Gehirns und Veränderung des Kortex?
- Wie werden durch maternale Hyperoxie hervorgerufene Effekte reguliert?
- Können die Effekte einer maternalen Hyperoxie durch längere Applikation noch gesteigert werden?
- Welchen Einfluss haben Katecholamine auf die Entwicklung des Gehirns?

3 Methoden

3.1 Tierhaltung, Tiermodell und Gewebepräparation

Alle Versuche mit und an Tieren erfolgten nach Genehmigung der jeweils zuständigen Landesbehörden (Landesamt für Landwirtschaft, Lebensmittelsicherheit und Fischerei Mecklenburg-Vorpommern: AZ 7221.3-1-043/16; Landesdirektion Sachsen: 24-9168.24-1/2010-5). In den Projekten wurden C57BL/6J Mäuse verwendet, welche unter 12 h/12 h Tag-Nacht-Zyklus gehalten wurden und denen Futter und Wasser *ad libitum* zur Verfügung stand. Zur Sicherstellung der entsprechenden Entwicklungsstadien wurden die Tiere zeitlich exakt verpaart, d.h. das jeweilige Männchen wurde nur eine Nacht zu den Weibchen gesetzt. Zur Gewebepräparation wurden die Tiere fachgerecht und schmerzfrei getötet, die Feten entnommen und mittels Stereomikroskop die Gehirne herauspräpariert. Diese wurde für 24 h in 4 % Paraformaldehyd fixiert, in 30 % Sukroselösung entwässert, in circa -60 °C kaltem Isopropanol schockgefroren und anschließend bis zur weiteren Verwendung bei -80 °C gelagert.

3.2 Sauerstoffbehandlung

Zur Behandlung der trächtigen Tiere wurden diese in ihren normalen Käfigen in einer auf 75% pO_2 vorgefluteten Sauerstoffkammer gehalten (siehe Abbildung 4). Die Behandlung erfolgte zur kurzzeitigen maternalen Hyperoxiebehandlung für 48 h vom Embryonalstadium (E) 14,5 bis E16,5. Zur chronischen maternalen Hyperoxiebehandlung wurden die Tiere von E5,5 bis E16,5 im 24 h Rhythmus abwechselnd in 75% Sauerstoff bzw. normaler Raumluft gehalten. Die jeweils 24 h Erholungsphase war notwendig, um das Wohl des trächtigen Tieres selbst sicher zu stellen (Wagenfuhr et al. 2015). Kurz vor der kurzzeitigen Hyperoxiebehandlung an E14,5 wurde einem Teil der Tiere das Thymidinanalogon BrdU intraperitoneal injiziert, sowie einen Tag nach der Hyperoxiebehandlung an E17,5 das Thymidinanalogon EdU.

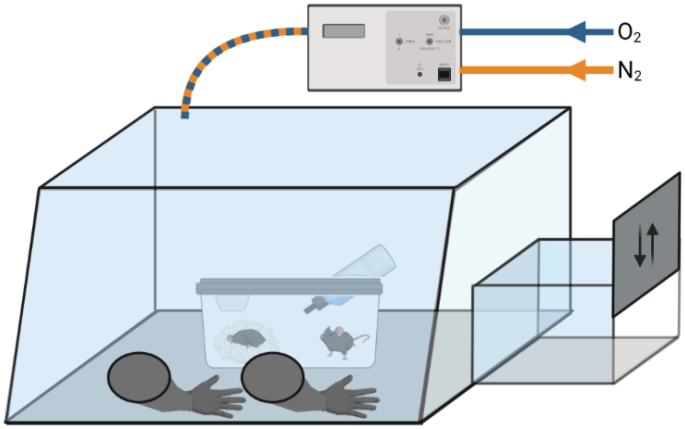

Abbildung 4: Schematische Zeichnung der verwendeten Sauerstoffkammer ITA950 (InerTec). Die aus transparentem Kunststoff bestehende Kammer verfügt über Sauerstoff- bzw. Stickstoff-Zuführungen zur exakten Einstellung des jeweilig gewünschten Sauerstoffpartialdrucks, welcher über Sensoren in der Box permanent gemessen wird. Zudem sind eine Schleuse zum Transfer der Käfig sowie Handschuhe zur Handhabung innerhalb der Kammer vorhanden. Erstellt mit BioRender.com.

3.3 Immunhistochemie

Die immunhistochemischen Analysen erfolgten mit Unterstützung von Frau Luisa Müller bezüglich NeuN Färbungen bei chronisch maternal hyperoxygenierten Tieren und maßgeblich durch Grit Weselek bezüglich der Färbungen und Analysen zur katecholaminergen Innervation des sich entwickelnden Gehirns. Zur immunhistochemischen Analyse verschiedener Marker wurden die Gehirne mittels Kryomikrotom koronar in 20 µm dünne Scheiben geschnitten und direkt auf Objektträger aufgezogen. Die Schnitte wurden mittels TBST gewaschen und zur Antigendemaskierung für 30 min in 95 °C heißem Zitratpuffer bzw. für BrdU-Färbungen bei 37 °C in 2 N HCl inkubiert. Nach erneutem Waschen erfolgte die Permeabilisierung und das Blockieren unspezifischer Bindungen mittels 0,2 % Triton-X Lösung bzw. mittels 10% Esel-Serum. Anschließend wurden die Schnitte bei 4 °C über Nacht mit verschiedenen Primärantikörpern inkubiert (Tabelle 1), gewaschen und mit Sekundärantikörper für 90 min bei Raumtemperatur inkubiert. Abschließend wurden die Schnitte 3 min mit Höchstlösung zur Kernfärbung bedeckt und mittels Fluoromount-G eingedeckelt. Die Analyse der Präparate erfolgte an verschiedenen Mikroskopen: Zeiss AxioObserver mit Apotome, Zeiss LSM900 mit AiryScan, Zeiss LSM 700 oder Leica DM IRE2.

Tabelle 1: Liste aller verwendeter Primärantikörper

Antikörper	**Firma**	**RRID**
chicken anti-NeuN	Merck	AB_11205760
goat anti-Iba1	Abcam	AB_2224402
guinea pig anti-vGluT2	Merck	AB_1587626
mouse anti-BrdU	Thermo Fisher Scientific	AB_2536432
mouse anti-Nestin	Chemicon	AB_2251134
mouse anti-NET	MAB Technologies	AB_2571639
mouse anti-phH3	Cell Signaling	AB_331748
mouse anti-Satb2	Abcam	AB_882455
rabbit anti-CC3	Cell Signaling	AB_2341188
rabbit anti-CD68	Abcam	AB_10975465
rabbit anti-Iba1	Wako	AB_839504
rabbit anti-MCM2	Abcam	AB_881276
rabbit anti-NeuN	Merck	AB_10807945
rabbit anti-Pax6	Covance	AB_291612
rabbit anti-Tbr1	Abcam	AB_2200219
rabbit anti-Tbr2	Abcam	AB_2721040
rabbit anti-TH	Pel-Freez	AB_461064
rat anti-CD68	BioRad	AB_324217
rat anti-Ctip2	Abcam	AB_2064130
rat anti-DAT	Merck	AB_2251134
sheep anti-TH	Pel-Freez	AB_461070

3.4 Analyse der Katecholamine

Zur Analyse der Katecholamine wurden ca. 200 µm Gewebe rund um die Ventrikel verschiedener Gehirnareale entfernt, gewogen und in Perchlorsäure homogenisiert (durchgeführt von Grit Weselek). Die Proben wurden bei 48000 g zentrifugiert und 50 µl des jeweiligen Überstandes wurden in einem Hochleistungs-Flüssigkeitschromatographie (High-Performance Liquid Chromatography, HPLC) System auf ihren Dopamin- und Noradrenalin-Gehalt hin untersucht (durchgeführt von Manfred Gerlach). Dabei kam ein Agilent 1100 System mit Nukleosil 120-5C18 reversen Phase Säule, Elektrochemischen Detektor und Agilent Chem Station for LC9D zum Einsatz, wobei das Detektionslimit bei 0,1 ng Katecholamine pro ml Probe lag.

4 Ergebnisse

4.1 Hyperoxygenation During Mid-Neurogenesis Accelerates Cortical Development in the Fetal Mouse Brain

Franz Markert & Alexander Storch

Frontiers in Cell and Developmental Biology, 2022, Band 10, Artikel 732682

Zusammenfassung:

In dieser Studie wurde untersucht, ob die Effekte einer kurzzeitigen maternalen Hyperoxie zu dauerhaften Veränderungen im Gehirn führt. Dazu wurden trächtige C57BL/6J Mäuse von Embryonalstadium (E) 14,5 bis E16,5 in 75% Sauerstoff gehalten und die Feten bzw. Jungtiere zu E16,5, Postnatalstadium (P) 0,5 und P3,5 auf den Status ihrer kortikalen Entwicklung hin untersucht. Die immunhistochemische Analyse zeigte, dass die Sauerstoffbehandlung zu einer beschleunigten Neurogenese führt, welche sich in einem bis P0,5 anhaltenden vergrößerten Kortex und mehr kortikalen Neuronen äußert, an P3,5 jedoch wieder normalisiert ist. Im speziellen wird durch die beschleunigte Neurogenese die Anzahl an $Ctip2^+$ Schicht V Neuronen an E16,5 gesteigert und adäquat zwischen P0,5 und P3,5 an das Level der Kontrolltiere angepasst. Diese Normalisierung erfolgt unter Beteiligung von $CD68^+/Iba1^+$ aktiven Mikroglia, welche $Ctip2^+$ Zellen angreifen und vermehrt $Ctip2^+$ Partikel phagozytieren, ohne dass diese Zeichen von Apoptose aufweisen. Insgesamt zeigt sich, dass kurzzeitige maternale Hyperoxie zu einem transienten Überschuss von Schicht V Neuronen führt, welcher jedoch kurz nach Geburt wieder normalisiert wird, sodass keine persistenten Effekte nachweisbar sind. Die Studie ermöglicht neue Einblicke in die Effekte von Sauerstoff, die Entwicklung der kortikalen Schicht V und die Beteiligung von Mikroglia während der Gehirnentwicklung.

frontiers in Cell and Developmental Biology

ORIGINAL RESEARCH
published: 17 March 2022
doi: 10.3389/fcell.2022.732682

Hyperoxygenation During Mid-Neurogenesis Accelerates Cortical Development in the Fetal Mouse Brain

Franz Markert[1] *and Alexander Storch*[1,2]*

[1]Department of Neurology, University of Rostock, Rostock, Germany, [2]German Center for Neurodegenerative Diseases (DZNE) Rostock/Greifswald, Rostock, Germany

Oxygen tension is well-known to affect cortical development. Fetal brain hyperoxygenation during mid-neurogenesis in mice (embryonic stage E14.5. to E16.5) increases brain size evoked through an increase of neuroprecursor cells. Nevertheless, it is unknown whether these effects can lead to persistent morphological changes within the highly orchestrated brain development. To shed light on this, we used our model of controlled fetal brain hyperoxygenation in time-pregnant C57BL/6J mice housed in a chamber with 75% atmospheric oxygen from E14.5 to E16.5 and analyzed the brains from E14.5, E16.5, P0.5, and P3.5 mouse embryos and pups *via* immunofluorescence staining. Mid-neurogenesis hyperoxygenation led to an acceleration of cortical development by temporal expansion of the cortical plate with increased $NeuN^+$ neuron counts in hyperoxic brains only until birth. More specifically, the number of $Ctip2^+$ cortical layer 5 (L5) neurons was increased at E16.5 and at birth in hyperoxic brains but normalized in the early postnatal stage (P3.5). The absence of cleaved caspase 3 within the extended $Ctip2^+$ L5 cell population largely excluded apoptosis as a major compensatory mechanism. Timed BrdU/EdU analyses likewise rule out a feedback mechanism. The normalization was, on the contrary, accompanied by an increase of active microglia within L5 targeting $Ctip2^+$ neurons without any signs of apoptosis. Together, hyperoxygenation during mid-neurogenesis phase of fetal brain development provoked a specific transient overshoot of cortical L5 neurons leading to an accelerated cortical development without detectable persistent changes. These observations provide insight into cortical and L5 brain development.

Keywords: oxygen, hyperoxia, corticogenesis, neural stem cells, apoptosis, brain development, microglia, cortical layers

OPEN ACCESS

Edited by:
Felipe Mora-Bermúdez, Max Planck Society, Germany

Reviewed by:
Christian Lange, Technical University Dresden, Germany
Jessica M. Rosin, University of British Columbia, Canada

***Correspondence:**
Alexander Storch
alexander.storch@med.uni-rostock.de

Specialty section:
This article was submitted to Stem Cell Research, a section of the journal Frontiers in Cell and Developmental Biology

Received: *29 June 2021*
Accepted: *20 January 2022*
Published: *17 March 2022*

Citation:
Markert F and Storch A (2022) Hyperoxygenation During Mid-Neurogenesis Accelerates Cortical Development in the Fetal Mouse Brain. Front. Cell Dev. Biol. 10:732682. doi: 10.3389/fcell.2022.732682

Abbreviations: CC3, cleaved caspase 3; CP, cortical plate; Ctip2, chicken ovalbumin upstream promotor transcription factor-interacting protein 2; E, embryonic day; L, layer; NeuN, neuronal nuclear protein; RBFOX3, RNA binding protein fox-1 homolog 3; OSVZ, outer subventricular zone; P, postnatal stage; Pax6, paired box 6; PBS, phosphate buffered saline; Satb2, special AT-rich sequence-binding protein 2; SVZ, subventricular zone; Tbr1, T-box brain protein 1; Tbr2, T-box brain protein 2; TBST, Tris buffered saline/Tween 20; vGluT2, vesicular glutamate transporter 2; VZ, ventricular zone.

INTRODUCTION

Oxygen tension during development is known to critically affect brain development (Fagel et al., 2006; Schneider et al., 2012; Porzionato et al., 2015; Wagenfuhr et al., 2015; Lange et al., 2016; Wagenfuhr et al., 2016). Thereby, the effects depend on timing and intensity of oxygen application: while short-term hyperoxygenation is able to enhance neurogenesis and brain size, chronic hyperoxygenation can lead to adverse effects (Wagenfuhr et al., 2015; Wagenfuhr et al., 2016; Markert et al., 2020). Indeed, short-term hyperoxygenation during mid-neurogenesis of fetal mouse brain development (embryonic stages E14.5 to E16.5) leads to an immediate expansion of a distinct proliferative cell population basal of the subventricular zone (SVZ) constituting a new neurogenic cell layer similar to the outer SVZ (OSVZ), which contributes to corticogenesis by heading for deeper cortical layers as a part of the cortical plate (CP) (Wagenfuhr et al., 2015). Finally, the number of $Ctip2^+$ neurons in the deeper layer 5 (L5) of the CP projecting into various brain regions is markedly increased (Hattox and Nelson 2007; Oswald et al., 2013; Wagenfuhr et al., 2015). This phenomenon is of high interest, since alterations within the cortical L5 cell population are directly linked to diseases such as schizophrenia (Kolomeets and Uranova 2019; Mi et al., 2019), which is also linked with oxidative stress and various other factors during development (Chew et al., 2013; Górny et al., 2020). Despite these known effects of maternal hyperoxygenation with subsequent changes of the oxygen tension of brain tissue *in utero*, a pilot study applying maternal oxygenation in humans, although in a more chronic treatment scheme, shows initial morphological changes of the head, but no differences in neurodevelopmental testing of the children (Edwards et al., 2018). These results raise not only concerns about the safety of maternal hyperoxygenation therapy (Rudolph 2020) but also the questions whether and how the brain is able to better compensate for changes of neuronal plasticity during development to normalize the cortical structure.

The process of embryonic/fetal brain development is highly orchestrated through main events like proliferation, differentiation, and migration of neuronal stem cells (Noctor et al., 2001; Talamillo et al., 2003; Haubensak et al., 2004; Noctor et al., 2004) and morphological and functional shaping of cortical cell populations (White and Barone 2001; Blanquie et al., 2017). Thereby, radial glia cells located at the ventricular surface develop into cortical neurons through the Pax6, Tbr2, and Tbr1 axis where the resulting cells migrate through the cortex and form the cortical inside-out layering (Englund et al., 2005; Agirman et al., 2017). The resulting number of neurons seems to be prenatally regulated through invading microglia capable of phagocytizing and controlling the number $Pax6^+$ or $Tbr2^+$ cells (Cunningham et al., 2013). Other suggested mechanisms include a feedback signal from cortical deep layer cells to the radial glia affecting the generation of upper layer cells as well as already occurring apoptosis of neuroprecursor cells (Blaschke et al., 1996; Toma et al., 2014). After birth, apoptosis of postmitotic neurons particularly becomes prominent in the cortex where around 50% of all neurons die (Dekkers et al., 2013; Wong and Marín 2019). This mechanism likely regulates the number of cortical neurons in an area-dependent manner through their electrical activity and indicates a specific postnatal connectivity control (Blanquie et al., 2017).

Although the short-term effects of hyperoxygenation during mid-neurogenesis of fetal mouse brain development with immediately enhanced neurogenesis particularly within cortical L5 are reported, the subsequent consequences of these phenomena during later cortical development remain enigmatic. We therefore used our established model of maternal hyperoxygenation to investigate the effects of increased oxygen tension during mid-neurogenesis (E14.5–E16.5) on later cortical development until the early postnatal state (Wagenfuhr et al., 2015). Moreover, the model allows the investigation of potential mechanisms mediating the reshape of the cortical structure during late fetal and early postnatal cortical development.

MATERIALS AND METHODS

Animals and Oxygen Treatment

C57BL/6J timed-pregnant mice were housed in their home cages within a preconditioned oxygen chamber (InerTec, Grenchen, Switzerland) at 75% oxygen or room air (21% oxygen; control condition). During the whole treatment protocol, all animals were handled by the same investigator. Fetuses of both groups showed an ordinary morphology. Pregnant mice for analysis of postnatal day 0.5 (P0.5) fetuses intraperitoneally received BrdU (50 mg/kg body weight) at E14.5, the start of hyperoxia treatment, and EdU (25 mg/kg body weight) at E17.5, 1 day after the end of the oxygen treatment. All data were gathered from randomly chosen embryos or pups from at least three independent litters per group. All animals were maintained and treated with permission of the local Department of Animal Welfare (Landesamt für Landwirtschaft, Lebensmittelsicherheit und Fischerei Mecklenburg-Vorpommern) (reference number 7221.3-1-043/16) and comply with the Tierschutzgesetz and Verordnung zur Umsetzung der Richtlinie 2010/63/EU from Germany. Of note, our study was initially designed including a hypoxia group (10% oxygen), but it was not possible to gather data for postnatal maternal hypoxia group as the mice tend to infanticide. To secure animal welfare and to be in line with German law, we had to cancel these experiments.

The brains of embryos and pups were dissected prior and immediately after oxygen treatment [E14.5 (for estimating the cortical volume) and E16.5] and postnatally at P0.5 and P3.5, fixed for 24 h in 4% paraformaldehyde (Merck, Darmstadt, Germany), and kept in 30% sucrose (Carl Roth, Karlsruhe, Germany) in DPBS (Thermo Fisher Scientific, Waltham, United States). Then brains were snap-frozen, sectioned coronal at 20-µm thickness using a cryomicrotome (Leica Biosystems, Nussloch, Germany), and mounted on Superfrost Plus slides (Thermo Fisher Scientific). The slides were stored at 4°C until staining.

Immunofluorescence

Slides were washed with wash buffer (Agilent, Santa Clara, United States), and heat-induced antigen retrieval was performed using 10 mM sodium citrate (Carl Roth) with 0.05% Tween 20 (SERVA, Heidelberg, Germany) for 30 min at 95°C or 2 N HCl for 30 min at 37°C for BrdU staining. After 20 min at room temperature, slides were washed with Tris buffered saline/Tween 20 (TBST), treated with TBST containing 0.2% Triton X-100 (Carl Roth) and 10% donkey serum (Merck) for 30 min, and were incubated with primary antibodies overnight at 4°C. The following primary antibodies were used: rabbit anti-NeuN (Merck, ABN78, RRID: AB_10807945), chicken anti-NeuN (Merck, ABN91, RRID: AB_11205760), rabbit anti-cleaved-caspase-3 (CC3; Cell Signaling, 9661S, RRID: AB_2341188), mouse anti-BrdU (Thermo Fisher Scientific, B35128, RRID: AB_2536432), rabbit anti-Tbr1 (Abcam, ab31940, RRID: AB_2200219), mouse anti-Satb2 (Abcam, ab51502, RRID: AB_882455), rat anti-Ctip2 (Abcam, ab18465, RRID: AB_2064130), rabbit anti-Ctip2 (Abcam, ab28448, AB_1140055), rabbit anti-Iba1 (Wako, 019-19741, RRID: AB_839504), goat anti-Iba1 (Abcam, ab5076, RRID: AB_2224402), rabbit anti-CD68 (Abcam, ab125212,RRID: AB_10975465), rat anti-CD68 (BioRad, MCA1957GA, AB_324217), or guinea pig anti-vGluT2 (Merck, AB2251-I, RRID: AB_1587626). Subsequently, slides were incubated with corresponding secondary antibodies (Thermo Fisher Scientific), and nuclei were stained with Hoechst 33258 (Merck). For EdU analysis, slides were stained using Click-iT staining kit (Thermo Fisher Scientific) as described by the manufacturer. Finally, slides were mounted with Fluoromount-G (Biozol, Eching, Germany).

Imaging and Measurements

Most images were taken with AxioObserver Z1 with Apotome using ZEN blue 2.3 software with Tiles and Position module (all from Carl Zeiss, Oberkochen, Germany). Z-stack images of microglia-targeting Ctip2$^+$ cells were taken with LSM900 with Airyscan (Carl Zeiss). Hoechst images of every sixth section with a thickness of 20 µm were taken with ×2.5 objective and subsequently used for determining the volume of the whole brain and the CP corresponding to the mouse brain atlas (Allen-Institute, 2008). Thereby, we used the corpus callosum and the lateral ventricles for orientation dorsal/between the hemispheres and for lateral the piriform region and the endopiriform nucleus. For caudal sections, we used the thinner subiculum layer in the extension of hippocampal C1 layer (excluded) for dorsal orientation (**Supplementary Figure S1**). The volume was calculated by adding up the data of each slice (midpoint type) and then multiplying by 120 (every sixth slice of 20-µm thickness).

For analysis of apoptosis, fluorescence images of the whole hemispheres from the developing parietal cortex areas were taken. CC3$^+$ cells were counted with ZEN blue 2.3 in the cortex from the dorsal to ventral site corresponding to the area described above. For double staining, CC3$^+$ were searched as described above and imaged as Z-stack with Apotome mode. For specific marker analysis, at least four images of the cortex were taken as Z-stack with 1-µm steps. The corresponding cells or VGlut2$^+$ synapses were counted in the middle focal plane using either ZEN analysis software (Tbr1, Ctip2, and Satb2) or ImageJ (BrdU, EdU, and NeuN). L5 neurons at postnatal stages were defined by high Ctip2 expression levels as described by McKenna et al. (2011). Iba1$^+$ cells and double/triple-stained cells were manually counted through the Z-stacks within the middle cortical sections in the rostro-caudal axis by the same investigator who was blinded for the treatment groups.

Statistics

All statistical analyses were performed with RGUI 3.4.1 (R Foundation for Statistical Computing, Vienna, Austria) or SPSS version 25.0 (SPSS Inc., Chicago, IL). If not otherwise stated, statistical significance was evaluated by unpaired two-sided *t*-test or two-way ANCOVA followed by pairwise *t*-test including Bonferroni correction. Cortical volume was analyzed independent of the developmental state due to its well-known physiological large volume expansion after birth. The numbers of analyzed embryos and pups gathered from at least three independent litters are indicated by "*n*." All data are displayed as means ± s.e.m. with the numbers of analyzed embryos and pups indicated for each experiment. The significance level was set to $p < 0.05$ (two-tailed test).

RESULTS

Oxygen-Induced Cortical Expansion During Fetal Brain Development is Equalized at Early Postnatal Stage

To assess the time course and putative long-term persistency of the effects of oxygen tension on the rapidly changing and highly regulated fetal cortical development, we applied the already introduced mouse model of maternal hyperoxygenation known to reliably control tissue oxygen tension and subsequently neurogenesis within the developing fetal mouse brain (Wagenfuhr et al., 2015; Wagenfuhr et al., 2016). We thus applied maternal hyperoxygenation to time-pregnant mice at mid-neurogenesis from embryonic stage E14.5 to E16.5 and investigated cortical morphology during embryonic development from E14.5 to early postnatal stage at P3.5 (**Figure 1A**). The hyperoxia and control groups showed no abnormalities in their spontaneous or litter care behavior. All embryos and pups displayed normal morphology at all developmental stages examined, but the brains of the hyperoxia group appeared visually and quantitatively increased in their size at E16.5, but not on other developmental stages (**Figures 1B,C**). Indeed, mouse embryos of the hyperoxia group showed a 1.2-fold increase in the volume of the CP as compared with normoxic controls at E16.5 ($p = 0.002$), which persisted until birth (P0.5; $p = 0.015$), but not until P3.5 ($p = 0.653$; unpaired two-sided *t*-test; $n = 4–9$; **Figure 1D**).

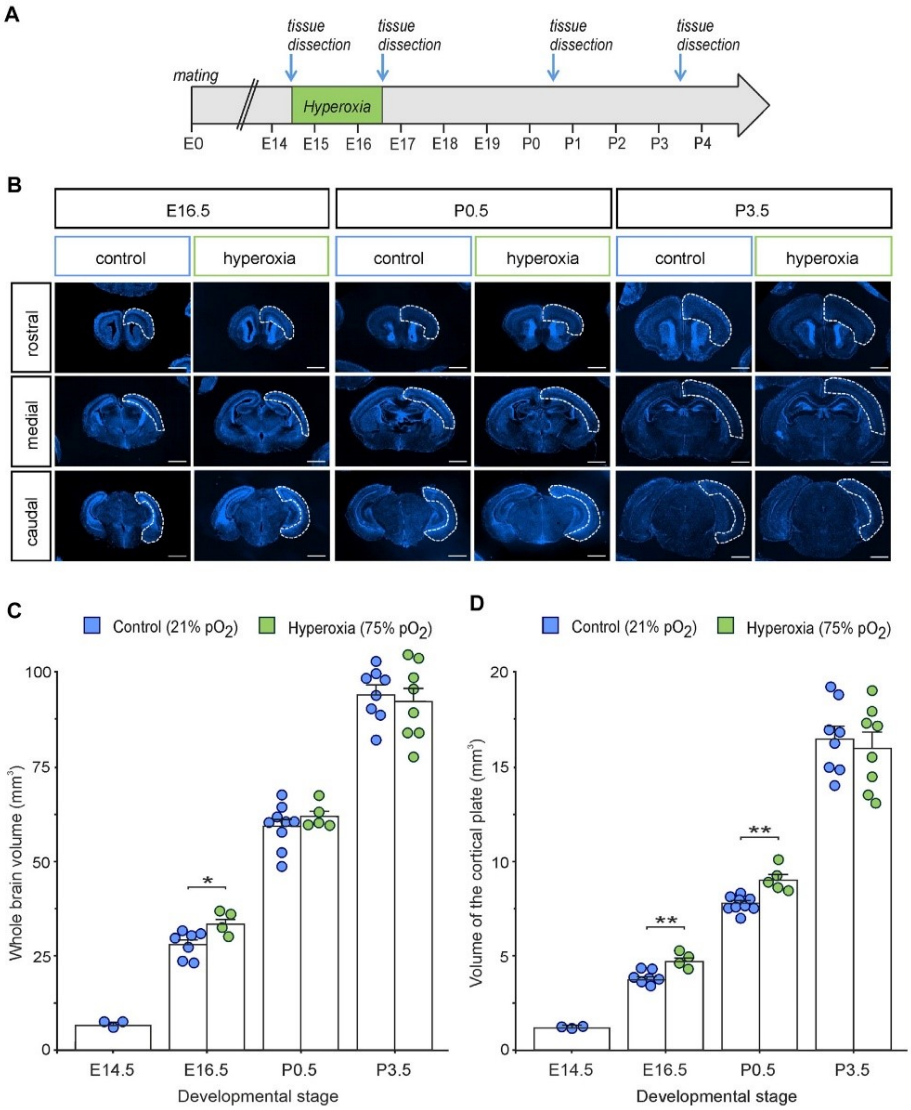

FIGURE 1 | The effects of fetal brain hyperoxia during mid-neurogenesis (E14.5 to E16.5) on volume of the cortical plate (CP) during later brain development in mice. **(A)** Experimental treatment scheme for fetal brain hyperoxygenation (by maternal application of 75% O_2) during mid-neurogenesis (E14.5 to E16.5). **(B)** Representative fluorescence images from rostral, middle, and caudal slices of E16.5, P0.5, and P3.5 brains. Slices were stained with Hoechst (blue). Dashed lines outline the cortical area used to estimate cortical volume. Scale bars, 1,000 µm. **(C,D)** Quantification of whole-brain volume **(C)** and the volume of the CP **(D)** showed increased cortical volume in hyperoxic brains at E16.5 and P0.5 (only CP) but not at P3.5 as compared to normoxic controls. Note that the value at E14.5 serves as starting point of volume just before the hyperoxic treatment, and thus, no hyperoxic condition was tested. Data are means ± s.e.m. [E14: $n = 3$; E16.5: $n = 7$ (control), $n = 4$ (hyperoxia); P0.5: $n = 9$ (control), $n = 5$ (hyperoxia); P3.5: $n = 8$ (control and hyperoxia)]. *$p < 0.05$ and **$p < 0.01$ from unpaired two-sided t-tests (non-significant comparisons are not marked for clarity).

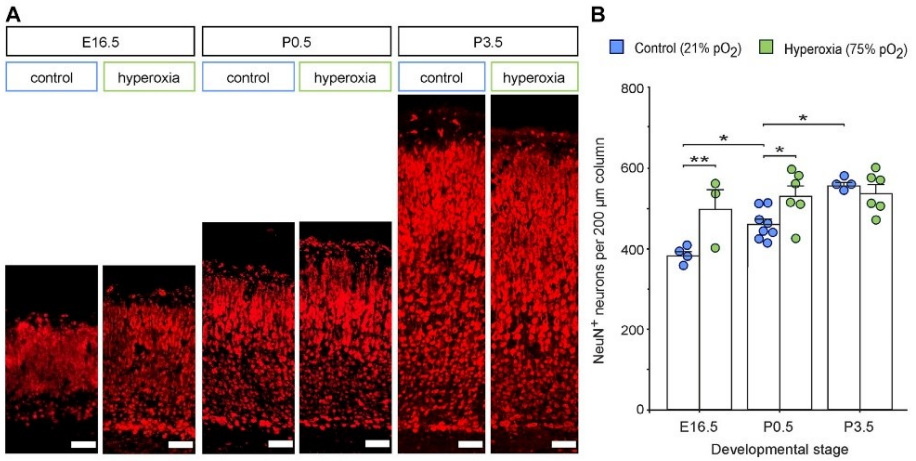

FIGURE 2 | The effects of fetal brain hyperoxia during mid-neurogenesis (E14.5 to E16.5) on the numbers of cortical neurons during later brain development in mice. **(A)** Representative fluorescence images from the CP in the middle sections along the rostro-caudal axis stained with NeuN (red). Scale bars, 50 µm. **(B)** Quantification of NeuN$^+$ cortical neurons in the brain slices. Data are means ± s.e.m. [E16.5: $n = 4$ (control), $n = 3$ (hyperoxia); P0.5: $n = 8$ (control), $n = 6$ (hyperoxia); P3.5: $n = 4$ (control), $n = 6$ (hyperoxia)]. $^*p < 0.05$ and $^{**}p < 0.01$ from two-way ANOVA with *post-hoc* two-sided *t*-test with Bonferroni correction (non-significant comparisons are not marked for clarity). For full statistics for **(B)**, see **Supplementary Table S1**.

Hyperoxygenation During Mid-Neurogenesis Accelerates But Does Not Increase Cortical Neurogenesis

To further evaluate cortical development, we used NeuN staining and analyzed the number of neurons within the middle cortical sections along the rostro-caudal axis (**Figure 2**). The hyperoxic embryos showed an increase of NeuN$^+$ neurons per volume at E16.5 with a 1.3-fold higher neuronal density as compared with normoxic control animals ($p = 0.005$), which persisted until birth (P0.5) with a still 1.2-fold higher neuronal density ($p = 0.013$), but not until P3.5 ($p = 0.581$, all from *post hoc* two-sided *t*-test with Bonferroni adjustment; **Figure 2B**). The neuronal density in the control group rose continuously between E16.5 and P3.5, while in the hyperoxia group, the maximum neuronal density seems to be already reached at earlier developmental stages at E16.5 (**Figure 2B**). Of note, neuronal density in the hyperoxia group never exceeded that in the control group, indicating an accelerated but not increased cortical neurogenesis (**Figure 2B**).

Postnatal Cortical Normalization Occurs in a Layer-Specific Manner

Whether the equalization of cortical volume and neuronal density at birth after fetal hyperoxygenation during the mid-neurogenesis phase is capable of functioning as a control mechanism for regulating neuronal layer specificity and neural circuits or whether it originates from increased raw cell numbers competitive to each other remains elusive. To shed light on this aspect, we performed a layer-specific analysis using a panel of markers Tbr1, Ctip2, and Satb2 of hyperoxic mouse embryos and pups through the developmental stages E16.5, P0.5, and P3.5 and performed a quantitative analysis for Tbr1$^+$ cells as characteristic for neurons of the SP and L6 (Hevner et al., 2001), Ctip2$^+$/Tbr1$^-$ cells representing L5 neurons (Arlotta et al., 2005), and Satb2$^+$ cells as neurons of the upper cortical layers (**Figure 3**) (Britanova et al., 2008). The number of Tbr1$^+$ cells in the CP decreased continuously from E16.5 to P3.5 (**Figure 3B**). Of note, the percentage of Tbr1$^+$ cells in the CP was reduced at E16.5, although the total number of Tbr1$^+$ cells was not affected (**Figure 3B**; **Supplementary Figure S2**).

Quantification of the percentage of L5-specific neurons (Ctip2$^+$/Tbr1$^-$ cells; (Hevner et al., 2001; Arlotta et al., 2005) showed a persistent increase within the hyperoxic group at E16.5 (1.5-fold) and P0.5 (1.6-fold; **Figure 3C**), which further supports our previous data and even further demonstrates that fetal brain hyperoxia evoked persistent effects on L5 (Wagenfuhr et al., 2015). The same layer marker panel revealed no differences in the number of Ctip2$^+$ cells at P3.5. Comparing the time course of Ctip2$^+$ cell numbers during cortical development, there was a slow drop of the percentage of Ctip2$^+$ cells within the CP between E16.5 and P3.5 in normoxic mice, but a later drop just after birth in hyperoxic mice, suggesting that the specific rearrangement of cortical L5 is postponed by hyperoxia (**Figure 3C**). We also found an increase in the absolute numbers of L5 neurons between E16.5 and P0.5. Since no more L5 neurons are generated at this time, we assume that this represents a change in the expression of Ctip2 rather than ongoing neurogenesis (McKenna et al., 2011; Toma et al., 2014).

The number of upper-layer Satb2$^+$ neurons was not affected by hyperoxia through all developmental stages (**Figure 3D**; **Supplementary Figure S2**).

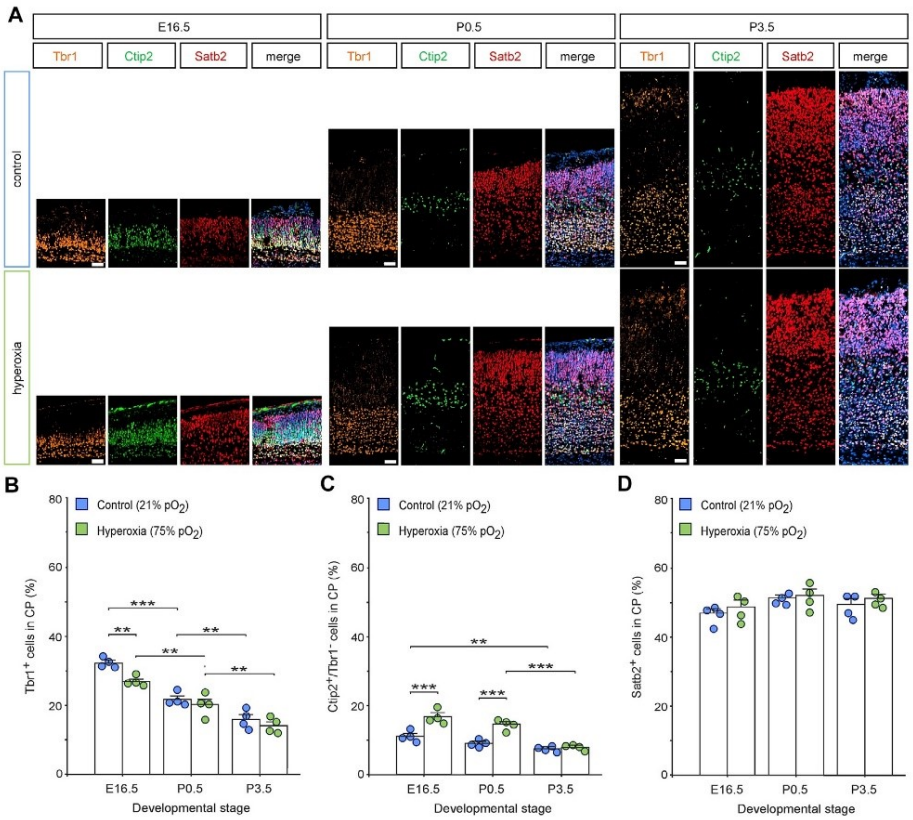

FIGURE 3 | The effects of fetal brain hyperoxygenation on layer-specific distribution of neurons. **(A)** Representative fluorescent images of Tbr1$^+$ (orange), Ctip2$^-$ cells (green), and Satb2$^+$ cells (red) from E16.5, P0.5, and P3.5 in the middle cortical sections along the rostro-caudal axis of hyperoxic and normoxic control mice. Hoechst (blue) was used to stain cell nuclei shown in the merged image. Scale bars, 50 µm. **(B–D)** Quantification of the distribution of Tbr1$^+$ cortical subplate/layer 6 neurons **(B)**, Ctip2$^+$/Tbr1$^-$ layer 5 neurons **(C)**, and Satb2$^+$ upper layer-specific neurons **(D)** showed a specific increase of layer 5 neurons at E16.5 and P0.5 but not at P3.5. Data are means ± s.e.m. ($n = 4$ for all animal groups). $^{**}p < 0.01$ and $^{***}p < 0.001$ from two-way ANOVA with *post-hoc* two-sided *t*-test with Bonferroni correction (non-significant comparisons are not marked for clarity). For full statistics, see **Supplementary Tables S2–S4**.

Microglia are Involved in Postnatal Cortical Normalization After Fetal Hyperoxygenation

The postnatal regulation of the CP after fetal hyperoxygenation prompted us to evaluate the possible underlying mechanisms. There are already known mechanisms capable of controlling the number of brain cells including neurons during development (Cunningham et al., 2013; Toma et al., 2014; Blanquie et al., 2017): apoptosis known to occur during early postnatal cortical development; feedback mechanisms where the increased number of neurons signals a feedback to neuronal stem cells or microglia able to phagocytose brain cells. We consequently analyzed Iba1 staining for the number of microglia, CC3 staining as an established marker for apoptosis, and time-delayed BrdU/EdU labelling for estimating the birthdate of the resulting neurons during brain development.

Immunohistochemical staining of Iba1$^+$ cells labelling resting and activated microglia (Imai et al., 1996; Morgan et al., 2010) revealed an already visually detectable increase in microglia residing in L5 of hyperoxic P0.5 mouse pups (**Figure 4A**), which was not present in E16.5 or P3.5 brains (**Supplementary Figure S3**). Quantification of these Iba1$^+$ cells revealed a specific 2.7-fold increase of microglial cells in L5 of hyperoxic mice ($p < 0.001$, *post hoc* two-sided *t*-test with Bonferroni adjustment), while the total number of Iba1$^+$ cells, other layers, and developmental stages was not affected by oxygen (**Figures 4B–E**; **Supplementary Figure S4**). Microglia within the CP were predominantly found at and after P0.5, but the invasion specifically of L5 is accelerated, although not exceeding the

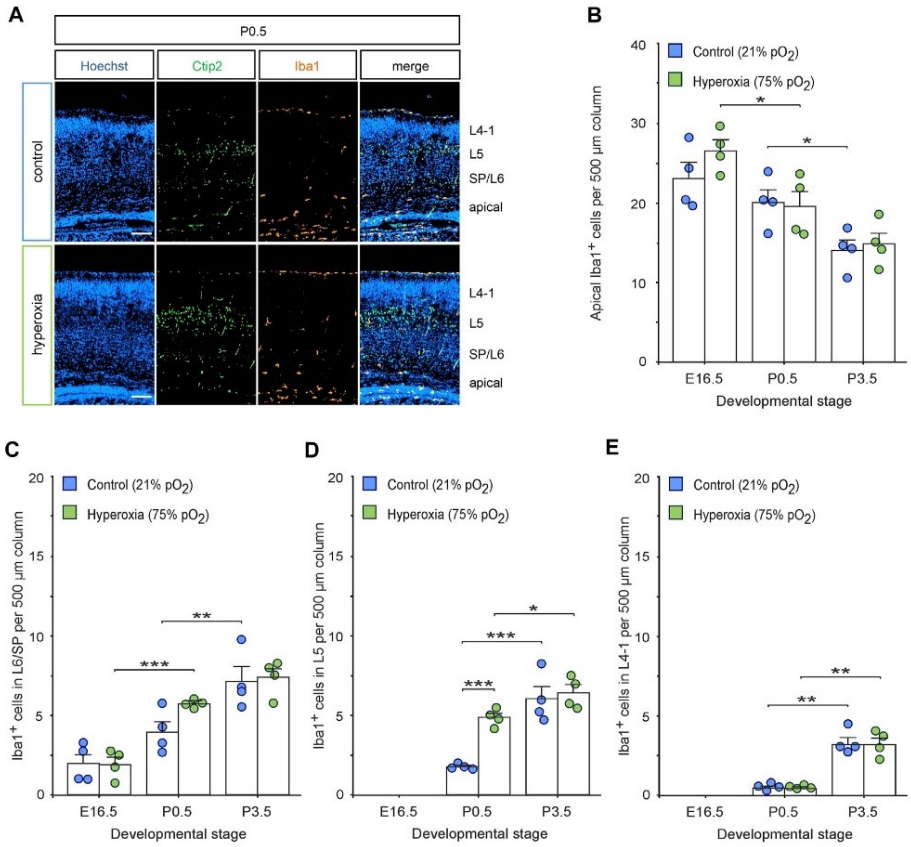

FIGURE 4 | The effects of hyperoxygenation on microglial distribution within the developing cortex. **(A)** Representative fluorescent images of Iba1$^+$ cells (orange) from P0.5 in the middle cortical sections along the rostro-caudal axis of hyperoxia-treated and control mice. Ctip2$^+$ (green) was used for layer determination, and Hoechst (blue) was used to stain cell nuclei. Scale bars represent 100 µm. **(B–E)** Quantification of Iba1$^+$ apical microglia **(B)**, within subplate/layer 6 (SP/L6) **(C)**, layer 5 (L5) **(D)**, and upper layers 4-1 (L4-1) **(E)** showed an increase of microglia within L5 at P0.5. Data are means ± s.e.m. ($n = 4$ for all animal groups). *$p < 0.05$, **$p < 0.01$, and ***$p < 0.001$ from two-way ANOVA with *post-hoc* two-sided *t*-test with Bonferroni correction (non-significant comparisons are not marked for clarity). For full statistics, see **Supplementary Tables S5–S8**.

number of microglia at P3.5. This is further supported by analysis of the apical and SP/L6 microglia, where the decrease of apical microglia and the successive increase of SP/L6 occurred between P0.5 and P3.5 in normoxic control mice, but already occurred between E16.5 and P0.5 in hyperoxic mice (the increase in Iba1$^+$ microglia in SP/L6 at P0.5 represents only a non-significant trend). Intriguingly, we could show that microglia in L5-targeted Ctip2$^+$ cells without morphological signs of apoptosis (**Figure 5A**). An analysis of Ctip2$^+$ and Satb2$^+$ cells targeted by microglia at time point P0.5 showed that Ctip2$^+$ cells were targeted by microglia significantly more often in the hyperoxia group than in the control group (**Figure 5B**). At the same time, there was no difference in the number of Satb2$^+$ cells targeted by microglia (**Figure 5C**; **Supplementary Figure S5**). We consequently analyzed the number of active microglia by using the combination of Iba1 and the microglia activation marker CD68 (Rabinowitz and Gordon 1991; Imai et al., 1996; Morgan et al., 2010; Jurga et al., 2020). Quantification revealed that there are indeed more active microglia in L5 and also apical, but not between these in L6/SP (**Figures 5D–H**). Further analyses revealed Ctip2$^+$ and Satb2$^+$ particles in these active microglia in L5, but—interestingly—only the number of active microglia containing Ctip2$^+$ particles was increased in hyperoxic as compared to control brains (**Figure 5I,J**).

To further evaluate whether adaptive mechanisms contribute to normalization of the number of neurons cortex after fetal hyperoxygenation, we performed a birth-dating analysis using BrdU application immediately before and EdU application 1 day

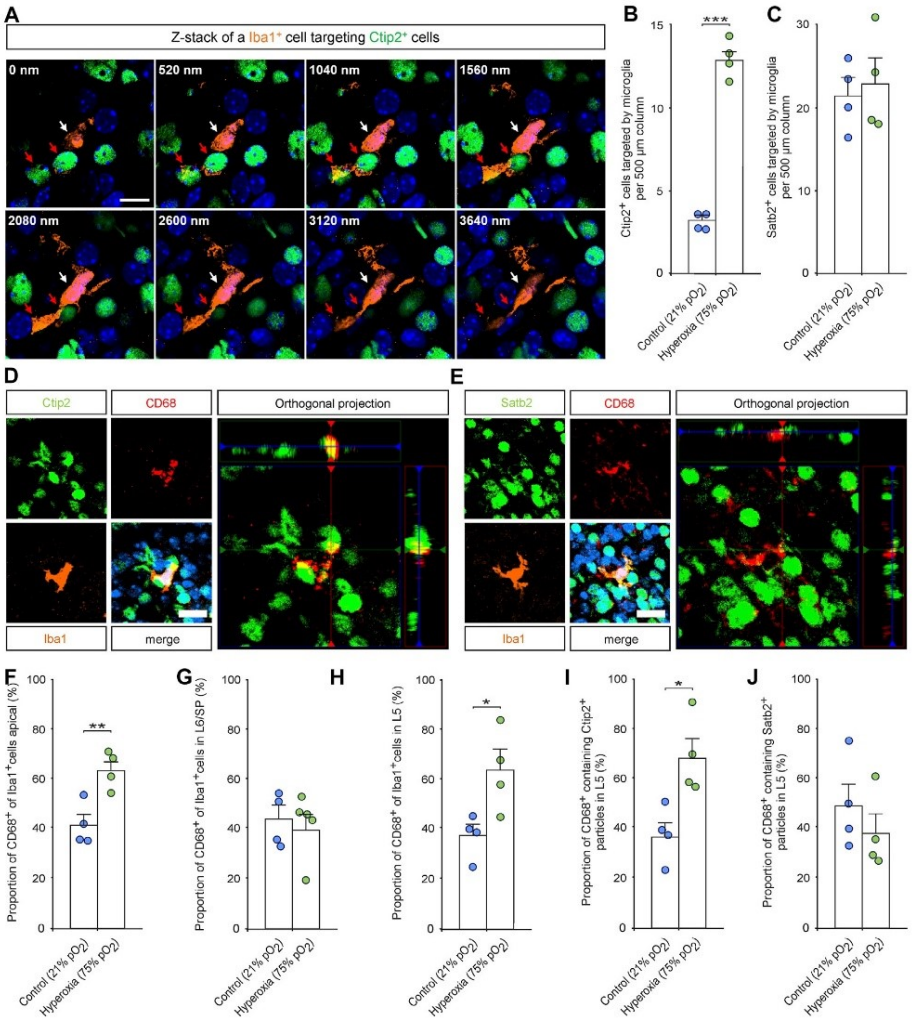

FIGURE 5 | The effects of hyperoxygenation on the layer-specific activation of microglia and their targeting and phagocytosis of neurons within the developing cortex. **(A)** Representative Z-stack images of an Iba1$^-$ microglia cell (white arrow) targeting Ctip2$^+$ cells (red arrows) in layer 5 of a P0.5 mouse cortex. Scale bars represent 10 µm. **(B,C)** Quantification of Ctip2$^+$ cells targeted by Iba1$^+$ microglia **(B)** and Satb2$^+$ cells targeted by Iba1$^+$ microglia **(C)** at P0.5. Data are means ± s.e.m. ($n = 4$). ***$p < 0.001$ from unpaired two-sided t-test (non-significant comparison is not marked for clarity). **(D,E)** Representative fluorescent images of triple staining with Iba1, CD68, and Ctip2 **(D)** or Satb2 **(E)** in the middle cortical sections along the rostro-caudal axis of hyperoxia-treated and control mice at P0.5. Orthogonal projections of CD68 and Ctip2/Satb2 show co-localization of the markers. Hoechst (blue) was used to stain cell nuclei. Scale bars represent 20 µm. **(F–H)** Quantification of CD68$^+$ microglia revealed an increase of active apical microglia **(F)** and L5 **(G)**, but not in L6/SP **(H)**. *$p < 0.05$, **$p < 0.01$, and ***$p < 0.001$ from unpaired two-sided t-test (non-significant comparisons are not marked for clarity; $n = 4$). **(I,J)** Quantification of CD68$^-$ microglia containing neuronal markers revealed an increase of microglia containing Ctip2 particles in hyperoxia-treated mice **(I)** while there is no difference regarding contained Satb2 particles **(J)**. *$p < 0.05$, **$p < 0.01$ from unpaired two-sided t-test (non-significant comparisons are not marked for clarity; $n = 4$).

after oxygen treatment and subsequent histological analyses of BrdU/EdU incorporation by cortical cells at P0.5 (see **Figure 6A** for experimental paradigm). Immunostaining of both markers showed that a large proportion of CP neurons were generated at E14.5 (BrdU$^+$), while cells generated at E17.5 (EdU$^+$) represent a much smaller part of the developing cortex (**Figures 6B,C**). Quantification of BrdU$^+$/EdU$^+$ cells in the CP revealed a significantly 1.4-fold increase in the number of BrdU$^+$ cells

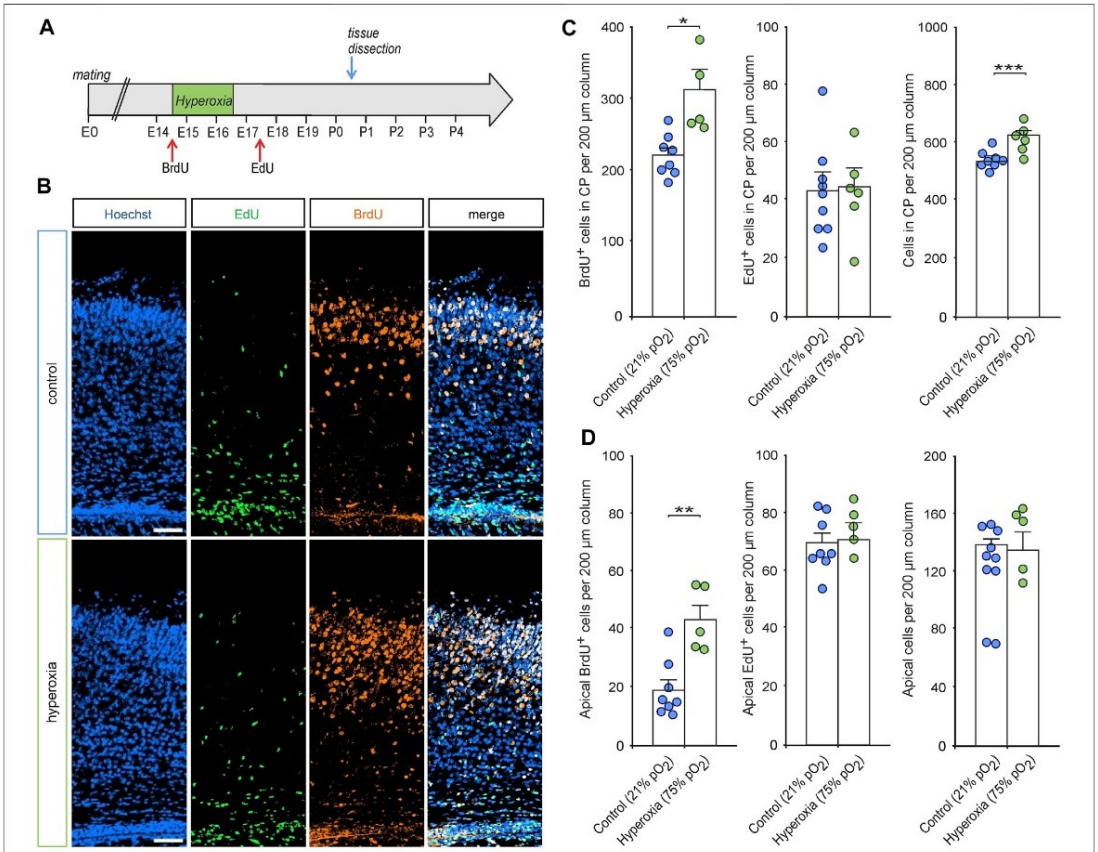

FIGURE 6 | The effects of hyperoxia on cell proliferation during and after oxygen treatment. **(A)** Experimental treatment scheme for BrdU/EdU application in fetal brain hyperoxygenation during mid-neurogenesis (E14.5 to E16.5). Mice received an intraperitoneal injection with BrdU immediately before oxygen treatment and with EdU 1 day after treatment (E17.5) and subsequently analyzed at P0.5. **(B)** Representative fluorescent images of EdU^- (green) and $BrdU^+$ cells (orange) from P0.5 in the middle cortical sections along the rostro-caudal axis of hyperoxia-treated and control mice. Hoechst (blue) was used to stain cell nuclei. Scale bars represent 50 µm. **(C,D)** Quantification of $BrdU^+$, EdU^+, and overall cells showed an increased number of CP neurons born during hyperoxia ($BrdU^+$ cells) but not after hyperoxia treatment (EdU^+ cells) within the CP **(C)** and the apical cortex **(D)** of P0.5 mouse pups. $^*p < 0.05$, $^{**}p < 0.01$, and $^{***}p < 0.001$ from unpaired two-sided *t*-test [non-significant comparisons are not marked for clarity; $n = 8$ (control) and $n = 5$ (hyperoxia)].

($p = 0.021$) in response to hyperoxia, but not of EdU^+ cells ($p = 0.886$, both from unpaired two-sided *t*-test), as a putative later feedback reaction. Thereby, the increased rate of $BrdU^+$ cells led to an increase of the overall cells in the CP. Notably, there were more $BrdU^+$ cells left at the apical side of the cortex ($p = 0.002$), but again, no change in EdU^+ cells ($p = 0.791$, both from unpaired two-sided *t*-test; **Figure 6D**).

We further analyzed $CC3^+$ apoptotic cells within the middle cortical sections along the rostro-caudal axis showing increased apoptosis in hyperoxic P0.5 mouse pups. Immunostaining with quantification showed that the overall number of $CC3^+$ cells in the hyperoxic group is increased by 2.6-fold with apoptosis predominantly occurring in the apical regions (**Figures 7A,B**). We then evaluated whether layer 5 cells of the cortex were apoptotic through double labelling of $CC3^+$ and $Ctip2^+$, but there was almost no cell possessing both markers (<0.1% of $Ctip2^+$ cells). Since apoptosis occurred mainly apical where increased proliferation could be detected in the hyperoxia group at E14.5, we analyzed the number of $BrdU^+/CC3^+$ and $EdU^+/CC3^+$ cells (**Figures 7C–E**). Quantification revealed that indeed apical $BrdU^+$ cells were more often apoptotic while EdU^+ cells were not. Since apical active microglia were detected more often in the hyperoxia group, we finally investigated whether there are changes in elimination of apoptotic cells by $Iba1^+/CD68^+$ active microglia. However, we have neither found any increase in the number of active microglia-targeting $CC3^+$ cells nor in the number of apoptotic cells that were engulfed by microglia in hyperoxic brain when compared to controls (**Figures 7F–H**).

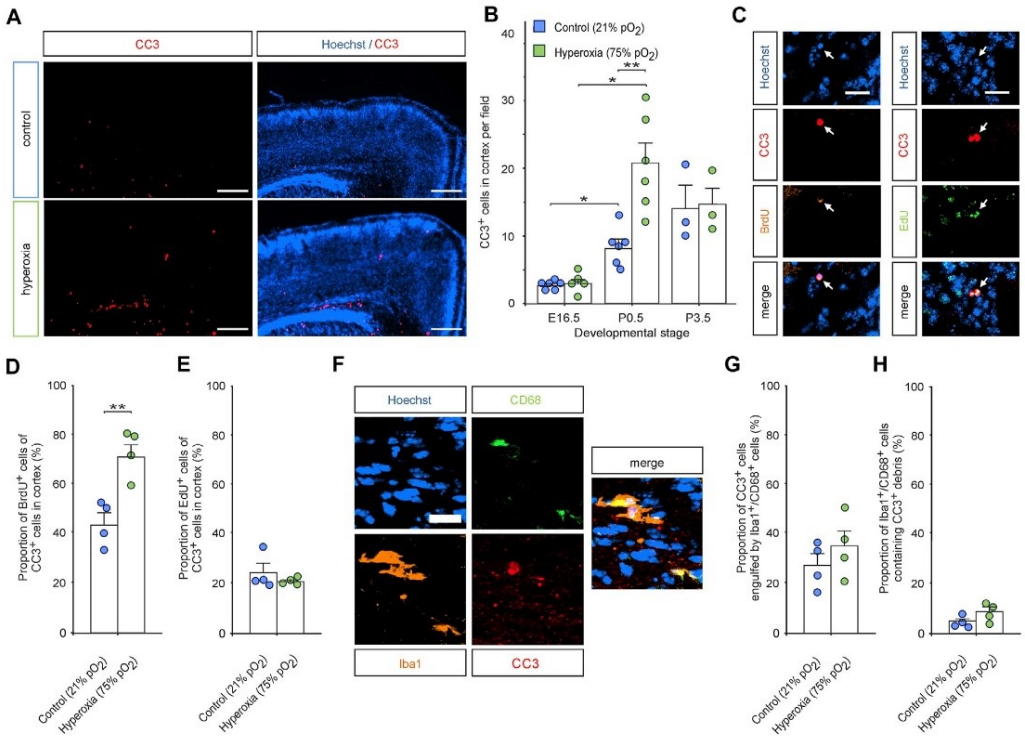

FIGURE 7 | The effects of hyperoxia on apoptosis in P0.5 mice cortex after mid-neurogenesis hyperoxygenation. **(A)** Representative fluorescent images of $CC3^+$ apoptotic cells (red) from P0.5 in the middle sections along the rostro-caudal axis of hyperoxia-treated and control mice. Hoechst (blue) was used to stain cell nuclei. Scale bars represent 200 µm. **(B)** Quantification of cortical $CC3^+$ cells shows increased apoptosis in brain slices of hyperoxia-treated mouse embryos at P0.5 but not at E16.5 or P3.5. Data are means ± s.e.m. [E16.5: $n = 6$ (control), $n = 5$ (hyperoxia); P0.5: $n = 6$; P3.5: $n = 3$]. $^*p < 0.05$ and $^{**}p < 0.01$ from robust ANOVA with *post-hoc* two-sided unpaired Wilcoxon test with Bonferroni correction. For full statistics, see **Supplementary Table S9**. **(C)** Representative fluorescent images of $BrdU^+$ (orange) and EdU^+ (green) cells double stained with CC3 in the middle cortical sections along the rostro-caudal axis of hyperoxia-treated and control mice at P0.5. Hoechst (blue) was used to stain cell nuclei. Scale bars represent 20 µm. **(D,E)** Quantification revealed that most of the apoptotic cells are $BrdU^+$ in the hyperoxia group, but not in controls **(D)**, and no differences were observed regarding apoptotic EdU^+ cells **(E)**. $^{**}p < 0.01$ from unpaired two-sided *t*-test (non-significant comparisons are not marked for clarity; $n = 4$). **(F)** Representative fluorescent image of $Iba1^+/CD68^+$ active microglia (orange/green) containing apoptotic cell debris ($CC3^+$, red) in the middle sections along the rostro-caudal axis of hyperoxia-treated mice at P0.5. Hoechst (blue) was used to stain cell nuclei. Scale bars represent 20 µm. **(G,H)** Quantification of neither the percentage of apoptotic cells engulfed by microglia **(G)** nor the number microglia engulfing apoptotic cells **(H)** revealed any differences between hyperoxia-treated vs control mice ($n = 4$).

Number of Excitatory Synapses Follows Normalization in L5

To provide first data on the effects on mid-neurogenesis hyperoxygenation on synaptic development, we analyzed the expression of the vesicular glutamate transporter 2 (vGluT2) as a common target for microglia pruning in later stages and a marker for the predominant form of excitatory synapses during early brain development (Nakamura et al., 2007; Schafer et al., 2012) (**Figure 8**). Double staining of vGluT2 and Ctip2 showed increased synaptic input into L5 in the hyperoxia animal group at P0.5: quantification in L5 showed that there were 1.7-fold more $vGluT2^+$ puncta in the hyperoxia group as compared with normoxic controls at P0.5 ($p = 0.006$), which did not persist until P3.5 (**Figure 8C**). Additionally, the number of $vGluT2^+$ puncta in L5 in the hyperoxia group at P0.5 temporary overshots that of controls at P0.5 and P3.5 ($p = 0.033$).

DISCUSSION

We present here that the short-term effects of hyperoxygenation during mid-neurogenesis of fetal mouse brain development (E14.5 to E16.5) with increased neuroprecursor cell proliferation within the SVZ/OSVZ (Wagenfuhr et al., 2015) translate into an accelerated cortical development but without

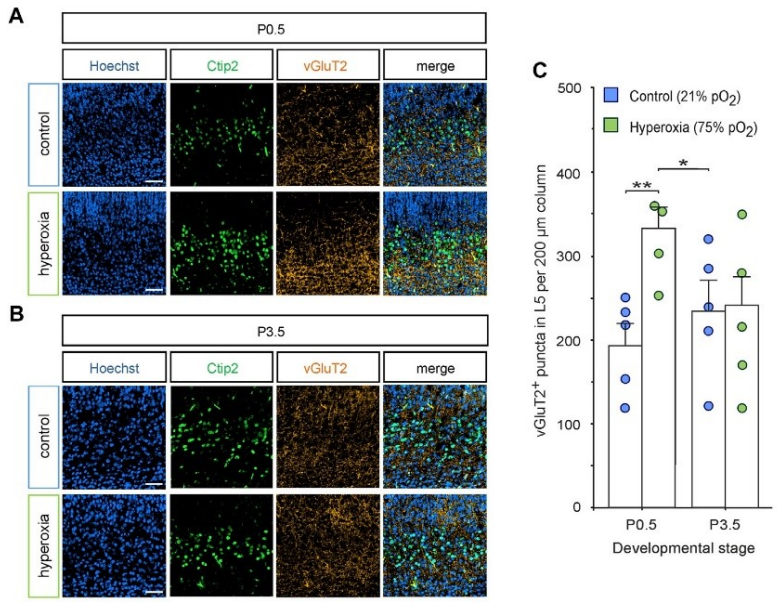

FIGURE 8 | Synaptic excitatory input into L5 is normalized together with L5 neurons. **(A,B)** Representative fluorescent images of vGluT2$^+$ synapses (orange) in L5 (Ctip2$^+$ cells, green) in the middle cortical sections along the rostro-caudal axis of hyperoxia-treated and control mice at P0.5 **(A)** and P3.5 **(B)**. Hoechst (blue) was used to stain cell nuclei. Scale bars represent 50 µm. **(C)** Quantification of vGluT2$^+$ puncta showed an increased number of puncta at P0.5, but not at P3.5. Data are means ± s.e.m. (n = 5 for all animal groups). *p < 0.05 and **p < 0.01 from two-way ANOVA with *post-hoc* two-sided t-test (non-significant comparisons are not marked for clarity). For full statistics, see **Supplementary Table S10**.

increase in cortical neurogenesis and cortical volume at early postnatal stage. Indeed, the CP is expanded through a specific overshoot amount of Ctip2$^+$/Tbr1$^-$ L5 neurons in later fetal development until birth in hyperoxic mouse cortex, which is normalized at early postnatal stage. This normalization is accompanied by an increase of microglial cells within L5 capable of targeting the respective neurons but no signs of L5 neuronal apoptosis.

We used our established model of maternal hyperoxygenation to investigate the effects of increased fetal brain oxygen tension during mid-neurogenesis (E14.5–E16.5) on later cortical development until the early postnatal state (Wagenfuhr et al., 2015; Wagenfuhr et al., 2016). Early chronic hyperoxygenation in this model causes severe reduction of neuroprecursor cell proliferation and the apical neuroprecursor cell pool (Markert et al., 2020). Contributing to this, Lange et al. (2016) reported that early hyperoxygenation from E10.5 to E13.5 is able to alter neuroprogenitor cell fate leading to a decrease of expanding neuroprogenitors. However, late or postnatal hyperoxygenation is known to cause brain damage accompanied by excessive loss of neurons (Gerstner et al., 2008; Yis et al., 2008; Tuzun et al., 2012), while short-term hyperoxygenation during mid-neurogenesis of fetal mouse brain development (E14.5 to E16.5) leads to an immediate expansion of a distinct proliferative cell population basal of the SVZ, which subsequently contributes to corticogenesis by heading for deeper cortical layers (Wagenfuhr et al., 2015). Finally, the amount of Ctip2$^+$ neurons in L5 projecting into various brain regions is markedly overshot after short-term maternal hyperoxygenation and at birth with a normalization until early postnatal stage (Hattox and Nelson 2007; Oswald et al., 2013; Wagenfuhr et al., 2015). Oxygen levels are known to directly regulate neuroprecursor cell maintenance, proliferation, and differentiation *in vitro* through the activation of several oxygen-sensitive signaling pathways (Chen et al., 2007; Pistollato et al., 2007; Giese et al., 2010; Mazumdar et al., 2010; Braunschweig et al., 2015; Mennen et al., 2020). Although the *in vitro* cell models are not directly comparable to our *in vivo* system, analyses of the fetal brain oxygen tension revealed that maternal hyperoxygenation of 75% leads to an increase of oxygen tension in the neurogenic niche of the VZ/SVZ from below 1.1% in maternal normoxic condition to oxygen levels above this threshold in hyperoxic animals, which is also supported by other colleagues (Wagenfuhr et al., 2015; Lange et al., 2016). Of note, there are no *in vivo* oxygen markers available for small laboratory animals to detect changes in oxygen levels in the range of 5%–20% to further define the tissue oxygen tension in the hyperoxic condition. However, maternal hyperoxia is unlikely to cause oxygen levels towards 20%, which is the commonly used oxygen tension in cell culture

experiments. Thus, the higher oxygen tension in hyperoxic brain tissue likely represents the *in vitro* condition of mild hyperoxia and provides a stimulating environment for maintenance and proliferation of neuroprecursor cells as demonstrated in cell culture (Chen et al., 2007; Chen et al., 2010; Santilli et al., 2010; Braunschweig et al., 2015; Qi et al., 2017) when compared to very low oxygen conditions.

The observed normalization of the brain morphology in the early postnatal stage indicates that the brain is able to compensate prenatally evoked morphological changes at least for an excess of cell population. Within the period of synaptogenesis during the first 30 postnatal days, neuronal programmed cell death or apoptosis is known to play a major role in shaping the neocortex with a peak around P5 in rodents in most studies (Southwell et al., 2012; Ahern et al., 2013; Blanquie et al., 2017). In the six-layered isocortex, the loss of neuronal density displays a layer-specific pattern and manifested itself mostly in L2–L4, whereas L1, L5, and L6 show fewer changes. We thus studied whether this physiological process is also mediating the normalization neuronal cell counts in L5 of hyperoxic mouse cortex in earlier postnatal stages by using CC3 staining (Fernandes-Alnemri et al., 1994; Nicholson et al., 1995; Wong et al., 2018). Surprisingly, almost none of L5 Ctip2$^+$ neurons showed CC3 marker expression, indicating that apoptosis is not involved in controlling the number of L5 neurons after mid-neurogenesis hyperoxygenation. The rare occurrence of apoptosis in L5 in the first days after birth is however in line with previous systematic studies of layer-specific postnatal apoptosis (Verney et al., 2000; Denaxa et al., 2018). However, we found an increase in the number of CC3$^+$ apoptotic cells in hyperoxic as compared to normoxic brain at P0.5, but their location was vastly limited to the apical proliferative zone outside the CP, and they were eliminated by active microglia. This phenomenon might be interpreted as an adaptive response of the physiological apical apoptosis at birth to the hyperoxia-induced increased proliferation of precursor cells at E14.5 and at the end of mid-neurogenesis phase at E16.5 (White and Barone 2001; Wagenfuhr et al., 2015). Putative feedback mechanisms regulating neuroprecursor cell proliferation such as activity-dependent negative feedback from developing neurons (Toma et al., 2014) might be involved in cortical re-shaping after mid-neurogenesis hyperoxygenation. We thus applied the thymidine analogue EdU at a time point when it is known that the brain enlarges (E17.5) and 1 day after the oxygen treatment and analyzed EdU uptake at birth (P0.5). Although hyperoxygenation provokes strong immediate effects on the number of CP neurons born at E14.5 as described earlier (Wagenfuhr et al., 2015), cells generated after the hyperoxygenation phase at E17.5 predominantly reside on the apical side of the developing cortex and do not yet contribute to CP morphology at birth. Moreover, there is no indication for an adaption regarding the number of neurons in the CP during the post-hyperoxygenation phase.

Microglia already physiologically colonize the developing brain at E10.5 where they regulate the number of precursor cells through phagocytosis (Cunningham et al., 2013; Arnò et al., 2014; Tronnes et al., 2016). Until E16.5, microglia exclusively reside within the proliferating zones while they start to invade into the CP as late as during the early postnatal stage (Squarzoni et al., 2014). The majority of microglia in the developing cerebral cortex have an activated morphology and express markers associated with activation, and functional studies revealed that microglia regulate neuroprecursor cell number in the developing cortex by phagocytosis (Cunningham et al., 2013). Interestingly, most precursor cells targeted by Iba1$^+$ microglia in the cortical proliferative zones did not show signs of cell death or apoptosis (Fricker et al., 2012; Cunningham et al., 2013). Our data suggest a very similar mechanism during the re-shaping of the cortical layers after mid-neurogenesis hyperoxygenation: increased numbers of Iba1$^+$ microglia, which also express CD68 as a marker for active microglia (Rabinowitz and Gordon 1991; Jurga et al., 2020), target and incorporate Ctip2$^+$ L5 neurons with no apoptotic signs at the critical stage P0.5. However, the number of targeted Satb2$^+$ cells or incorporated Satb2$^+$ particles at the same time remains unaffected, suggesting a specific effect on Ctip2$^+$ L5 neurons. Nevertheless, our study is limited to immunohistochemical staining and cannot exclude other effects such as a critical change in microglial support for surviving of L5 cells (Ueno et al., 2013). In addition, the study is limited to a rather small sample size. Non-significant trends like the increased number of microglia in SP/L6 at E16.5 could potentially be relevant. Since there are no changes in microglial activity or absolute L6-specific Tbr1$^+$ neurons, this may reflect an accelerated invasion of the cortical plate where microglia migrate from apical through SP and L6 to L5 (Swinnen et al., 2013). Consequently, future functional studies with activation and depletion of microglia during late prenatal and early postnatal cortical development are warranted to investigate the exact microglia–L5 neuron interactions in cortical re-shaping after critical insults during mid-neurogenesis such as hyperoxygenation. These data in conjunction with no indications for changes in cell migration [data on cortical layering herein and Wagenfuhr et al., (2015)] or compensatory reduction or shift of precursor proliferation strongly suggest different mechanisms to normalize the overshoot amount of neuroprecursor cells depending on the brain region with CC3-mediated apoptosis as one major mechanism within the apical proliferative zone (VZ/SVZ) and microglia playing a key role in cortical L5.

To first shed light on alterations of early synaptic connectivity within the developing cortex by mid-neurogenesis hyperoxygenation, we further analyzed the expression of vGluT2 as a common marker for the predominant form of excitatory synapses during early brain development (Nakamura et al., 2007). We detected a temporary overshoot of glutamatergic synaptic input into L5 in the hyperoxia animal group at P0.5 with normalization until P3.5 in fairly accurate parallelism to the changes in cortical L5 neurogenesis. Although the underlying mechanisms of this normalization need to be determined by functional studies as outlined above, it might also be mediated through activated microglia, because microglia

have been reported to have a pivotal role in remodeling of developing synapses in the early postnatal brain (Schafer et al., 2012). To determine whether the morphological changes in response to hyperoxygenation during mid-neurogenesis translate into behavioral disruption, early postnatal behavioral testing of the pups using righting reflex test, gait analysis, and negative geotaxis test (Lubics et al., 2005; Fan et al., 2008) is urgently required in future studies. Our observations might then be of interest for investigating layer 5-specific neurodevelopmental disorders (Kolomeets and Uranova 2019; Mi et al., 2019) and their potential therapeutic/prophylactic interventions.

Together, the present data demonstrate that fetal brain hyperoxygenation during mid-neurogenesis from embryonic stage E14.5 to E16.5 accelerates cortical development in the fetal mouse brain. The cortical CP is expanded through a specific overshoot amount of L5 neurons at E16.5 and at birth in hyperoxic mouse cortex, which is subsequently normalized at early postnatal stage. This normalization is accompanied by an increase of microglial cells within L5 capable of targeting and incorporating the respective neurons with no signs of L5 neuronal apoptosis. Indeed, our data strongly suggest different mechanisms to the overshoot number of neuroprogenitor cells depending on the brain region with CC3-mediated apoptosis as the mechanism within the apical proliferative zone and microglial targeting in cortical L5. However, future functional studies on microglia using ablation and/or stimulation of microglia are warranted to finally confirm that an increased microgliosis in L5 is responsible or at least contribute to postnatal adaption to prenatal hyperoxia effects on corticogenesis.

DATA AVAILABILITY STATEMENT

The raw data supporting the conclusion of this article will be made available by the authors, without undue reservation.

ETHICS STATEMENT

The animal study was reviewed and approved by Landesamt für Landwirtschaft, Lebensmittelsicherheit und Fischerei Mecklenburg-Vorpommern, reference number 7221.3-1-043/16, and complies with the Tierschutzgesetz and Verordnung zur Umsetzung der Richtlinie 2010/63/EU from Germany.

AUTHOR CONTRIBUTIONS

AS created, designed, and supervised the project; analyzed the data; and wrote the manuscript. FM designed the project, performed the experiments; and wrote the manuscript. All authors contributed to the article and approved the submitted version.

FUNDING

This work was supported by regular funds of the University Medical Centre Rostock.

ACKNOWLEDGMENTS

We thank the team of the core facility Zentrale Versuchstierhaltung at the University of Rostock for providing the timed-pregnant mice and Uta Naumann her technical assistance. We also like to thank the Department of Neurology at the Technische Universität Dresden for lending us the oxygen chamber.

SUPPLEMENTARY MATERIAL

The Supplementary Material for this article can be found online at: https://www.frontiersin.org/articles/10.3389/fcell.2022.732682/full#supplementary-material

REFERENCES

Agirman, G., Broix, L., and Nguyen, L. (2017). Cerebral Cortex Development: an Outside-in Perspective. *FEBS Lett.* 591, 3978–3992. doi:10.1002/1873-3468.12924

Ahern, T. H., Krug, S., Carr, A. V., Murray, E. K., Fitzpatrick, E., Bengston, L., et al. (2013). Cell Death Atlas of the Postnatal Mouse Ventral Forebrain and Hypothalamus: Effects of Age and Sex. *J. Comp. Neurol.* 521, 2551–2569. doi:10.1002/cne.23298

Allen-Institute (2008). Developing Mouse Brain Atlas. Available at: https://developingmouse.brain-map.org/.

Arlotta, P., Molyneaux, B. J., Chen, J., Inoue, J., Kominami, R., and Macklis, J. D. (2005). Neuronal Subtype-specific Genes that Control Corticospinal Motor Neuron Development *In Vivo*. *Neuron* 45, 207–221. doi:10.1016/j.neuron.2004.12.036

Arnò, B., Grassivaro, F., Rossi, C., Bergamaschi, A., Castiglioni, V., Furlan, R., et al. (2014). Neural Progenitor Cells Orchestrate Microglia Migration and Positioning into the Developing Cortex. *Nat. Commun.* 5, 5611. doi:10.1038/ncomms6611

Blanquie, O., Yang, J.-W., Kilb, W., Sharopov, S., Sinning, A., and Luhmann, H. J. (2017). Electrical Activity Controls Area-specific Expression of Neuronal Apoptosis in the Mouse Developing Cerebral Cortex. *eLife* 6, e27696. doi:10.7554/eLife.27696

Blaschke, A. J., Staley, K., and Chun, J. (1996). Widespread Programmed Cell Death in Proliferative and Postmitotic Regions of the Fetal Cerebral Cortex. *Development* 122, 1165–1174. doi:10.1242/dev.122.4.1165

Braunschweig, L., Meyer, A. K., Wagenführ, L., and Storch, A. (2015). Oxygen Regulates Proliferation of Neural Stem Cells through Wnt/β-Catenin Signalling. *Mol. Cell Neurosci.* 67, 84–92. doi:10.1016/j.mcn.2015.06.006

Britanova, O., de Juan Romero, C., Cheung, A., Kwan, K. Y., Schwark, M., Gyorgy, A., et al. (2008). Satb2 Is a Postmitotic Determinant for Upper-Layer Neuron Specification in the Neocortex. *Neuron* 57, 378–392. doi:10.1016/j.neuron.2007.12.028

Chen, H.-L., Pistollato, F., Hoeppner, D. J., Ni, H.-T., McKay, R. D. G., and Panchision, D. M. (2007). Oxygen Tension Regulates Survival and Fate of Mouse central Nervous System Precursors at Multiple Levels. *Stem Cells* 25, 2291–2301. doi:10.1634/stemcells.2006-0609

Chen, X., Tian, Y., Yao, L., Zhang, J., and Liu, Y. (2010). Hypoxia Stimulates Proliferation of Rat Neural Stem Cells with Influence on the Expression of Cyclin D1 and C-Jun N-Terminal Protein Kinase Signaling Pathway *In Vitro*. *Neuroscience* 165, 705–714. doi:10.1016/j.neuroscience.2009.11.007

Chew, L.-J., Fusar-Poli, P., and Schmitz, T. (2013). Oligodendroglial Alterations and the Role of Microglia in white Matter Injury: Relevance to Schizophrenia. *Dev. Neurosci.* 35, 102–129. doi:10.1159/000346157

Cunningham, C. L., Martínez-Cerdeño, V., and Noctor, S. C. (2013). Microglia Regulate the Number of Neural Precursor Cells in the Developing Cerebral Cortex. *J. Neurosci.* 33, 4216–4233. doi:10.1523/jneurosci.3441-12.2013

Dekkers, M. P. J., Nikoletopoulou, V., and Barde, Y.-A. (2013). Death of Developing Neurons: New Insights and Implications for Connectivity. *J. Cel Biol* 203, 385–393. doi:10.1083/jcb.201306136

Denaxa, M., Neves, G., Rabinowitz, A., Kemlo, S., Liodis, P., Burrone, J., et al. (2018). Modulation of Apoptosis Controls Inhibitory Interneuron Number in the Cortex. *Cel Rep.* 22, 1710–1721. doi:10.1016/j.celrep.2018.01.064

Edwards, L. A., Lara, D. A., Sanz Cortes, M., Hunter, J. V., Andreas, S., Nguyen, M. J., et al. (2018). Chronic Maternal Hyperoxygenation and Effect on Cerebral and Placental Vasoregulation and Neurodevelopment in Fetuses with Left Heart Hypoplasia. *Fetal Diagn. Ther.* 46, 45–57. doi:10.1159/000489123

Englund, C., Fink, A., Lau, C., Pham, D., Daza, R. A., Bulfone, A., et al. (2005). Pax6, Tbr2, and Tbr1 Are Expressed Sequentially by Radial Glia, Intermediate Progenitor Cells, and Postmitotic Neurons in Developing Neocortex. *J. Neurosci.* 25, 247–251. doi:10.1523/jneurosci.2899-04.2005

Fagel, D. M., Ganat, Y., Silbereis, J., Ebbitt, T., Stewart, W., Zhang, H., et al. (2006). Cortical Neurogenesis Enhanced by Chronic Perinatal Hypoxia. *Exp. Neurol.* 199, 77–91. doi:10.1016/j.expneurol.2005.04.006

Fan, L.-W., Chen, R.-F., Mitchell, H. J., Lin, R. C. S., Simpson, K. L., Rhodes, P. G., et al. (2008). α-Phenyl-n-tert-butyl-nitrone Attenuates Lipopolysaccharide-Induced Brain Injury and Improves Neurological Reflexes and Early Sensorimotor Behavioral Performance in Juvenile Rats. *J. Neurosci. Res.* 86, 3536–3547. doi:10.1002/jnr.21812

Fernandes-Alnemri, T., Litwack, G., and Alnemri, E. S. (1994). CPP32, a Novel Human Apoptotic Protein with Homology to *Caenorhabditis elegans* Cell Death Protein Ced-3 and Mammalian Interleukin-1 Beta-Converting Enzyme. *J. Biol. Chem.* 269, 30761–30764. doi:10.1016/s0021-9258(18)47344-9

Fricker, M., Neher, J. J., Zhao, J.-W., Thery, C., Tolkovsky, A. M., and Brown, G. C. (2012). MFG-E8 Mediates Primary Phagocytosis of Viable Neurons during Neuroinflammation. *J. Neurosci.* 32, 2657–2666. doi:10.1523/jneurosci.4837-11.2012

Gerstner, B., DeSilva, T. M., Genz, K., Armstrong, A., Brehmer, F., Neve, R. L., et al. (2008). Hyperoxia Causes Maturation-dependent Cell Death in the Developing white Matter. *J. Neurosci.* 28, 1236–1245. doi:10.1523/jneurosci.3213-07.2008

Giese, A.-K., Frahm, J., Hübner, R., Luo, J., Wree, A., Frech, M. J., et al. (2010). Erythropoietin and the Effect of Oxygen during Proliferation and Differentiation of Human Neural Progenitor Cells. *BMC Cel Biol* 11, 94. doi:10.1186/1471-2121-11-94

Górny, M., Bilska-Wilkosz, A., Iciek, M., Hereta, M., Kamińska, K., Kamińska, A., et al. (2020). Alterations in the Antioxidant Enzyme Activities in the Neurodevelopmental Rat Model of Schizophrenia Induced by Glutathione Deficiency during Early Postnatal Life. *Antioxidants* 9, 538. doi:10.3390/antiox9060538

Hattox, A. M., and Nelson, S. B. (2007). Layer V Neurons in Mouse Cortex Projecting to Different Targets Have Distinct Physiological Properties. *J. Neurophysiol.* 98, 3330–3340. doi:10.1152/jn.00397.2007

Haubensak, W., Attardo, A., Denk, W., and Huttner, W. B. (2004). From the Cover: Neurons Arise in the Basal Neuroepithelium of the Early Mammalian Telencephalon: A Major Site of Neurogenesis. *Proc. Natl. Acad. Sci.* 101, 3196–3201. doi:10.1073/pnas.0308600100

Hevner, R. F., Shi, L., Justice, N., Hsueh, Y.-P., Sheng, M., Smiga, S., et al. (2001). Tbr1 Regulates Differentiation of the Preplate and Layer 6. *Neuron* 29, 353–366. doi:10.1016/s0896-6273(01)00211-2

Imai, Y., Ibata, I., Ito, D., Ohsawa, K., and Kohsaka, S. (1996). A Novel Geneiba1in the Major Histocompatibility Complex Class III Region Encoding an EF Hand Protein Expressed in a Monocytic Lineage. *Biochem. Biophys. Res. Commun.* 224, 855–862. doi:10.1006/bbrc.1996.1112

Jurga, A. M., Paleczna, M., and Kuter, K. Z. (2020). Overview of General and Discriminating Markers of Differential Microglia Phenotypes. *Front. Cel. Neurosci.* 14, 198. doi:10.3389/fncel.2020.00198

Kolomeets, N. S., and Uranova, N. A. (2019). Reduced Oligodendrocyte Density in Layer 5 of the Prefrontal Cortex in Schizophrenia. *Eur. Arch. Psychiatry Clin. Neurosci.* 269, 379–386. doi:10.1007/s00406-018-0888-0

Lange, C., Turrero Garcia, M., Decimo, I., Bifari, F., Eelen, G., Quaegebeur, A., et al. (2016). Relief of Hypoxia by Angiogenesis Promotes Neural Stem Cell Differentiation by Targeting Glycolysis. *Embo J.* 35, 924–941. doi:10.15252/embj.201592372

Lubics, A., Reglődi, D., Tamás, A., Kiss, P., Szalai, M., Szalontay, L., et al. (2005). Neurological Reflexes and Early Motor Behavior in Rats Subjected to Neonatal Hypoxic-Ischemic Injury. *Behav. Brain Res.* 157, 157–165. doi:10.1016/j.bbr.2004.06.019

Markert, F., Müller, I., Badstübner-Meeske, K., and Storch, A. (2020). Early Chronic Intermittent Maternal Hyperoxygenation Impairs Cortical Development by Inhibition of Pax6-Positive Apical Progenitor Cell Proliferation. *J. Neuropath Exp. Neurol.* 79, 1223–1232. doi:10.1093/jnen/nlaa072

Mazumdar, J., O'Brien, W. T., Johnson, R. S., LaManna, J. C., Chavez, J. C., Klein, P. S., et al. (2010). O2 Regulates Stem Cells through Wnt/β-Catenin Signalling. *Nat. Cel Biol* 12, 1007–1013. doi:10.1038/ncb2102

McKenna, W. L., Betancourt, J., Larkin, K. A., Abrams, B., Guo, C., Rubenstein, J. L. R., et al. (2011). Tbr1 and Fezf2 Regulate Alternate Corticofugal Neuronal Identities during Neocortical Development. *J. Neurosci.* 31, 549–564. doi:10.1523/jneurosci.4131-10.2011

Mennen, R. H., de Leeuw, V. C., and Piersma, A. H. (2020). Oxygen Tension Influences Embryonic Stem Cell Maintenance and Has Lineage Specific Effects on Neural and Cardiac Differentiation. *Differentiation* 115, 1–10. doi:10.1016/j.diff.2020.07.001

Mi, Z., Yang, J., He, Q., Zhang, X., Xiao, Y., and Shu, Y. (2019). Alterations of Electrophysiological Properties and Ion Channel Expression in Prefrontal Cortex of a Mouse Model of Schizophrenia. *Front. Cel. Neurosci.* 13, 54. doi:10.3389/fncel.2019.00554

Morgan, J. T., Chana, G., Pardo, C. A., Achim, C., Semendeferi, K., Buckwalter, J., et al. (2010). Microglial Activation and Increased Microglial Density Observed in the Dorsolateral Prefrontal Cortex in Autism. *Biol. Psychiatry* 68, 368–376. doi:10.1016/j.biopsych.2010.05.024

Nakamura, K., Watakabe, A., Hioki, H., Fujiyama, F., Tanaka, Y., Yamamori, T., et al. (2007). Transiently Increased Colocalization of Vesicular Glutamate Transporters 1 and 2 at Single Axon Terminals during Postnatal Development of Mouse Neocortex: a Quantitative Analysis with Correlation Coefficient. *Eur. J. Neurosci.* 26, 3054–3067. doi:10.1111/j.1460-9568.2007.05868.x

Nicholson, D. W., Ali, A., Thornberry, N. A., Vaillancourt, J. P., Ding, C. K., Gallant, M., et al. (1995). Identification and Inhibition of the ICE/CED-3 Protease Necessary for Mammalian Apoptosis. *Nature* 376, 37–43. doi:10.1038/376037a0

Noctor, S. C., Flint, A. C., Weissman, T. A., Dammerman, R. S., and Kriegstein, A. R. (2001). Neurons Derived from Radial Glial Cells Establish Radial Units in Neocortex. *Nature* 409, 714–720. doi:10.1038/35055553

Noctor, S. C., Martínez-Cerdeño, V., Ivic, L., and Kriegstein, A. R. (2004). Cortical Neurons Arise in Symmetric and Asymmetric Division Zones and Migrate through Specific Phases. *Nat. Neurosci.* 7, 136–144. doi:10.1038/nn1172

Oswald, M. J., Tantirigama, M. L. S., Sonntag, I., Hughes, S. M., and Empson, R. M. (2013). Diversity of Layer 5 Projection Neurons in the Mouse Motor Cortex. *Front. Cel. Neurosci.* 7, 174. doi:10.3389/fncel.2013.00174

Pistollato, F., Chen, H. L., Schwartz, P. H., Basso, G., and Panchision, D. M. (2007). Oxygen Tension Controls the Expansion of Human CNS Precursors and the Generation of Astrocytes and Oligodendrocytes. *Mol. Cel Neurosci* 35, 424–435. doi:10.1016/j.mcn.2007.04.003

Porzionato, A., Macchi, V., Zaramella, P., Sarasin, G., Grisafi, D., Dedja, A., et al. (2015). Effects of Postnatal Hyperoxia Exposure on the Rat Dentate Gyrus and Subventricular Zone. *Brain Struct. Funct.* 220, 229–247. doi:10.1007/s00429-013-0650-3

Qi, C., Zhang, J., Chen, X., Wan, J., Wang, J., Zhang, P., et al. (2017). Hypoxia Stimulates Neural Stem Cell Proliferation by Increasing HIF"1Ĩ± Expression and Activating Wnt/Ĩ²-Catenin Signaling. *Cel Mol Biol (Noisy-le-grand)* 63, 12–19. doi:10.14715/cmb/2017.63.7.2

Rabinowitz, S. S., and Gordon, S. (1991). Macrosialin, a Macrophage-Restricted Membrane Sialoprotein Differentially Glycosylated in Response to Inflammatory Stimuli. *J. Exp. Med.* 174, 827–836. doi:10.1084/jem.174.4.827

Rudolph, A. M. (2020). Maternal Hyperoxygenation for the Human Fetus: Should Studies Be Curtailed? *Pediatr. Res.* 87, 630–633. doi:10.1038/s41390-019-0604-4

Santilli, G., Lamorte, G., Carlessi, L., Ferrari, D., Rota Nodari, L., Binda, E., et al. (2010). Mild Hypoxia Enhances Proliferation and Multipotency of Human Neural Stem Cells. *PloS one* 5, e8575. doi:10.1371/journal.pone.0008575

Schafer, D. P., Lehrman, E. K., Kautzman, A. G., Koyama, R., Mardinly, A. R., Yamasaki, R., et al. (2012). Microglia Sculpt Postnatal Neural Circuits in an Activity and Complement-dependent Manner. *Neuron* 74, 691–705. doi:10.1016/j.neuron.2012.03.026

Schneider, C., Krischke, G., Rascher, W., Gassmann, M., and Trollmann, R. (2012). Systemic Hypoxia Differentially Affects Neurogenesis during Early Mouse Brain Maturation. *Brain Dev.* 34, 261–273. doi:10.1016/j.braindev.2011.07.006

Southwell, D. G., Paredes, M. F., Galvao, R. P., Jones, D. L., Froemke, R. C., Sebe, J. Y., et al. (2012). Intrinsically Determined Cell Death of Developing Cortical Interneurons. *Nature* 491, 109–113. doi:10.1038/nature11523

Squarzoni, P., Oller, G., Hoeffel, G., Pont-Lezica, L., Rostaing, P., Low, D., et al. (2014). Microglia Modulate Wiring of the Embryonic Forebrain. *Cel Rep.* 8, 1271–1279. doi:10.1016/j.celrep.2014.07.042

Swinnen, N., Smolders, S., Avila, A., Notelaers, K., Paesen, R., Ameloot, M., et al. (2013). Complex Invasion Pattern of the Cerebral Cortex Bymicroglial Cells during Development of the Mouse Embryo. *Glia* 61, 150–163. doi:10.1002/glia.22421

Talamillo, A., Quinn, J. C., Collinson, J. M., Caric, D., Price, D. J., West, J. D., et al. (2003). Pax6 Regulates Regional Development and Neuronal Migration in the Cerebral Cortex. *Develop. Biol.* 255, 151–163. doi:10.1016/s0012-1606(02)00046-5

Toma, K., Kumamoto, T., and Hanashima, C. (2014). The Timing of Upper-Layer Neurogenesis Is Conferred by Sequential Derepression and Negative Feedback from Deep-Layer Neurons. *J. Neurosci.* 34, 13259–13276. doi:10.1523/JNEUROSCI.2334-14.2014

Tronnes, A. A., Koschnitzky, J., Daza, R., Hitti, J., Ramirez, J. M., and Hevner, R. (2016). Effects of Lipopolysaccharide and Progesterone Exposures on Embryonic Cerebral Cortex Development in Mice. *Reprod. Sci.* 23, 771–778. doi:10.1177/1933719115618273

Tuzun, F., Kumral, A., Ozbal, S., Dilek, M., Tugyan, K., Duman, N., et al. (2012). Maternal Prenatal omega-3 Fatty Acid Supplementation Attenuates Hyperoxia-induced Apoptosis in the Developing Rat Brain. *Int. J. Dev. Neurosci.* 30, 315–323. doi:10.1016/j.ijdevneu.2012.01.007

Ueno, M., Fujita, Y., Tanaka, T., Nakamura, Y., Kikuta, J., Ishii, M., et al. (2013). Layer V Cortical Neurons Require Microglial Support for Survival during Postnatal Development. *Nat. Neurosci.* 16, 543–551. doi:10.1038/nn.3358

Verney, C., Takahashi, T., Bhide, P. G., Nowakowski, R. S., and Caviness, V. S., Jr. (2000). Independent Controls for Neocortical Neuron Production and Histogenetic Cell Death. *Dev. Neurosci.* 22, 125–138. doi:10.1159/000017434

Wagenführ, L., Meyer, A. K., Braunschweig, L., Marrone, L., and Storch, A. (2015). Brain Oxygen Tension Controls the Expansion of Outer Subventricular Zone-like Basal Progenitors in the Developing Mouse Brain. *Development* 142, 2904–2915. doi:10.1242/dev.121939

Wagenführ, L., Meyer, A. K., Marrone, L., and Storch, A. (2016). Oxygen Tension within the Neurogenic Niche Regulates Dopaminergic Neurogenesis in the Developing Midbrain. *Stem Cell Dev.* 25, 227–238. doi:10.1089/scd.2015.0214

White, L. D., and Barone, S. (2001). Qualitative and Quantitative Estimates of Apoptosis from Birth to Senescence in the Rat Brain. *Cell Death Differ* 8, 345–356. doi:10.1038/sj.cdd.4400816

Wong, F. K., Bercsenyi, K., Sreenivasan, V., Portalés, A., Fernández-Otero, M., and Marín, O. (2018). Pyramidal Cell Regulation of Interneuron Survival Sculpts Cortical Networks. *Nature* 557, 668–673. doi:10.1038/s41586-018-0139-6

Wong, F. K., and Marín, O. (2019). Developmental Cell Death in the Cerebral Cortex. *Annu. Rev. Cel Dev. Biol.* 35, 523–542. doi:10.1146/annurev-cellbio-100818-125204

Yis, U., Kurul, S. H., Kumral, A., Cilaker, S., Tugyan, K., Genc, S., et al. (2008). Hyperoxic Exposure Leads to Cell Death in the Developing Brain. *Brain Dev.* 30, 556–562. doi:10.1016/j.braindev.2008.01.010

Conflict of Interest: The authors declare that the research was conducted in the absence of any commercial or financial relationships that could be construed as a potential conflict of interest.

Publisher's Note: All claims expressed in this article are solely those of the authors and do not necessarily represent those of their affiliated organizations, or those of the publisher, the editors and the reviewers. Any product that may be evaluated in this article, or claim that may be made by its manufacturer, is not guaranteed or endorsed by the publisher.

frontiers

Hyperoxygenation during mid-neurogenesis accelerates cortical development in the fetal mouse brain

Franz Markert and Alexander Storch

Supplementary Figures:

- **Supplementary Figure S1.** Example for the determination of the volume of the cortical plate.
- **Supplementary Figure S2.** Effects of maternal hyperoxygenation on the absolute number of layer specific neurons.
- **Supplementary Figure S3.** Effects of maternal hyperoxygenation on the distribution of microglia in a P16.5 and P3.5 mouse cortex.
- **Supplementary Figure S4.** Effects of hyperoxygenation on the total number of microglia within the developing cortex.
- **Supplementary Figure S5.** $Iba1^+$ cells are able to target $Satb2^+$ cells.

Supplementary Tables:

- **Supplementary Table S1.** Statistics determined for $NeuN^+$ cortical neurons.
- **Supplementary Table S2.** Statistics determined for $Tbr1^+$ cortical neurons.
- **Supplementary Table S3.** Statistics determined for $Ctip^+/Tbr1^-$ neurons.
- **Supplementary Table S4.** Statistics determined for $Satb2^+$ cortical neurons.
- **Supplementary Table S5.** Statistics determined for apical $Iba1^+$ cells.
- **Supplementary Table S6.** Statistics determined for subplate/layer 6 (SP/L6) $Iba1^+$ cells.
- **Supplementary Table S7.** Statistics determined for layer 5 (L5) $Iba1^+$ cells
- **Supplementary Table S8.** Statistics determined for layer 4-1 (L4-1) $Iba1^+$ cells.
- **Supplementary Table S9.** Statistics determined for absolute $CC3^+$ cell counts.
- **Supplementary Table S10.** Statistics determined for $vGluT2^+$ synapses in L5.
- **Supplementary Table S11.** Statistics determined for absolute $Tbr1^+$ neuron counts.
- **Supplementary Table S12.** Statistics determined for absolute $Ctip^+/Tbr1^-$ neuron counts.
- **Supplementary Table S13.** Statistics determined for absolute $Satb2^+$ neuron counts.
- **Supplementary Table S14.** Statistics determined for total $Iba1^+$ cell counts.

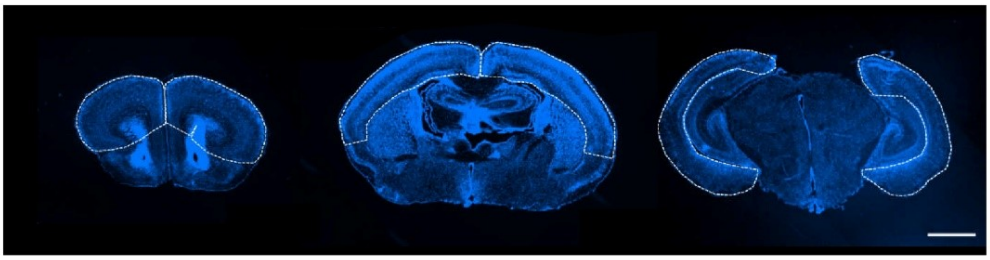

Supplementary Figure S1. Example for the determination of the volume of the cortical plate (CP). Every 6th Hoechst stained slice of a mouse brain was outlined as shown in the figure (left to right: rostral, middle and caudal section) and used to calculate the volume. Scale bar, 1000 µm.

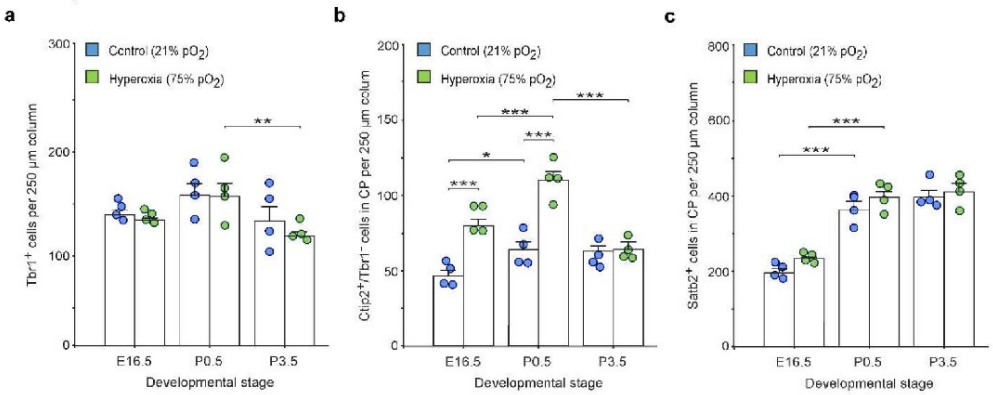

Supplementary Figure S2. Effects of maternal hyperoxygenation on the absolute number of layer specific neurons. Quantification of absolute Tbr1$^+$, Ctip2$^+$/Tbr1$^-$ and Satb2$^+$ cells within 250 µm wide cortical columns of E16.5, P0.5 and P3.5 mice. Data are means±s.e.m. (n = 4). * p<0.05, ** p<0.01, *** p<0.001 from two-way ANOVA with *post-hoc* two-sided t-test with Bonferroni correction. For full statistics, see **Supplementary Tables S11-S13**.

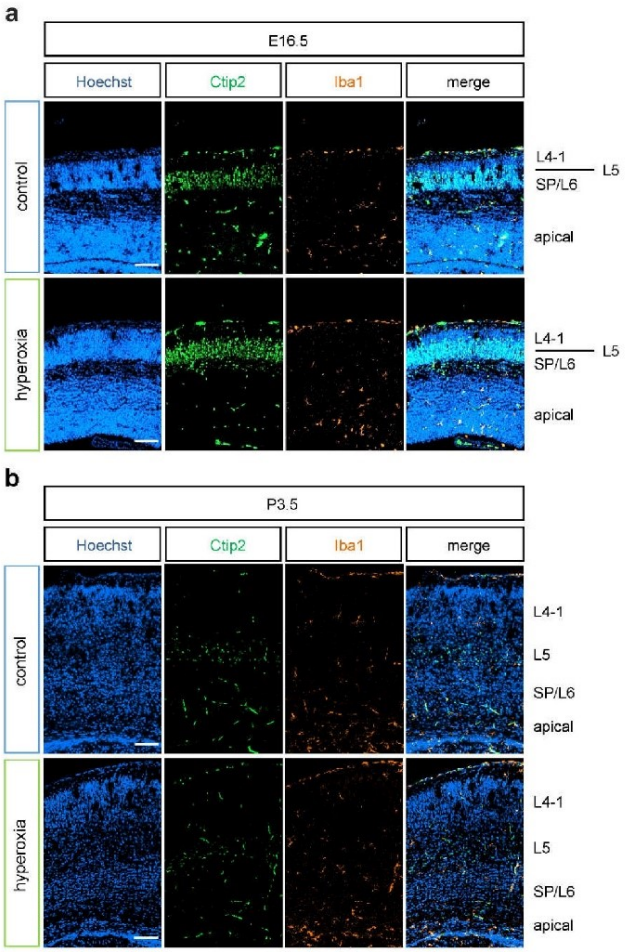

Supplementary Figure S3: Effects of fetal brain hyperoxygenation on the distribution of microglia in E16.5 and P3.5 mouse cortex. Representative fluorescent images of $Iba1^+$ cells (orange) from (**a**) E16.5 and (**b**) P3.5 in the middle cortical sections along the rostro-caudal axis–of hyperoxia treated and control mice showed no differences. $Ctip2^+$ (green) was used for layer determination and Hoechst (blue) was used to stain cell nuclei. Scale bars represent 100 µm.

[3]

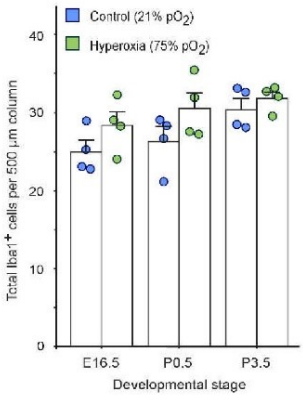

Supplementary Figure S4. Effects of hyperoxygenation on the total number of microglia within the developing cortex. Quantification of the total number of Iba1$^+$ microglia showed no differences with respect to hyperoxia treatment. Data are means±s.e.m. (n = 4). * p<0.05, ** p<0.01, *** p<0.001 from two-way ANOVA with *post-hoc* two-sided t-test with Bonferroni correction. For full statistics, see **Supplementary Table S14.**

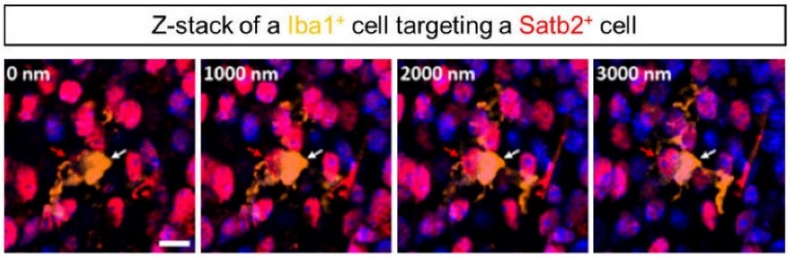

Supplementary Figure S5. Iba1$^+$ cells are able to target Satb2$^+$ cells. Representative z-stack images of a microglia cell (white arrow) targeting Satb2$^+$ cells (red arrow) in a P0.5 mouse cortex. Scale bars represent 10 µm.

[4]

Supplementary Tables

Supplementary Table S1. Statistics determined for $NeuN^+$ cortical neurons in various development stages (E16.5, P0.5, P3.5) after different oxygen exposures during mid-neurogenesis (**Figure 1e**). Two-way ANOVA with *post-hoc* t-test and Bonferroni adjustment with atmospheric oxygen concentrations and development stage as fixed factors revealed that atmospheric oxygen concentration and developmental stage have a significant interaction effect on $NeuN^+$ neuron counts (p=0.028, F-value=4.2) and significant differences among atmospheric oxygen concentrations (p=0.006, F-value=8.8) and developmental stages (p<0.001, F-value=9.3). Displayed are Bonferroni-adjusted P-values (E16.5: n=4 [control], n=3 [hyperoxia]; P0.5: n=8 [control], n=6 [hyperoxia]; P3.5: n=4 [control], n=6 [hyperoxia]). **(A)** Significances among the different atmospheric oxygen concentrations. **(B)** Significances among the different developmental stages. Bold values indicate significant differences.

A

	E16.5	**P0.5**	**P3.5**
Normoxia (21% O_2) vs. Hyperoxia (75% O_2)	**0.005**	**0.013**	0.581

B

	Normoxia (21% O_2)	**Hyperoxia (75% O_2)**
E16.5 vs. P0.5	**0.0459**	1
E16.5 vs. P3.5	**< 0.001**	0,769
P0.5 vs. P3.5	**0.011**	1

Supplementary Table S2. Statistics determined for $Tbr1^+$ cortical neurons in various development stages (E16.5, P0.5, P3.5) after different oxygen exposures during mid-neurogenesis (**Figure 2b**). Two-way ANOVA with *post-hoc* t-test and Bonferroni adjustment with atmospheric oxygen concentrations and development stage as fixed factors revealed that atmospheric oxygen concentration and developmental stage have no significant interaction effect on $Tbr1^+$ neuron counts (p=0.210, F-value=1.7), but significant differences among atmospheric oxygen concentrations (p=0.006, F-value=9.8) and developmental stages (p<0.001, F-value=84.3). Displayed are Bonferroni-adjusted P-values (n = 4). **(A)** Significances among the different atmospheric oxygen concentrations. **(B)** Significances among the different developmental stages. Bold values indicate significant differences.

A

	E16.5	**P0.5**	**P3.5**
Normoxia (21% O_2) vs. Hyperoxia (75% O_2)	**0.004**	0.333	0.278

B

	Normoxia (21% O_2))	**Hyperoxia (75% O_2)**
E16.5 vs. P0.5	**< 0.001**	**0.002**
E16.5 vs. P3.5	**< 0.001**	**< 0.001**
P0.5 vs. P3.5	**0.005**	0.004

[6]

Supplementary Table S3. Statistics determined for $Ctip^{+}/Tbr1^{-}$ cortical neurons in various development stages (E16.5, P0.5, P3.5) after different oxygen exposures during mid-neurogenesis (**Figure 2c**). Two-way ANOVA with *post-hoc* t-test and Bonferroni adjustment with atmospheric oxygen concentrations and development stage as fixed factors revealed that atmospheric oxygen concentration and developmental stage have a significant interaction effect on $Ctip^{+}/Tbr1^{-}$ cortical neuron counts (p=0.002, F-value=9.5) and significant differences among atmospheric oxygen concentrations (p<0.001, F-value=49.2) and developmental stages (p=0.002, F-value=44.9). Displayed are Bonferroni-adjusted P-values (n = 4). **(A)** Significances among the different atmospheric oxygen concentrations. **(B)** Significances among the different developmental stages. Bold values indicate significant differences.

A

	E16.5	**P0.5**	**P3.5**
Normoxia (21% O_2) vs. Hyperoxia (75% O_2)	**< 0.001**	**< 0.001**	0.629

B

	Normoxia (21% O_2))	**Hyperoxia (75% O_2)**
E16.5 vs. P0.5	0.135	0.092
E16.5 vs. P3.5	**0.003**	**< 0.001**
P0.5 vs. P3.5	0.309	**< 0.001**

Supplementary Table S4. Statistics determined for $Satb2^+$ cortical neurons in various development stages (E16.5, P0.5, P3.5) after different oxygen exposures during mid-neurogenesis (**Figure 2d**). Two-way ANOVA with *post-hoc* t-test and Bonferroni adjustment (n = 4) with atmospheric oxygen concentrations and development stage as fixed factors revealed that atmospheric oxygen concentration and developmental stage have no significant interaction effect on $Satb2^+$ neuron counts (p=0.922, F-value=0.1), no significant differences among atmospheric oxygen concentrations (p=0.922, F-value=3.6), but significant differences among developmental stages (p=0.048, F-value=3.6). Displayed are Bonferroni-adjusted P-values (n = 4). **(A)** Significances among the different atmospheric oxygen concentrations. **(B)** Significances among the different developmental stages. Bold values indicate significant differences.

A

	E16.5	**P0.5**	**P3.5**
Normoxia (21% O_2) vs. Hyperoxia (75% O_2)	0.411	0.748	0.437

B

	Normoxia (21% O_2))	**Hyperoxia (75% O_2)**
E16.5 vs. P0.5	0.141	0.369
E16.5 vs. P3.5	0.720	0.774
P0.5 vs. P3.5	1	1

Supplementary Table S5. Statistics determined for apical Iba1$^+$ cells in various development stages (E16.5, P0.5, P3.5) after different oxygen exposures during mid-neurogenesis (**Figure 4b**). Two-way ANOVA with *post-hoc* t-test and Bonferroni adjustment with atmospheric oxygen concentrations and development stage as fixed factors revealed that atmospheric oxygen concentration and developmental stage have no significant interaction effect on apical Iba1$^+$ cell counts (p=0.465, F-value=0.8) and no significant differences among atmospheric oxygen concentrations (p=0.363, F-value=0.9), but significant differences among developmental stages (p<0.001, F-value=20.9). Displayed are Bonferroni-adjusted P-values (n = 4). **(A)** Significances among the different atmospheric oxygen concentrations. **(B)** Significances among the different developmental stages. Bold values indicate significant differences.

A

	E16.5	**P0.5**	**P3.5**
Normoxia (21% O_2) vs. Hyperoxia (75% O_2)	0.146	0.819	0.744

B

	Normoxia (21% O_2)	**Hyperoxia (75% O_2)**
E16.5 vs. P0.5	0.605	**0.020**
E16.5 vs. P3.5	**0.003**	**< 0.001**
P0.5 vs. P3.5	**0.049**	0.064

Supplementary Table S6. Statistics determined for subplate/layer 6 (SP/L6) Iba1$^+$ cells in various development stages (E16.5, P0.5, P3.5) after different oxygen exposures during mid-neurogenesis (**Figure 4c**). Two-way ANOVA with *post-hoc* t-test and Bonferroni adjustment with atmospheric oxygen concentrations and development stage as fixed factors revealed that atmospheric oxygen concentration and developmental stage have no significant interaction effect on SP/L6 Iba1$^+$ cells counts (p=0.295, F-value=1.3) and no significant differences among atmospheric oxygen concentrations (p=0.203, F-value=1.7), but significant differences among developmental stages (p<0.001, F-value=38.6). Displayed are Bonferroni-adjusted P-values (n = 4). **(A)** Significances among the different atmospheric oxygen concentrations. **(B)** Significances among the different developmental stages. Bold values indicate significant differences.

A

	E16.5	**P0.5**	**P3.5**
Normoxia (21% O_2) vs. Hyperoxia (75% O_2)	0.942	0.054	0.772

B

	Normoxia (21% O_2)	**Hyperoxia (75% O_2)**
E16.5 vs. P0.5	0.096	**< 0.001**
E16.5 vs. P3.5	**< 0.001**	**< 0.001**
P0.5 vs. P3.5	**0.005**	0.211

[10]

Supplementary Table S7. Statistics determined for layer 5 (L5) Iba1$^+$ cells in various development stages (P0.5, P3.5) after different oxygen exposures during mid-neurogenesis (**Figure 4d**). Two-way ANOVA with *post-hoc* t-test and Bonferroni adjustment with atmospheric oxygen concentrations and development stage as fixed factors revealed that atmospheric oxygen concentration and developmental stage have a significant interaction effect on L5 Iba1$^+$ cells counts (p=0.014, F-value=8.1) and significant differences among atmospheric oxygen concentrations (p=0.003, F-value=13.2) and developmental stages (p<0.001, F-value=37.5). Displayed are Bonferroni-adjusted P-values (n = 4). **(A)** Significances among the different atmospheric oxygen concentrations. **(B)** Significances among the different developmental stages. Bold values indicate significant differences.

A

	P0.5	**P3.5**
Normoxia (21% O_2) vs. Hyperoxia (75% O_2)	**< 0.001**	0.588

B

	Normoxia (21% O_2))	**Hyperoxia (75% O_2)**
P0.5 vs. P3.5	**< 0.001**	**0.039**

Supplementary Table S8. Statistics determined for layer 4-1 (L4-1) $Iba1^+$ cells in various development stages (P0.5, P3.5) after different oxygen exposures during mid-neurogenesis (**Figure 4e**). Two-way ANOVA with *post-hoc* t-test and Bonferroni adjustment with atmospheric oxygen concentrations and development stage as fixed factors revealed that atmospheric oxygen concentration and developmental stage have no significant interaction effect on L4-1 $Iba1^+$ cells counts (p=0.945, F-value=0.0) and no significant differences among atmospheric oxygen concentrations (p=0.945, F-value=0.0), but significant differences among developmental stages (p<0.001, F-value=85.8). Displayed are Bonferroni-adjusted P-values (n = 4). **(A)** Significances among the different atmospheric oxygen concentrations. **(B)** Significances among the different developmental stages. Bold values indicate significant differences.

A

	P0.5	**P3.5**
Normoxia (21% O_2) vs. Hyperoxia (75% O_2)	0.920	1.000

B

	Normoxia (21% O_2)	**Hyperoxia (75% O_2)**
P0.5 vs. P3.5	**< 0.001**	**< 0.001**

Supplementary Table S9. Statistics determined for $CC3^+$ cell counts in various development stages (E16.5, P0.5, P3.5) after different oxygen exposures during mid-neurogenesis (**Figure 7b**). Robust ANOVA using raov function from Rfit package with *post-hoc* unpaired Wilcoxon-test and Bonferroni adjustment (n = 3) with atmospheric oxygen concentrations and development stage as fixed factors revealed that atmospheric oxygen concentration and developmental stage have a significant interaction effect on $CC3^+$ cell counts (p=0.001, F-value=9.1) and significant differences among atmospheric oxygen concentrations (p=0.004, F-value=10.4) and developmental stages (p<0.001, F-value=30.1). **(A)** Significances among the different atmospheric oxygen concentrations. **(B)** Significances among the different developmental stages. Bold values indicate significant differences.

A

	E16.5	**P0.5**	**P3.5**
Normoxia (21% O_2) vs. Hyperoxia (75% O_2)	0.564	**0.008**	1.000

B

	Normoxia (21% O_2))	**Hyperoxia (75% O_2)**
E16.5 vs. P0.5	**0.014**	**0.024**
E16.5 vs. P3.5	0.075	0.107
P0.5 vs. P3.5	0.276	0.786

Supplementary Table S10: Statistics determined for vGluT2$^+$ synapses in L5 (P0.5, P3.5) after different oxygen exposures during mid-neurogenesis (**Figure 8**). Two-way ANOVA with *post-hoc* t-test with atmospheric oxygen concentrations and development stage as fixed factors revealed that atmospheric oxygen concentration and developmental stage have a significant interaction effect on VGlut2$^+$ synapses (p=0.046, F-value=4.7) and significant differences among atmospheric oxygen concentrations (p=0.030, F-value=5.6), but no significant differences among developmental stages (p=0.371, F-value=0.8). Displayed are P-values (n = 5). **(A)** Significances among the different atmospheric oxygen concentrations. **(B)** Significances among the different developmental stages. Bold values indicate significant differences.

A

	P0.5	**P3.5**
Normoxia (21% O_2) vs. Hyperoxia (75% O_2)	**0.006**	0.881

B

	Normoxia (21% O_2))	**Hyperoxia (75% O_2)**
P0.5 vs. P3.5	0.394	**0.045**

Supplementary Table S11. Statistics determined for absolute $Tbr1^+$ cortical neuron counts in various development stages (E16.5, P0.5, P3.5) after different oxygen exposures during mid-neurogenesis (**Supplementary Figure S2a**). Two-way ANOVA with *post-hoc* t-test and Bonferroni adjustment with atmospheric oxygen concentrations and development stage as fixed factors revealed that atmospheric oxygen concentration and developmental stage have no significant interaction effect on $Tbr1^+$ neuron counts (p=0.780, F-value=0.3) and no significant differences among atmospheric oxygen concentrations (p=0.338, F-value=1.0), but significant differences among developmental stages (p=0.014, F-value=5.5). Displayed are Bonferroni-adjusted P-values (n = 4). **(A)** Significances among the different atmospheric oxygen concentrations. **(B)** Significances among the different developmental stages. Bold values indicate significant differences.

A

	E16.5	**P0.5**	**P3.5**
Normoxia (21% O_2) vs. Hyperoxia (75% O_2)	0.654	0.895	0.278

B

	Normoxia (21% O_2))	**Hyperoxia (75% O_2)**
E16.5 vs. P0.5	0.567	0.327
E16.5 vs. P3.5	1.000	0.852
P0.5 vs. P3.5	0.261	**0.036**

Supplementary Table S12. Statistics determined for absolute $Ctip2^+/Tbr1^-$neuron counts in various development stages (E16.5, P0.5, P3.5) after different oxygen exposures during mid-neurogenesis (**Supplementary Figure S2b**). Two-way ANOVA with *post-hoc* t-test and Bonferroni adjustment with atmospheric oxygen concentrations and development stage as fixed factors revealed that atmospheric oxygen concentration and developmental stage have a significant interaction effect on $Ctip2^+/Tbr1^-$ neuron counts ($p<0.001$, F-value=10.8) and significant differences among atmospheric oxygen concentrations ($p<0.001$, F-value=53.2) and developmental stages ($p<0.001$, F-value=19.1). Displayed are Bonferroni-adjusted *P*-values (n = 4). **(A)** Significances among the different atmospheric oxygen concentrations. **(B)** Significances among the different developmental stages. Bold values indicate significant differences.

A

	E16.5	**P0.5**	**P3.5**
Normoxia (21% O_2) vs. Hyperoxia (75% O_2)	**< 0.001**	**< 0.001**	0.574

B

	Normoxia (21% O_2)	**Hyperoxia (75% O_2)**
E16.5 vs. P0.5	**0.047**	**< 0.001**
E16.5 vs. P3.5	0.208	0.057
P0.5 vs. P3.5	1.000	**< 0.001**

Supplementary Table S13. Statistics determined for absolute $Satb2^+$ cortical neuron counts in various development stages (E16.5, P0.5, P3.5) after different oxygen exposures during mid-neurogenesis (**Supplementary Figure S2c**). Two-way ANOVA with *post-hoc* t-test and Bonferroni adjustment (n = 4) with atmospheric oxygen concentrations and development stage as fixed factors revealed that atmospheric oxygen concentration and developmental stage have no significant interaction effect on $Satb2^+$ neuron counts (p=0.828, F-value=0.2), no significant differences among atmospheric oxygen concentrations (p=0.066, F-value=3.8), but significant differences among developmental stages (p<0.001, F-value=76.9). **(A)** Significances among the different atmospheric oxygen concentrations. **(B)** Significances among the different developmental stages. Bold values indicate significant differences.

A

	E16.5	**P0.5**	**P3.5**
Normoxia (21% O_2) vs. Hyperoxia (75% O_2)	0.153	0.225	0.527

B

	Normoxia (21% O_2))	**Hyperoxia (75% O_2)**
E16.5 vs. P0.5	**< 0.001**	**< 0.001**
E16.5 vs. P3.5	**< 0.001**	**< 0.001**
P0.5 vs. P3.5	0.573	1.000

Supplementary Table S14. Statistics determined for total Iba1$^+$ cell counts (E16.5, P0.5, P3.5) after different oxygen exposures during mid-neurogenesis (**Supplementary Figure S4**). Two-way ANOVA with *post-hoc* t-test and Bonferroni adjustment with atmospheric oxygen concentrations and development stage as fixed factors revealed that atmospheric oxygen concentration and developmental stage have no significant interaction effect on total Iba1$^+$ cell counts (p=0.643, F-value=0.5), but significant differences among atmospheric oxygen concentrations (p=0.030, F-value=5.5) and significant differences among developmental stages (p=0.034, F-value=4.1). Displayed are Bonferroni-adjusted P-values (n = 4). Significances among the different developmental stages. Bold values indicate significant differences.

A

	E16.5	**P0.5**	**P3.5**
Normoxia (21% O_2) vs. Hyperoxia (75% O_2)	0.144	0.069	0.541

B

	Normoxia (21% O_2))	**Hyperoxia (75% O_2)**
E16.5 vs. P0.5	1.000	0.989
E16.5 vs. P3.5	0.072	0.411
P0.5 vs. P3.5	0.234	1.000

4.2 Early Chronic Intermittent Maternal Hyperoxygenation Impairs Cortical Development by Inhibition of Pax6-Positive Apical Progenitor Cell Proliferation

Franz Markert, Luisa Müller, Kathrin Badstübner-Meeske & Alexander Storch

Journal of Neuropathology & Experimental Neurology, 2020, Band 79, Nummer 11, Seiten 1223 - 1232

Zusammenfassung:

Im Hinblick auf den proliferationssteigernden Effekt einer maternalen Sauerstoffbehandlung bei Mäusen von Embryonalstadium (E)14,5 bis E16,5 wurde in dieser Studie untersucht, inwieweit sich eine chronische Behandlung mit Sauerstoff auf die kortikale Entwicklung auswirkt. Dazu wurden trächtige C57BL/6J Mäuse intermittierend in 75% Sauerstoff gehalten und die Feten zum E16,5 mittels Immunhistochemie auf neuronale Proliferations- und Differenzierungsmarker hin untersucht. Die chronische Sauerstoffbehandlung führt zu einer Verringerung der Anzahl an neuronalen Vorläuferzellen und einer Reduktion von mitotischen Zellen in den betroffenen Kortizes. Diese Veränderungen resultieren in einer abnormalen kortikalen Schichtung, sodass mehr $Tbr1^+$-Neurone der inneren Schicht des Kortex, dafür weniger $Satb2^+$-Neurone der äußeren Schichten zu finden sind. Passend dazu wird eine verringerte Expression des neuronalen Markers NeuN in den oberen kortikalen Schichten festgestellt. Die Ergebnisse zeigen, dass eine zeitige chronisch intermittierende Sauerstoffbehandlung, im Gegensatz zur kurzzeitigen Sauerstoffbehandlung, zu verringerter Proliferation neuronaler Stammzellen und einer veränderten kortikalen Schichtung führt. Die Applikationsdauer sowie der Zeitpunkt der Applikation einer Sauerstoffbehandlung scheinen daher maßgeblich den Effekt auf die kortikale Entwicklung zu beeinflussen. Zur Aufklärung der zugrundeliegenden Mechanismen, sowie der Frage inwieweit diese Veränderungen persistieren, sind weitere Folgestudien in Form von Zellzyklusanalysen, neuronalen Migrationsanalysen sowie Verhaltensanalysen notwendig.

J Neuropathol Exp Neurol
Vol. 79, No. 11, November 2020, pp. 1223–1232
doi: 10.1093/jnen/nlaa072

ORIGINAL ARTICLE

Early Chronic Intermittent Maternal Hyperoxygenation Impairs Cortical Development by Inhibition of Pax6-Positive Apical Progenitor Cell Proliferation

Franz Markert, MSc, Luisa Müller, MSc, Kathrin Badstübner-Meeske, PhD, and Alexander Storch, MD

Abstract

Maternal hyperoxygenation is a feasible, noninvasive method to treat fetal diseases, such as heart hypoplasia, but effects of maternal hyperoxygenation on the developing brain remain poorly understood. Previous studies showed that short-term maternal hyperoxygenation during midneurogenic phase (E14–E16) but not in earlier development (E10–E12) increases oxygen tension and enhances neurogenesis in the developing mouse cortex. We investigated effects of early chronic maternal hyperoxygenation (CMH) as a potential clinical treatment. Pregnant C57BL/6J mice were housed in a chamber at 75% atmospheric oxygen and the brains of E16 fetuses were analyzed using immunohistochemistry. The mitosis marker phH3 showed a significant reduction of proliferation in the dorsolateral cortices of CMH-treated E16 fetuses. Numbers of Tbr2-positive intermediate progenitor cells were unaffected whereas numbers of Pax6-positive apical progenitor cells were significantly reduced in CMH-treated mice. This resulted in altered cortical plate development with fewer Satb2-positive upper layer neurons but more Tbr1-positive neurons corresponding to the deeper layer 6. Thus, maternal hyperoxygenation affects the developing cortex depending on timing and length of applied oxygen. Early CMH causes a severe reduction of neuroprogenitor proliferation likely affecting cortical development. Further studies are needed to investigate the mechanisms underlying these findings and to assess the clinical and neurodevelopmental outcomes of the pups.

Key Words: Corticogenesis, Hyperoxia, Maternal hyperoxygenation, Neural stem cells, Oxygen tension.

INTRODUCTION

Ventilation therapy in respiratory or lung diseases is standard of care in humans of all ages and oxygen therapy is often necessary in newborns, particularly for the survival of premature infants (1–3). On the other hand, oxygen therapy to specifically change tissue oxygen tension is rarely used in evidence-based medicine. Currently, there is interest in maternal hyperoxygenation for influencing fetal development, mainly for heart hypoplasia (4–6). Indeed, maternal hyperoxygenation affects fetal pulmonary blood flow and oxygen saturation and eventually heart hypoplasia (7–9). While most of the available clinical studies address short-term protocols, a few trials address the effects of long-term protocols (10). However, besides the potential effects of oxygenation on congenital heart diseases, experimental evidence shows that oxygen is an important signaling molecule in neural development. Specifically, various research groups reported that neural progenitor cells reside in a hypoxic niche in both embryonic and adult brain (11–13), and numerous in vitro data regarding oxygen tension have revealed oxygen as a key factor for proliferation and differentiation of rodent and human neural stem and progenitor cells (14–19). In contrast, only very few studies systematically investigated the effects of various oxygen tensions in brain tissue by maternal hyperoxygenation or altering angiogenesis and confirmed that altered oxygen conditions affect the developing brain in vivo by regulating the balance between neural stem cell maintenance and their differentiation (12, 20, 21).

As the available data from in vivo studies addressed only the effects of short-term maternal hyperoxygenation resulting in increased neurogenesis during cortical development, the effects of chronic maternal hyperoxygenation (CMH) are poorly understood. Contrary to short-term maternal hyperoxygenation, a recent pilot study in humans showed that CMH impairs fetal neuronal development resulting in reduced head growth of infants, although no alterations in neurodevelopmental assessments were observed (22). These observations raise the question whether CMH protocols have different effects on brain development as compared with short-term protocols. We thus investigated the effects of an intense CMH on neural development, including the neural stem cell expansion phase. We used pregnant C57BL/6J mice as a

From the Department of Neurology, University of Rostock (FM, LM, KB-M, AS); and German Center for Neurodegenerative Diseases (DZNE) Rostock (AS), Rostock, Germany.
Send correspondence to: Alexander Storch, MD, Department of Neurology, University of Rostock, Gehlsheimer Straße 20, 18147 Rostock, Germany; E-mail: alexander.storch@med.uni-rostock.de
This study was supported by regular funds of the University Medical Centre Rostock.
The authors have no duality or conflicts of interest to declare.

model known to be susceptible to increased fetal brain oxygen tension, particularly within the stem cells niches of the developing brain, after treatment of the mother animals with 75% atmospheric oxygen (21).

MATERIALS AND METHODS

Animals and Oxygen Treatment

For oxygen treatment, C57BL/6J timed-pregnant mice were housed in their home-cages within an oxygen-chamber (InerTec, Grenchen, Switzerland) with a probe for oxygen. Further, for CMH mice were treated from E5 to E16 with cycles of 75% oxygen for one day followed by one day at room air (Fig. 1A). This intermittent treatment scheme was necessary since hyperoxygenation lasting longer than 48 hours affects the health of adult mice (12). Control mice were kept in room air straight next to the oxygen chamber ensuring the same environmental conditions besides oxygenation. All animals were handled by the same investigator during the entire treatment protocol. The fetuses in both groups showed an ordinary morphology with ~7 fetuses per litter. All data were gathered from randomly chosen fetuses from at least 3 independent litters per group. All animals were maintained and treated with permission of the local Department of Animal Welfare (Landesamt für Landwirtschaft, Lebensmittelsicherheit und Fischerei Mecklenburg-Vorpommern) and comply with the Tierschutzgesetz and Verordnung zur Umsetzung der Richtlinie 2010/63/EU from Germany.

Immediately after oxygen exposure, the embryonic brains were dissected, fixed for 24 hours in 4% paraformaldehyde (Merck, Darmstadt, Germany) and kept in 30% sucrose (Carl Roth, Karlsruhe, Germany) in Dulbecco's Phosphate-Buffered Saline (Thermo Fisher Scientific, Waltham, MA). Then brains were snap-frozen, sectioned coronal at 20 µm thickness with microtome (Leica Biosystems, Nussloch, Germany) and mounted on Superfrost Plus slides (Thermo Fisher Scientific). The slides were stored at 4°C until staining.

Immunofluorescence

Slides were washed with TBST Wash Buffer (Agilent, Santa Clara, CA) and heat-induced antigen retrieval was performed using citrate buffer containing 10 mM sodium citrate (Carl Roth) and 0.05% TWEEN 20 (SERVA, Heidelberg, Germany) for 30 minutes at 95°C. After 20 minutes at room temperature, slides were washed with TBST and treated with TBST containing 0.2% Triton X-100 (Carl Roth) and 10% donkey serum (Merck) for 30 minutes. Next, slides were incubated with Isolectin IB4 (Thermo Fisher Scientific) or primary antibodies overnight at 4°C. The following primary antibodies were used: Mouse anti-phospho-histone H3 (phH3; Cell Signaling, Danvers, MA; 9706, 1:100); mouse anti-Satb2 (Abcam, Cambridge, UK; ab51502, 1:500); rabbit anti-cleaved-caspase-3 (Cell Signaling; 9661S; 1:200); rabbit anti-NeuN (Merck; ABN78, 1:600); rabbit anti-Pax6 (Covance, San Diego, CA; PRB-278P, 1:300); rabbit anti-Tbr1 (Abcam; ab31940, 1:250); rabbit anti-Tbr2 (Abcam; ab183991, 1:600); and rat anti-Ctip2 (Abcam; ab18465, 1:500).

Subsequently, slides were incubated with corresponding secondary antibodies (Thermo Fisher Scientific) and nuclei were stained with Hoechst 33258 (Merck). To preserve immunofluorescence, slides were mounted with Prolong Antifade Diamond (Thermo Fisher Scientific) and stored at 4°C for microscopy.

Imaging and Measurements

Images were taken with Axio.Observer.Z1 with Apotome using ZEN blue 2.3 software with Tiles and Position module (all from Carl Zeiss, Oberkochen, Germany). Images from at least 4 different brain slices of the medial dorso-lateral telencephalon were taken at 20× magnification. For all markers with exception of the apoptosis marker cleaved caspase 3 (CC3) images were taken with apotome and Z-stack mode with 1-µm steps. For CC3 standard fluorescence images from the whole hemisphere were taken. CC3-positive cells were counted with ZEN blue 2.3 in the cortex from the dorsal to ventral site. Mitotic cells (phH3-positive cells) were counted with ZEN blue 2.3 within different layers of a 500-µm-wide cortical columns. Neurons (NeuN-positive), apical progenitor (AP) cells (Pax6-positive), and intermediate progenitor (IP) cells (Tbr2-positive) were counted within 200-µm-wide cortical columns using ImageJ. Tbr2-positive, phH3-positive, and NeuN-positive cells were counted through all Z-stacks of the corresponding brain slices. Pax6-positive, Tbr1-positive, Ctip2-positive, and Satb2-positive cells were counted in the medial focal plane of each brain slice. The boundary between the ventricular zone (VZ) and subventricular zone (SVZ) was defined by the shape of the nucleus and the density of Pax6-positive and Tbr2-positive cells. While most cells in the VZ show a stretched shape of the nucleus, cells in the SVZ possess an elliptical nucleus. In addition, the VZ was defined by its high density of Pax6-positive cells and SVZ was defined by its high density of Tbr2-positive cells where the basal decreasing density of cells marks the SVZ-intermediate zone (IZ) boundary (23). For quantification of mitotic cells in the hippocampal area, all phH3-positive cells were counted and subsequently correlated to the analyzed area. For adequate presentation, mitotic cell numbers were calculated to cells per mm^3. For vascularization analyses, the medial focal plane of each brain slice was used. Subsequently, binary images were created with a fixed threshold and the percentage of the covered area excluding the meninges was computed. The thicknesses of the cortex and the cortical plate (CP) of each fetus were measured from the ventricular surface or cortical subplate to the pial surface. For this purpose, at least 5 positions from dorsal to ventral along the ventricle (100-µm intervals) were analyzed in 3 sections of the medial cortex of each fetus.

Statistics

All statistics were performed with RGUI 3.4.1 (R Foundation for Statistical Computing, Vienna, Austria). If not otherwise stated, statistical significance was evaluated by unpaired two-sided *t*-test. The number of analyzed fetuses, gathered from at least 3 independent litters, is indicated by "n." The significance level was set to 0.05.

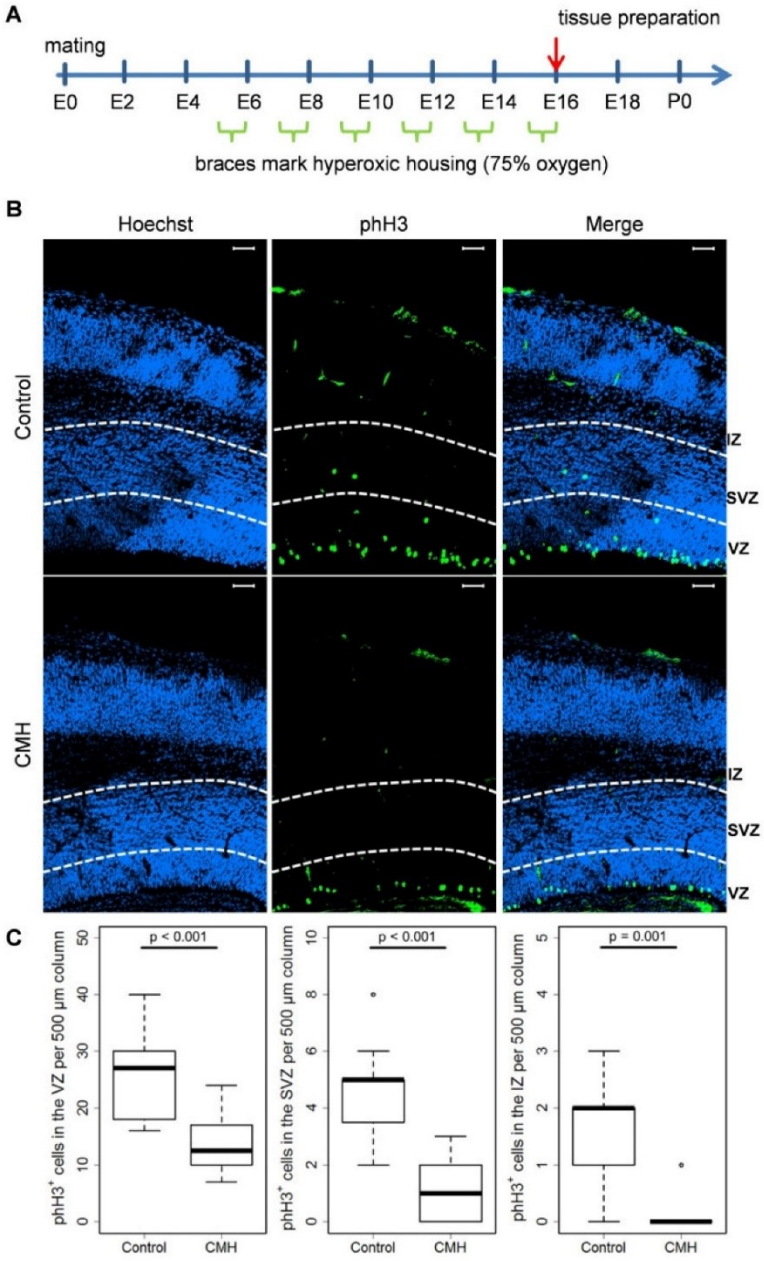

FIGURE 1. Chronic maternal hyperoxygenation (CMH) in mice leads to reduced mitosis in E16 dorso-lateral cortices. **(A)** Experimental setup. Timed-pregnant mice were treated from E5 to E16 with cycles of 75% oxygen for one day followed by one day at room air. Controls were kept at room air. **(B)** Representative immunofluorescence images of mitotic cells (phH3-positive cells, green) counterstained with Hoechst (blue). Dashed lines separate ventricular zone ([VZ], bottom, subventricular zone [SVZ], mid, and intermediate zone [IZ], top). Scale bars: 50 µm. **(C)** Quantification of phH3-positive mitotic cells within VZ, SVZ, and IZ in 500-µm-wide columns. Bars represent significant differences with displayed p-values (unpaired two-sided *t*-test or Wilcoxon-test for phH3-positive in the IZ; n = 9).

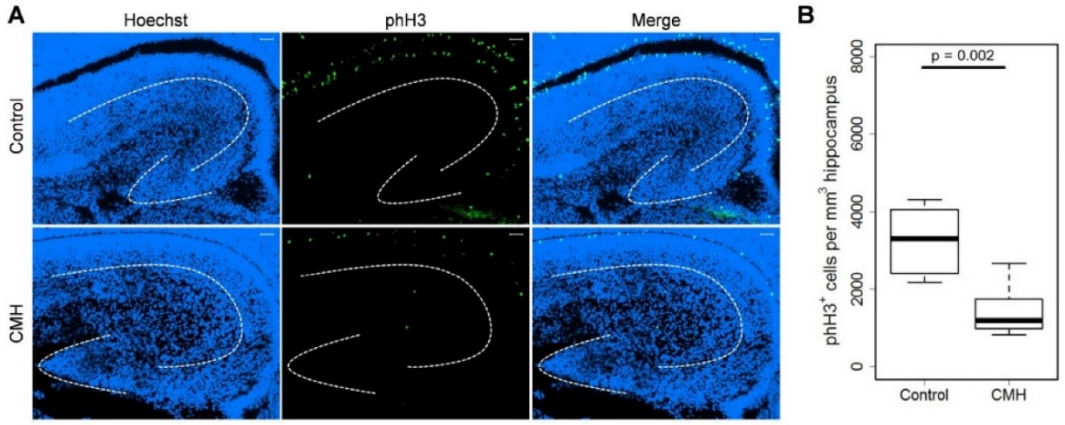

FIGURE 2. Chronic maternal hyperoxygenation (CMH) reduces early hippocampal mitosis in E16 mouse fetuses. **(A)** Representative immunofluorescence images of mitotic cells (phH3-positive cells, green) counterstained with Hoechst (blue). Dashed lines indicate CA1–CA3 region (top, right) and the hippocampal fissure (bottom, left). Scale bars: 50 μm. **(B)** Quantification of phH3-positive mitotic cells density in the early hippocampus. Bar represents significant difference with displayed p values (unpaired two-sided *t*-test; n = 6).

RESULTS

Maternal Hyperoxygenation Differentially Affects Proliferation in the Developing Brain Depending on Exposure Length

Short-term (48 hours) maternal hyperoxygenation leads to increased fetal brain oxygen tension and shows developmental stage-dependent effects in the proliferating zones of the mouse brain with enhancing progenitor cell proliferation, particularly in the IZ during late neurogenic phase of brain development (E14–E16), but expressed no effects in the earlier expansion/neurogenic phase from E10–E12 (12). The effects of CMH covering the expansion and neurogenic phase remained unclear. We therefore treated pregnant C57BL/6J mice from E5 to E16 with cycles of 75% oxygen for one day followed by one day at room air (Fig. 1A; intermittent treatment scheme was applied to avoid toxic effects on the adult mother [12]). The results were compared with control mice kept at room air ensuring the same environmental conditions besides the oxygen treatment. Representative immunofluorescence images of mitotic cells marked by phH3 in the VZ, the SVZ and the IZ representing the proliferating zones in the developing mouse brain from apical to basal membrane are displayed in Figure 1B. In contrast to short-term hyperoxygenation (12), quantitative immunohistochemistry analyses revealed that CMH-treated mice showed a significantly reduced number of mitotic cells by a factor of 0.5 in the VZ, 0.2 in the SVZ and nearly depleted in the IZ compared with controls (Fig. 1C). To investigate whether reduced cell proliferation is limited to the cortical area, we additionally analyzed cell proliferation within the developing hippocampal formation. These analyses revealed that CMH also affects hippocampal development with reduced mitotic activity in the VZ of the hippocampus (Fig. 2).

Early CMH Reduces the Number of AP but Not IP Cells

We next ascertained whether the differential effects on cell proliferation of short-term versus chronic maternal hyperoxia translates into different numbers of the various progenitor cell types of mouse developing cortex. The first population comprises dividing Pax6-positive radial glial cells as one major type of AP at the ventricular surface of the VZ (24–31). The second class of neural progenitors originate from radial glial cells by asymmetric mitoses are referred to as Tbr2-positive IPs and form the SVZ (29, 30, 32–35). CMH led to a morphological thinner VZ compared with normoxic controls. We found that there were reduced numbers of Pax6-positive cells compared control conditions with pronounced effects in the VZ (Pax6-positive cells reduced by a factor of 0.8), while the SVZ was not affected (Fig. 3).

To analyze IPs as the second major class of neural progenitors, we performed quantitative histology on Tbr2-positive cells. CMH did not change Tbr2-positive IP cell counts in any cell layer (Fig. 4). To clarify whether the specific reduction of Pax6-positive cells arises from reduced proliferation only or from apoptotic effects, we performed immunohistochemistry for the apoptosis marker CC3. Both CMH-treated and control mice showed few apoptotic cells but with no difference between both groups (Fig. 5A, B). Because Wagenführ et al and Lange et al showed vascularization effects associated with oxygenation (12, 20), we additionally performed immunohistochemical staining for IB4 as an established marker for vessels (Fig. 5C, D). Quantification of percentual vessel covered area revealed no differences between CMH-treated mice and control mice (Fig. 5D). In summary, CMH treatment of the fetal brain resulted in specific reduction of Pax6-positive AP production, but did not change the generation of IPs. This specific reduction of Pax6-positive

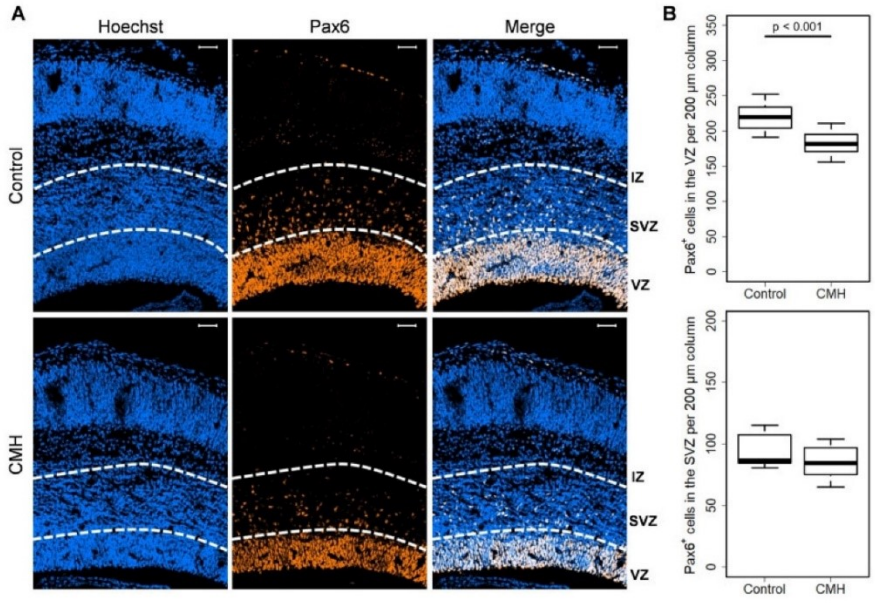

FIGURE 3. Chronic maternal hyperoxygenation (CMH) in mice reduces the number of basal progenitor cells in E16 dorso-lateral cortices. **(A)** Representative immunofluorescence images of basal progenitor cells (Pax6-positive cells, orange) counterstained with Hoechst (blue). Dashed lines separate ventricular zone ([VZ], bottom, subventricular zone [SVZ], mid, and intermediate zone [IZ], top). Scale bars: 50 µm. **(B)** Quantification of Pax6-positive basal progenitor cells within VZ and SVZ in 200-µm-wide columns; bars represent significant differences with displayed p values (unpaired two-sided *t*-test; n = 8 for controls, n = 10 for CMH).

APs likely arises from reduced proliferation, but not due to apoptosis or altered vascularization.

Early CMH Treatment Results in Altered Cortical Development

The proliferating zones near the apical surface constantly contribute neurons to the CP forming its typical inside-out layer pattern during cortical development (36). Pax6 represents a key factor in this highly orchestrated process (37). We next investigated whether the effects of CMH on progenitor cell proliferation and particularly the number of Pax6-positive APs translated into an alteration of the development of the CP. Immunofluorescence images of the rostral telencephalon revealed an aberrant NeuN expression profile in the CP in CMH-treated fetal brains. While NeuN expressing cells clearly mark the subplate and deeper layers of the CP, cells in the upper layers showed less NeuN expression (Fig. 6A). Quantification of NeuN expression using fixed illumination settings thereby resulted in a reduced number of NeuN-positive cells by a factor of 0.8 in the rostral CP (Fig. 6B). However, the aberrant NeuN expression profile in the upper layers of CP did not result in morphological changes since cortical thickness was not affected in CMH-treated mice compared with controls (Fig. 6C). This prompted us to analyze the individual cortical layers with a combination of Tbr1, Ctip2, and Satb2 markers. Immunohistochemical investigation of these markers revealed a reduced number of Satb2-positive cells representing upper layer neurons in CMH-treated fetuses. Despite this, the numbers of deeper layer neurons stained with Tbr1 were increased while the number of Ctip2-positive cells were unaffected (Fig. 7). In summary, CMH-treated mice were grossly morphologically unaffected but showed an altered cortical layering. There were more deeper layer neurons originating in early development but fewer upper layer neurons originating in later development in CMH-treated fetuses.

DISCUSSION

Maternal hyperoxygenation is used to treat heart hypoplasia in fetuses (4–6). Although there are promising effects regarding heart hypoplasia, maternal hyperoxygenation also influences neuronal development by specifically affecting neurogenesis (12, 20). While these in vivo studies addressed only short-term hyperoxygenation, the present study investigates the effects of CMH as a novel clinical approach on cortical development compared with normoxic controls. We thereby demonstrated that CMH with 75% oxygen affected the cortical development of C57BL6/J mouse fetuses, but in an opposite way compared with short-term maternal hyperoxygenation: While short-term maternal hyperoxygenation for 48 hours enhances the number of mitotic cells in the SVZ at developmental stage E14–E16 but has no effects at E10–E12, CMH from E5 to E16 leads to a significant reduction of mi-

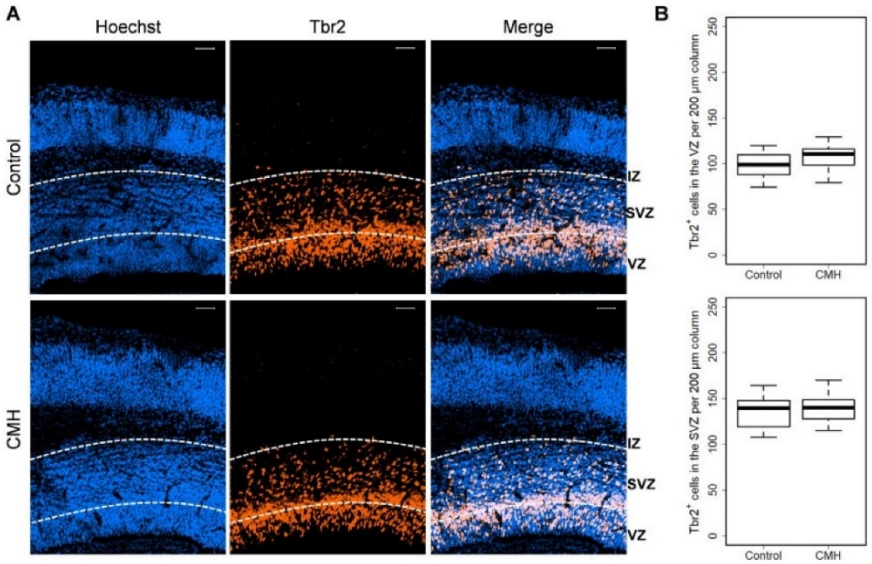

FIGURE 4. Intermediate progenitor cells in dorso-lateral cortices of E16 mice remains unaffected by chronic maternal hyperoxygenation (CMH). **(A)** Representative immunofluorescence images of intermediate progenitor cells (Tbr2-positive cells, orange) counterstained with Hoechst (blue). Dashed lines separate ventricular zone ([VZ], bottom, subventricular zone [SVZ], mid, and intermediate zone [IZ], top). Scale bars: 50 µm. **(B)** Quantification of Tbr2-positive intermediate progenitor cells within VZ and SVZ in 200-µm-wide columns. Unpaired two-sided *t*-tests revealed no significant differences between control and CMH animals for all layers (n = 8).

totic cells in all proliferating zones of the developing cortex. Because mitosis in the very early hippocampal development was also reduced, we conclude that this effect is likely not limited to the developing cortex.

To investigate the affected cell populations in the proliferating zones of the developing cortex, we next performed immunostainings for APs and IPs. Here, CMH leads to significantly reduced numbers of Pax6-positive cells representing APs going along with a morphologically thinner VZ. Unexpectedly, the number of sequentially resulting IPs was not affected (33). When comparing to short-term hyperoxygenation of fetal brain tissue, we suppose that there is a critical length and/or developmental stage for the effects of hyperoxygenation on neuroprogenitor populations. While short-term hyperoxygenation for 48 hours from E10 to E12 does not lead to significant changes in the number of IPs (12), a 72-hour period from E10 to E13 shifts the progenitor population from APs to an increased number of IPs as also was observed in the later midneurogenic phase at E14–E16 (12, 20). Since our CMH treatment scheme covers the developmental stages from E5 to E16, we conclude that the longer oxygen application leads to the stronger shift toward neuroprogenitor differentiation. Excluding apoptotic effects, the unaffected number of IPs in CMH-treated mice might result from reduced mitosis during development—even in earlier developmental stages as investigated in short-term hyperoxygenation studies—which offsets the oxygen-driven differentiation of APs sequentially dividing in IPs (38). However, as we needed to include rescue days with exposure of the dams to normal oxygen conditions (12), we cannot fully rule out that the sequential exposure or the exposure during very specific developmental processes might be—at least in part—also responsible for the contrary effects of CMH compared with short-term hyperoxygenation.

Since IPs contribute to cells of the CP via symmetric division and Tbr2 and Pax6 are both main regulators of cortical development, we investigated if CMH affect cortical morphology and NeuN expression as a marker for mature neurons (37, 39, 40). CMH induces an aberrant NeuN expression profile with reduced expression of NeuN in the upper cortical layers of rostral cortices. This aberrant NeuN expression profile could be the result of the decreased proliferation and subsequently reduced number of Pax6-positive APs, which may affect cortical neurogenesis. This hypothesis is supported by current evidence from Pax6 research, where timed and conditional knockout models show similar but more severe morphological changes compared with hyperoxygenic brains with markedly reduced numbers of neurons especially in superficial layers of the rostral cortex leading to severe decrease of brain sizes and hampered cognitive functions (37, 41). The more severe phenotype in Pax6 knockout models eventually leading to smaller brain sizes, which were not observed in CMH-treated mice, might be explained by the more consequent knock-out of Pax6-positive APs in genetic models compared with CMH animals. To deepen our knowledge of the underlying mechanisms, we have used Tbr1, Ctip2, and Satb2 antibodies as a panel of cortical layer markers. In CMH-treated

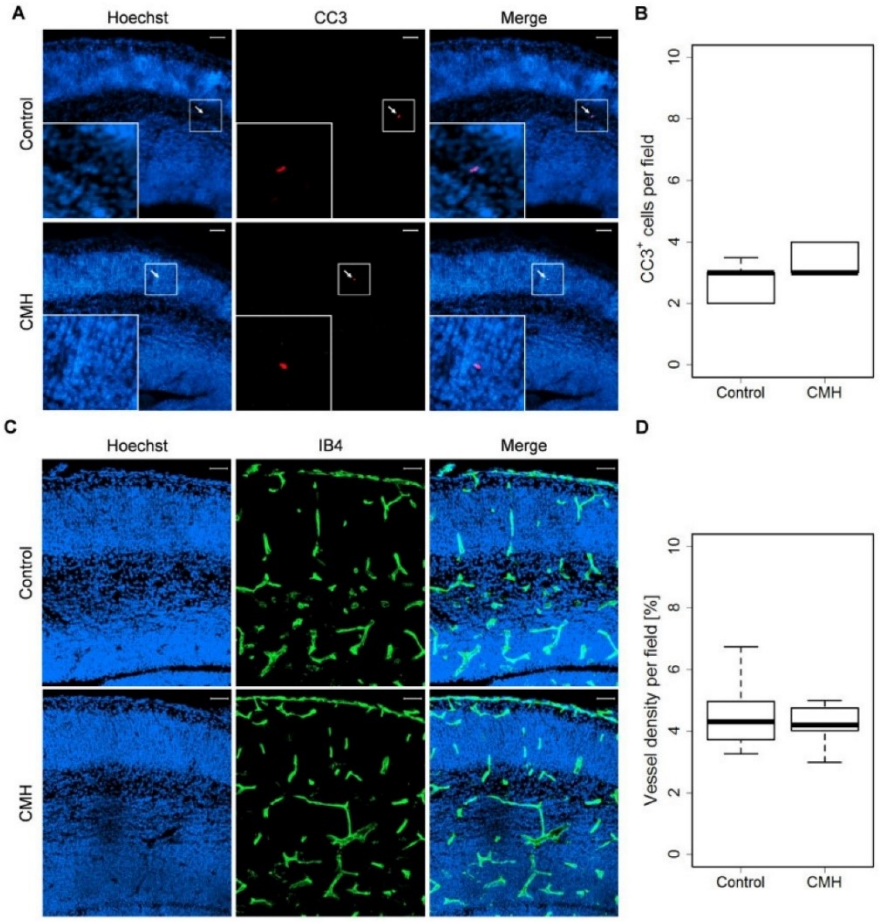

FIGURE 5. Apoptosis rate and vascularization in the E16 mouse cortex are not affected by chronic maternal hyperoxygenation (CMH). **(A)** Representative immunofluorescence images of apoptotic cells (cleaved caspase 3 [CC3]-positive cells, red) counterstained with Hoechst (blue). White arrows indicate apoptotic cells. White square is shown magnified in the left corner. Scale bars: 50 μm. **(B)** Quantification of CC3-positive apoptotic cells counted in the medial cortex per brain slice. Wilcoxon rank sum test revealed no significant differences between control and CMH animals (n = 6). **(C)** Representative orthogonal projected immunofluorescence images of vessels (IB4-positive, green) counterstained with Hoechst (blue). Scale bars: 50 μm. **(D)** Quantification of vessel density (IB4-positive) in the early hippocampal area. Unpaired two-sided *t*-test revealed no significant differences between control and CMH animals (n = 6).

mice, the reduced number of Satb2-positive cells that represent upper layer neurons supports our results of the aberrant NeuN expression profile. Interestingly, the number of deeper layer neurons represented by Tbr1-positive cells is enhanced. Since our CMH treatment protocol covers the early neurogenic expansion phase, an early increased proliferation leading to an exhaustion of proliferation capacity at E16 could be possible. Thereby, a probable increased proliferation at earlier stages could lead to relatively unremarkable cortical morphology, but reduced proliferation in later stages (42, 43). In addition, this theory would explain the increased number of deeper layer neurons that arise at earlier stages. Consequently, with exhaustion of proliferative capacities, which may lead also to the demonstrated reduced number of Pax6-positive cells at E16, the number of upper layer neurons is decreased. However, we cannot exclude other hypothesis that could be an aberrant migration and/or maturation, where the specific events of cortical development are delayed in CMH-treated mice or hampered migration occurs (44–46). Therefore, further studies are needed to investigate the specific effects of CMH protocols on the developing brain at various of developmental stages.

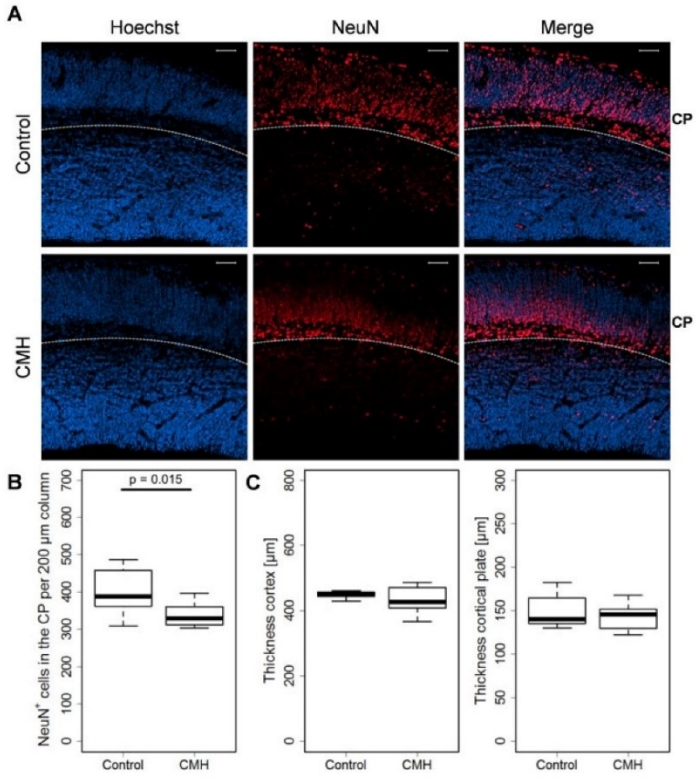

FIGURE 6. Chronic maternal hyperoxygenation (CMH) disturbs proper cortical layering in E16 mouse brain. **(A)** Representative immunofluorescence images of NeuN expressing neurons (red) counterstained with Hoechst (blue). Dashed lines separate cortical plate (top) from basal cortical zones (bottom). Scale bars: 50 µm. **(B)** Quantification of cortical NeuN-positive neurons within the cortical plate in 200-µm-wide columns. **(C)** Quantification of radial thickness of the cortex and the cortical plate. Bars represent significant differences with displayed p-values (unpaired two-sided *t*-test; n = 9 for NeuN-positive quantification; n = 7 for radial thickness measurements). CP, cortical plate.

A recent clinical pilot study investigating the effects of CMH for treatment of heart hypoplasia in humans resulted in a reduction of head growth in 6-month-old infants who underwent CMH therapy in utero (22). Therefore, Edwards et al adjusted their treatment protocol using longer daily exposure but with a lower fraction of inspired oxygen (FiO_2) and added evaluations of placental health, fetal head growth, and cerebral maturity. Although, the infants showed no differences in neurodevelopmental testing compared with controls, the study by Edwards et al together with our data indicate that intense or very early CMH treatment schemes may lead to abnormal neural development with contrary results to short-term hyperoxygenation. A direct comparison with our data is limited by oxygenation exposure, treatment protocol and species. Edwards et al started their treatment protocol around gestational week 26 with ~50% fraction of inspired oxygen controlled by analysis of the maternal arterial partial pressure of oxygen. We here used 75% oxygen, known to be effective in mice and for the comparability with short-term hyperoxygenation protocols, but we were technically not able to measure blood oxygenation due to handling issues within the oxygen chamber and to avoid any form of stress (12, 21). Additionally, we used a CMH protocol that starts at E5 to include the neural stem cell expansion phase and therefore we cannot exclude specific effects raised in the early treatment phase. Particularly, the increased number Tbr1-positive cells indicate early effects of the oxygen treatment. Nevertheless, both specialized treatment schemes raise concerns about the effects of CMH on proper development of the brain.

In conclusion, maternal hyperoxygenation leads to increased oxygen tension in fetal brain tissue and affects cortical development in mice with a specific pattern depending on timing and length within the developmental process. While short-term maternal hyperoxygenation during midneurogenic phase can even enhance neurogenesis, a longer and very early oxygen application, such as CMH leads to severe reduction of proliferation and numbers of APs, likely ending in reduced neuron numbers and brain size as well as hampered cognitive functions (41). Although the consequences of maternal hyperoxygenation on brain function, such as cognition need to be determined, the

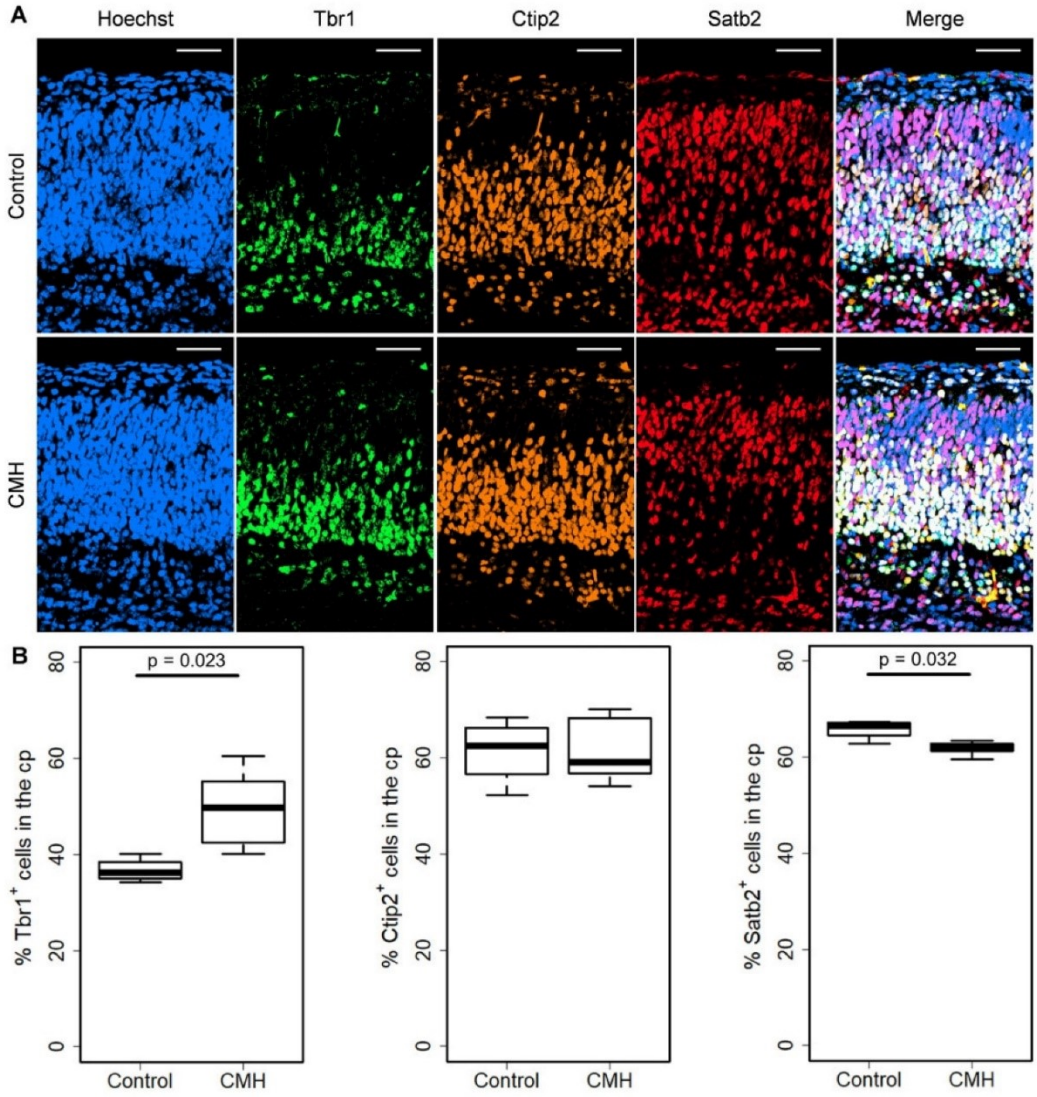

FIGURE 7. Chronic maternal hyperoxygenation (CMH) changes the distribution of neurons within the cortical layers. **(A)** Representative immunofluorescence images of Tbr1 (green), Ctip2 (orange), and Satb2 (red) expressing neurons counterstained with Hoechst (blue). Scale bars: 50 μm. **(B)** Quantification of cortical Tbr1-positive, Ctip-positive, and Satb2-positive neurons as percentage of all cells within the cortical plate (CP). Bars represent significant differences with displayed p values (unpaired two-sided *t*-test; n = 4 for controls; n = 5 for CMH).

effects of long-time maternal hyperoxygenation protocols on brain development require clarification. Further studies are thus needed to investigate the pathophysiological mechanisms underlying these findings and to assess the clinical and neurodevelopmental outcomes of the pups.

ACKNOWLEDGMENTS

We thank the team of the core facility Zentrale Versuchstierhaltung at the University of Rostock for providing the timed-pregnant mice and Uta Naumann, Jette Abel, and Franziska Alfen for their technical assistance.

REFERENCES

1. Manja V, Saugstad OD, Lakshminrusimha S. Oxygen saturation targets in preterm infants and outcomes at 18–24 months: A systematic review. Pediatrics 2017;139:e20161609
2. Sola A, Golombek SG, Montes Bueno MT, et al. Safe oxygen saturation targeting and monitoring in preterm infants: Can we avoid hypoxia and hyperoxia? Acta Paediatr 2014;103:1009–18
3. Sweet DG, Carnielli V, Greisen G, et al. European consensus guidelines on the management of respiratory distress syndrome—2016 update. Neonatology 2017;111:107–25
4. Kohl T. Chronic intermittent materno-fetal hyperoxygenation in late gestation may improve on hypoplastic cardiovascular structures associated with cardiac malformations in human fetuses. Pediatr Cardiol 2010;31:250–63
5. Lara DA, Morris SA, Maskatia SA, et al. Pilot study of chronic maternal hyperoxygenation and effect on aortic and mitral valve annular dimensions in fetuses with left heart hypoplasia. Ultrasound Obstet Gynecol 2016;48:365–72
6. Zeng S, Zhou J, Peng Q, et al. Sustained maternal hyperoxygenation improves aortic arch dimensions in fetuses with coarctation. Sci Rep 2016;6:39304
7. Channing A, Szwast A, Natarajan S, et al. Maternal hyperoxygenation improves left heart filling in fetuses with atrial septal aneurysm causing impediment to left ventricular inflow. Ultrasound Obstet Gynecol 2015;45:664–9
8. Dildy GA, Clark SL, Loucks CA. Intrapartum fetal pulse oximetry: The effects of maternal hyperoxia on fetal arterial oxygen saturation. Am J Obstet Gynecol 1994;171:1120–4
9. Haydon ML, Gorenberg DM, Nageotte MP, et al. The effect of maternal oxygen administration on fetal pulse oximetry during labor in fetuses with nonreassuring fetal heart rate patterns. Am J Obstet Gynecol 2006;195:735–8
10. Co-Vu J, Lopez-Colon D, Vyas HV, et al. Maternal hyperoxygenation: A potential therapy for congenital heart disease in the fetuses? A systematic review of the current literature. Echocardiography 2017;34:1822–33
11. Zhu LL, Wu LY, Yew DT, et al. Effects of hypoxia on the proliferation and differentiation of NSCs. Mol Neurobiol 2005;31:231–42
12. Wagenfuhr L, Meyer AK, Braunschweig L, et al. Brain oxygen tension controls the expansion of outer subventricular zone-like basal progenitors in the developing mouse brain. Development 2015;142:2904–15
13. Lee YM, Jeong CH, Koo SY, et al. Determination of hypoxic region by hypoxia marker in developing mouse embryos in vivo: A possible signal for vessel development. Dev Dyn 2001;220:175–86
14. Braunschweig L, Meyer AK, Wagenfuhr L, et al. Oxygen regulates proliferation of neural stem cells through Wnt/beta-catenin signalling. Mol Cell Neurosci 2015;67:84–92
15. Krabbe C, Bak ST, Jensen P, et al. Influence of oxygen tension on dopaminergic differentiation of human fetal stem cells of midbrain and forebrain origin. PLoS One 2014;9:e96465
16. Milosevic J, Schwarz SC, Krohn K, et al. Low atmospheric oxygen avoids maturation, senescence and cell death of murine mesencephalic neural precursors. J Neurochem 2005;92:718–29
17. Ortega JA, Sirois CL, Memi F, et al. Oxygen levels regulate the development of human cortical radial glia cells. Cereb Cortex 2017;27:3736–51
18. Yamazaki K, Fukushima K, Sugawara M, et al. Functional comparison of neuronal cells differentiated from human induced pluripotent stem cell-derived neural stem cells under different oxygen and medium conditions. J Biomol Screen 2016;21:1054–64
19. Storch A, Paul G, Csete M, et al. Long-term proliferation and dopaminergic differentiation of human mesencephalic neural precursor cells. Exp Neurol 2001;170:317–25
20. Lange C, Turrero Garcia M, Decimo I, et al. Relief of hypoxia by angiogenesis promotes neural stem cell differentiation by targeting glycolysis. EMBO J 2016;35:924–41
21. Wagenfuhr L, Meyer AK, Marrone L, et al. Oxygen tension within the neurogenic niche regulates dopaminergic neurogenesis in the developing midbrain. Stem Cells Dev 2016;25:227–38
22. Edwards LA, Lara DA, Sanz Cortes M, et al. Chronic maternal hyperoxygenation and effect on cerebral and placental vasoregulation and neurodevelopment in fetuses with left heart hypoplasia. Fetal Diagn Ther 2019;46:1–13
23. Molnár Z, Clowry GJ, Sestan N, et al. New insights into the development of the human cerebral cortex. J Anat 2019;235:432–51
24. Gotz M, Stoykova A, Gruss P. Pax6 controls radial glia differentiation in the cerebral cortex. Neuron 1998;21:1031–44
25. Haubensak W, Attardo A, Denk W, et al. Neurons arise in the basal neuroepithelium of the early mammalian telencephalon: A major site of neurogenesis. Proc Natl Acad Sci USA 2004;101:3196–201
26. Hutton SR, Pevny LH. SOX2 expression levels distinguish between neural progenitor populations of the developing dorsal telencephalon. Dev Biol 2011;352:40–7
27. Malatesta P, Hartfuss E, Gotz M. Isolation of radial glial cells by fluorescent-activated cell sorting reveals a neuronal lineage. Development 2000;127:5253–63
28. Noctor SC, Flint AC, Weissman TA, et al. Neurons derived from radial glial cells establish radial units in neocortex. Nature 2001;409:714–20
29. Noctor SC, Martinez-Cerdeno V, Ivic L, et al. Cortical neurons arise in symmetric and asymmetric division zones and migrate through specific phases. Nat Neurosci 2004;7:136–44
30. Noctor SC, Martinez-Cerdeno V, Kriegstein AR. Distinct behaviors of neural stem and progenitor cells underlie cortical neurogenesis. J Comp Neurol 2008;508:28–44
31. Noctor SC, Flint AC, Weissman TA, et al. Dividing precursor cells of the embryonic cortical ventricular zone have morphological and molecular characteristics of radial glia. J Neurosci 2002;22:3161–73
32. Bulfone A, Martinez S, Marigo V, et al. Expression pattern of the Tbr2 (Eomesodermin) gene during mouse and chick brain development. Mech Dev 1999;84:133–8
33. Englund C, Fink A, Lau C, et al. Pax6, Tbr2, and Tbr1 are expressed sequentially by radial glia, intermediate progenitor cells, and postmitotic neurons in developing neocortex. J Neurosci 2005;25:247–51
34. Gal JS, Morozov YM, Ayoub AE, et al. Molecular and morphological heterogeneity of neural precursors in the mouse neocortical proliferative zones. J Neurosci 2006;26:1045–56
35. Miyata T, Kawaguchi A, Saito K, et al. Asymmetric production of surface-dividing and non-surface-dividing cortical progenitor cells. Development 2004;131:3133–45
36. Agirman G, Broix L, Nguyen L. Cerebral cortex development: An outside-in perspective. FEBS Lett 2017;591:3978–92
37. Georgala PA, Manuel M, Price DJ. The generation of superficial cortical layers is regulated by levels of the transcription factor Pax6. Cereb Cortex 2011;21:81–94
38. Mohyeldin A, Garzon-Muvdi T, Quinones-Hinojosa A. Oxygen in stem cell biology: A critical component of the stem cell niche. Cell Stem Cell 2010;7:150–61
39. Mihalas AB, Elsen GE, Bedogni F, et al. Intermediate progenitor cohorts differentially generate cortical layers and require Tbr2 for timely acquisition of neuronal subtype identity. Cell Rep 2016;16:92–105
40. Sessa A, Ciabatti E, Drechsel D, et al. The Tbr2 molecular network controls cortical neuronal differentiation through complementary genetic and epigenetic pathways. Cereb Cortex 2017;27:3378–96
41. Tuoc TC, Radyushkin K, Tonchev AB, et al. Selective cortical layering abnormalities and behavioral deficits in cortex-specific Pax6 knock-out mice. J Neurosci 2009;29:8335–49
42. Quinn JC, Molinek M, Martynoga BS, et al. Pax6 controls cerebral cortical cell number by regulating exit from the cell cycle and specifies cortical cell identity by a cell autonomous mechanism. Dev Biol 2007;302:50–65
43. Stoykova A, Hatano O, Gruss P, et al. Increase in reelin-positive cells in the marginal zone of Pax6 mutant mouse cortex. Cereb Cortex 2003;13:560–71
44. Talamillo A, Quinn JC, Collinson JM, et al. Pax6 regulates regional development and neuronal migration in the cerebral cortex. Dev Biol 2003;255:151–63
45. Nishimura YV, Sekine K, Chihama K, et al. Dissecting the factors involved in the locomotion mode of neuronal migration in the developing cerebral cortex. J Biol Chem 2010;285:5878–87
46. Tsai JW, Chen Y, Kriegstein AR, et al. LIS1 RNA interference blocks neural stem cell division, morphogenesis, and motility at multiple stages. J Cell Biol 2005;170:935–45

4.3 Catecholaminergic Innervation of Periventricular Neurogenic Regions of the Developing Mouse Brain

Mareike Fauser, Grit Weselek, Christine Hauptmann, Franz Markert, Manfred Gerlach, Andreas Hermann & Alexander Storch

Frontiers in Neuroanatomy, 2020, Band 14, Artikel 558435

Zusammenfassung:

In dieser Studie wurde der Einfluss der Katecholamine Dopamin (DA) und Noradrenalin (NA) auf die fetale Neurogenese in verschiedenen Regionen des Gehirns untersucht. Dazu wurden die ventrikulären bzw. subventrikulären Zonen, welche das gesamte Ventrikelsystem umgeben, von verschiedenen Hirnregionen zu den Embryonalstadien (E) 14,5, E16,5 und zum Postnatalstadium (P) 0 isoliert und mittels HPLC auf ihren DA- und NA-Gehalt sowie mittels Immunhistochemie auf die Anzahl an $MCM2^+$ neuralen Stammzellen hin untersucht. Die Ergebnisse zeigen von E14,5 zu P0,5 eine kontinuierliche Abnahme an Stammzellen in allen Regionen. Der NA-Gehalt der jeweiligen Zonen steigt in diesem Zeitraum kontinuierlich an, während der DA-Gehalt nur an den lateralen Ventrikel zunimmt, in allen anderen Regionen allerdings abnimmt. Dabei offenbart sich eine starke inverse Korrelation der Anzahl an Vorläuferzellen mit dem NA-Gehalt der jeweiligen Regionen, nicht jedoch mit dem DA-Gehalt. Dies deutet auf einen potenziellen inhibitorischen Effekt durch NA auf die Vorläuferzellen des periventrikulären Systems während der Gehirnentwicklung hin. Die Daten stellen die Grundlage für weitere funktionelle Untersuchungen von Katecholaminen und insbesondere der noradrenergen Innervation und deren potenziell inhibitorischen Effekt auf neurale Stammzellen während der Entwicklung des Gehirns dar.

frontiers in Neuroanatomy

ORIGINAL RESEARCH
published: 23 September 2020
doi: 10.3389/fnana.2020.558435

Catecholaminergic Innervation of Periventricular Neurogenic Regions of the Developing Mouse Brain

Mareike Fauser[1†], Grit Weselek[1,2,3†], Christine Hauptmann[2], Franz Markert[1], Manfred Gerlach[4], Andreas Hermann[2,3,5‡] and Alexander Storch[1,3‡]*

[1]Department of Neurology, University of Rostock, Rostock, Germany, [2]Division of Neurodegenerative Diseases, Department of Neurology, Technische Universität Dresden, Dresden, Germany, [3]German Centre for Neurodegenerative Diseases (DZNE), Bonn, Germany, [4]Clinic for Child and Adolescent Psychiatry, Psychosomatics and Psychotherapy, Center for Mental Health, University Hospital Würzburg, Würzburg, Germany, [5]Translational Neurodegeneration Section "Albrecht-Kossel", Department of Neurology, University of Rostock, Rostock, Germany

OPEN ACCESS

Edited by:
Shigeo Okabe,
The University of Tokyo, Japan

Reviewed by:
Nobuhiko Yamamoto,
Osaka University, Japan
Yongsoo Kim,
Penn State Milton S. Hershey Medical Center, United States

***Correspondence:**
Alexander Storch
alexander.storch@med.uni-rostock.de

[†]*These authors have contributed equally to this work and share first authorship*

[‡]*These authors have contributed equally to this work and share last authorship*

Received: *02 May 2020*
Accepted: *28 August 2020*
Published: *23 September 2020*

Citation:
Fauser M, Weselek G, Hauptmann C, Markert F, Gerlach M, Hermann A and Storch A (2020) Catecholaminergic Innervation of Periventricular Neurogenic Regions of the Developing Mouse Brain. Front. Neuroanat. 14:558435. doi: 10.3389/fnana.2020.558435

The major catecholamines—dopamine (DA) and norepinephrine (NE)—are not only involved in synaptic communication but also act as important trophic factors and might ultimately be involved in mammalian brain development. The catecholaminergic innervation of neurogenic regions of the developing brain and its putative relationship to neurogenesis is thus of pivotal interest. We here determined DA and NE innervation around the ventricular/subventricular zone (VZ/SVZ) bordering the whole ventricular system of the developing mouse brain from embryonic day 14.5 (E14.5), E16.5, and E19.5 until postnatal day zero (P0) by histological evaluation and HPLC with electrochemical detection. We correlated these data with the proliferation capacity of the respective regions by quantification of $MCM2^+$ cells. During development, VZ/SVZ catecholamine levels dramatically increased between E16.5 and P0 with DA levels increasing in forebrain VZ/SVZ bordering the lateral ventricles and NE levels raising in midbrain/hindbrain VZ/SVZ bordering the third ventricle, the aqueduct, and the fourth ventricle. Conversely, proliferating $MCM2^+$ cell counts dropped between E16.5 and E19.5 with a special focus on all VZ/SVZs outside the lateral ventricles. We detected an inverse strong negative correlation of the proliferation capacity in the periventricular neurogenic regions (log-transformed $MCM2^+$ cell counts) with their NE levels ($r = -0.932$; $p < 0.001$), but not their DA levels ($r = 0.440$; $p = 0.051$) suggesting putative inhibitory effects of NE on cell proliferation within the periventricular regions during mouse brain development. Our data provide the first framework for further demandable studies on the functional importance of catecholamines, particularly NE, in regulating neural stem/progenitor cell proliferation and differentiation during mammalian brain development.

Keywords: brain development, ventricular zone, catecholamines, norepinephrine, dopamine, neurogenesis

INTRODUCTION

There is a multitude of research exploring the distribution of the major catecholamines—namely dopamine (DA) and norepinephrine (NE, also called noradrenaline)—in the mammalian brain including mammalian brain development. Noradrenergic neurons in the Locus coeruleus (LC) as the major noradrenergic formation in the mammalian brain are among the earliest born neurons followed by the dopaminergic system in later embryonic stages (Coyle, 1977; Steindler and Trosko, 1989; Pattyn et al., 2000; Aroca et al., 2006). LC neurons widely spread all over the brain with the striatum as one major exception (Foote et al., 1983; Erdtsieck-Ernste et al., 1991; Aston-Jones et al., 1995). Although the LC noradrenergic neurons are born early in development at around murine embryonic day 9 (E9)–E11 (all embryonic stages in this article are adapted to mouse embryonic ages post-fertilization through Carnegie stage comparisons; Lauder and Bloom, 1974; Coyle, 1977; Coyle and Molliver, 1977), the ascending noradrenergic projections throughout the brain needs several more days and reach the diencephalon at E13–E14 and cortical regions at E16–E17 with an increase in NE content as measured by HPLC of various brain areas starting around E15 to E17 in rodents depending on the brain region (Olson and Seiger, 1972; Lauder and Bloom, 1974; Coyle, 1977; Kohno et al., 1982; Berger and Verney, 1984; Murrin et al., 2007). The cortical distribution and density of NE fibers achieve their final pattern at postnatal day 7 (P7) and the adult extent in the 3rd to 4th postnatal week (Berger and Verney, 1984; Murrin et al., 2007). Similarly, tyrosine hydroxylase (TH) immunoreactivity in the ventral midbrain is detected from E11 to E12, and DA immunoreactivity is found from E12 (Olson and Seiger, 1972; Lauder and Bloom, 1974; Tomasini et al., 1997). This again contrasts with the later increase in DA tissue content from E13 to E15 (Ribary et al., 1986; Tomasini et al., 1997). The reported time offset between cellular and histological development of catecholaminergic systems and their subsequent functional development urgently necessitates the additive measurement of tissue levels of catecholaminergic neurotransmitters. Together, the development of both major catecholaminergic systems of the mammalian brain starts at a similar embryonic (postconceptional) age, is well pronounced during late embryonic development, and become functional just before birth. However, the available studies on catecholaminergic systems development strongly focused on neurotransmitter function within the nigrostriatal and mesolimbic dopaminergic system and the LC noradrenergic system innervating the cerebral cortex.

Catecholamines are not only involved in synaptic communication but also act as important trophic factors (Felten et al., 1982; Gustafson and Moore, 1987; Berger-Sweeney and Hohmann, 1997). In this respect, NE is considered to play a trophic role in brain maturation particularly cortical dendritic structuring (Felten et al., 1982; Gustafson and Moore, 1987; Berger-Sweeney and Hohmann, 1997). However, most studies used mechanical or toxic lesions of the NE system during the early postnatal period and only addressed cortical development (for review see Berger-Sweeney and Hohmann, 1997). The one study using prenatal lesioning of the NE system by intrauterine 6-hydroxydopamine application at E17 revealed no major alterations in cortical morphology in adulthood but did not study other brain regions (Lidov and Molliver, 1982). The more recent approach to disrupt NE innervation by knocking-out the gene encoding for dopamine-β-hydroxylase (DbH), the rate-limiting enzyme of NE production, showed that NE is essential for rodent fetal development with almost 100% mortality within the first days of life (Thomas et al., 1995). The brain morphology of these animals has however not been reported in detail yet. Substitution of NE by L-3, 4-dihydroxyphenylserine (DOPS) bypassing DbH restored NE synthesis and completely rescued the survival of DbH knock-out animals. However, in these mice, the postnatal development of the cerebellum and the noradrenergic systems was independent of NE (Jin et al., 2004). The reason for the prenatal mortality of DbH knock-out mice remains unclear but is most likely due to cardiovascular instability, which for unknown reasons stabilizes shortly after birth allowing the withdrawal of DOPS supplementation. Whether this instability arises from central or peripheral pathology remains enigmatic. The lethal phenotype without indirect NE supplementation during crucial developmental stages makes it impossible to accurately study embryonic/fetal brain development under NE depletion in this model. These data together with the recently described role of norepinephrine as a negative regulator of neural stem cell proliferation in the adult brain (Weselek et al., 2020) raised the question of whether catecholamines show analogous trophic actions during embryonic brain development beyond cortical development. We therefore comparatively determined the catecholaminergic innervation and the neural stem/progenitor cell proliferation capacity of the ventricular zone/subventricular zone (VZ/SVZ) bordering the whole ventricular system of the developing mouse brain from E14.5 until postnatal day zero (P0).

MATERIALS AND METHODS

Animals and Tissue Processing

Whole brains were dissected from embryos from timed-pregnant C57BL/6J mice at E14.5, E16.5, E19.5 (histology only), or newborn C57BL/6J mice (P0). All animal protocols were reviewed and approved by Animal Welfare Committee at the Technische Universität Dresden and Landesdirektion Sachsen, Dresden, Germany (governmental authorities). The tissue was fixed for 24 h in 4% paraformaldehyde (Merck, Darmstadt, Germany) and kept in 30% sucrose (Carl Roth, Karlsruhe, Germany) in PBS (Thermo Fisher Scientific, Waltham, MA, USA). Then brains were snap-frozen, coronal sections at 20 μm thickness were prepared using a cryotome (Leica Biosystems, Nussloch, Germany) and mounted on Superfrost Plus slides (Thermo Fisher Scientific, Waltham, MA, USA). The slides were stored at 4°C until staining. A total of three animals per group were examined for each experiment; all data

were gathered from randomly chosen fetuses from three independent litters.

Immunohistochemistry

Cryosections were pre-incubated in 3% blocking donkey serum (Jackson Immunoresearch, West Grove, IA, USA) containing 0.2% Triton X-100 (Thermo Fisher Scientific, Waltham, MA, USA) in PBS for 2 h at room temperature and then incubated overnight at 4°C with primary antibodies followed by secondary fluorescence conjugated antibodies for 1 h at room temperature. Cell nuclei were counterstained with 4,6-diamidino-2-phenylindole (DAPI, Thermo Fisher Scientific, Waltham, MA, USA). The following primary antibodies were used: sheep or rabbit anti-TH 1:500 (Pel-Freez, Rogers, Arkansas, RRID:AB_461070 and RRID:AB_461064); mouse anti-Nestin 1:500 (Chemicon, Thermo Fisher Scientific, RRID:AB_2251134); rat anti-DAT 1:500 (Merck, RRID:AB_2190413); rabbit anti-MCM2 1:500 (Abcam, Cambridge, UK, RRID:AB_881276; mouse anti-NET 1:200 (MAB Technologies, Neenah, WI, USA, RRID:AB_2571639). Fluorescence labeled secondary antibodies were purchased from (Molecular Probes, Thermo Fisher Scientific, Waltham, MA, USA). Images were captured using a fluorescence microscope (Leica DM IRE2, Wetzlar, Germany) or a Zeiss confocal microscope (LSM 700; Zeiss, Oberkochen, Germany) equipped with DAPI/UV, krypton, krypton/argon, and helium lasers.

HPLC Assay of Tissue Catecholamine Content

Tissue from the same periventricular regions (200 μm surrounding the ventricles) as those used for immunohistochemistry was microdissected from mouse brains at E14.5, E16.5, P0 and adult (8–12 weeks of age, male). For this purpose, the brains were removed from out of the skull and sliced into coronal sections of approximately 1 mm which were kept on ice or a cooling plate until further preparation. With the help of a dissection microscope (magnification: ×100) approximately 200 μm tissue surrounding the ventricles at the appropriate zone was removed by one experienced experimenter (Grit Weselek) and the pieces were snap-frozen in liquid nitrogen. The 200 μm were chosen to secure enough material for HPLC analysis while including the major part of VZ/SVZ. For further HPLC analysis, the tissue samples were thawed, weighed, and sonicated in 0.05 M perchloric acid for 60 s resulting in 10% (w/v) homogenate suspensions. The mean ± s.e.m. weights of tissue samples of 22 ± 2 (range: 9–45) mg per tissue sample were in the typical range of previous studies (Wagner et al., 1982) and did not show any significant differences between experimental conditions (two-way ANOVA with VZ regions and developmental stages as fixed factors revealed no significant interaction effect of VZ regions and stages on tissue sample weights ($p = 0.225$, F-value = 1.4) and no significant differences among VZ regions ($p = 0.468$, F-value = 0.9) and stages ($p = 0.840$, F-value = 0.2). These were centrifuged at 48,000× g for 20 min at 4°C, and 50 μl samples of the supernatants injected directly into high-performance liquid chromatography (HPLC) system with electrochemical detection (Gynkotek GmbH, Germering, Germany) for analysis of tissue DA, NE, and epinephrine according to the method described in detail previously (Wagner et al., 1982; Gerlach et al., 1996; Kuhn et al., 1996). The HPLC system consisted of an AGILENT 1100 series (Bio-Rad, Munich, Germany), a Nucleosil 120-5C18 reverse phase (250 × 4.6 mm) analytical column (Macherey-Nagel, Düren, Germany), an electrochemical detector (model 1640; Bio-Rad, Munich, Germany). Detector data were recorded and analyses using an AGILENT Chem Station for LC9D (Bio-Rad). Concentrations were calculated from the peak height with the aid of an external standard. The detection limit of the HPLC system was 0.1 ng/ml (corresponding to 1 ng/g brain tissue) for all catecholamines. The investigator was blind to the experimental condition.

Cell Counting and Statistical Analysis

For quantification of proliferating mini-chromosome maintenance protein 2 $(MCM2)^+$ cells within the ventricular zone/subventricular zone (VZ/SVZ) of the various periventricular regions [lateral wall of the lateral ventricles ($LV_{lateral}$), medial wall of the lateral ventricles (LV_{medial}), third ventricle (3V), aqueduct (Aq) and fourth ventricle (4V) according to the Prenatal Mouse Brain Atlas by Schambra (Schambra, 2008)], in any given experiment the number of $MCM2^+$ cells was determined in a 130 μm section along the VZ/SVZ of every 12th coronal section using laser scanning confocal microscopy images processed with ImageJ [National Institutes of Health (NIH), Bethesda, MD, USA]. Data are displayed as normalized to 100 μm^2 VZ/SVZ surface area for each region. Statistical analyses were done with SPSS software, version 21.0 or newer (SPSS, Chicago, IL, USA). We applied various linear and nonlinear regression analyses and logarithm functions nicely matching the $MCM2^+$ cell counts and NE levels and rendered a correlation coefficient (r^2) that was 0.858. Curve linearization was thus made by log transformation of results. Correlation analyses to assess the association of stem cell proliferation within the VZ/SVZ with catecholamine levels by using multiple linear regression analyses and Pearson correlation. Comparisons were made, as appropriate, with a two-sample t-test, Mann–Whitney U test, or χ^2 test. Two-sided p-values of less than 0.05 were deemed statistically significant.

RESULTS

Formation of a Rostrocaudal Proliferation Gradient Within the VZ/SVZ During Mouse Brain Development

Even though the proliferation capacity of the forebrain proliferative zone (ventricular zone/subventricular zone [VZ/SVZ]) bordering the lateral ventricles on their lateral side ($LV_{lateral}$) during mouse brain development is already described in detail, the time course of proliferation changes within the VZ/SVZ of the medial wall of the LV (LV_{medial}) and within the more caudal VZ/SVZ bordering the third ventricle (3V), the aqueduct (Aq) and the fourth ventricle (4V) is

not described in detail yet. To determine the proliferation capacity within the VZ/SVZ of the developing mouse brain, we here used the DNA replication licensing factor MCM2 as an established proliferation marker of Nestin$^+$ neural stem/progenitor cells (von Bohlen und Halbach, 2011). As shown in **Figures 1A,B**, quantitative immunohistochemistry revealed a dramatic reduction to almost complete loss of proliferating (MCM2$^+$) neural stem/progenitor cells within all proliferative zones between E14.5 and E19.5 except for the VZ/SVZ of $LV_{lateral}$. There were no relevant changes in proliferation patterns between E19.5 and P0. Together, we demonstrated the formation of a rostrocaudal gradient of the VZ/SVZ proliferation capacity during mouse brain development established between E14.5 and E16.5 and persisting until birth with high proliferation capacity in the rostral part (proliferative zone of the $LV_{lateral}$) down to a low proliferation capacity in the VZ/SVZ surrounding the third-to-fourth ventricle.

Catecholaminergic Innervation of the VZ/SVZ During Mouse Brain Development

Catecholaminergic innervation of the developing mouse brain was determined by immunostaining against the common catecholaminergic marker tyrosine hydroxylase (TH), the dopamine transporter (DAT), and norepinephrine transporter (NET) at E14.5, E16.5, and P0. **Figure 2** shows representative immunohistological microphotographs of TH as well as of DAT and NET staining during mouse brain development. Histology data demonstrated an increase of TH$^+$ fibers in all VZ/SVZ and adjacent regions during development after E14.5, but differential patterns of DAT$^+$ and NET$^+$ fibers: While DAT$^+$ innervation increased between E16.5 and P0 within the striatum and the adjacent proliferative zone of the $LV_{lateral}$, we did not detect relevant changes in striatal NET$^+$ fibers in the respective region. In all other VZ/SVZ regions, we detected no relevant changes in DAT$^+$ fiber density during brain development (**Figure 2**). In contrast, NET$^+$ fiber intensity displayed an increase during development after E14.5 in brain tissue surrounding the caudal VZ/SVZ regions of the 3V and Aq.

To confirm the functional catecholaminergic innervation of the VZ/SVZ, i.e., the actual catecholamine releases, we measured the levels of DA, NE, and epinephrine in microdissected proliferative zones periventricular regions containing the VZ/SVZ of the developing mouse brain at E14.5, E16.5, and P0 using an HPLC-electrochemical detection-based method. Since the thickness of the VZ/SVZ areas varies within the developing brain and changes during the developmental process and may thus not exactly correspond to the analyzed tissue samples, the preparation method used does not fully rule out partial contamination of HPLC samples with periventricular regions outside the VZ/SVZ. Nevertheless, in agreement with the DAT histology data, DA showed increased levels in the VZ/SVZ of the $LV_{lateral}$ at P0, while there was a continuous decline during development in the caudal VZ/SVZ regions (**Figure 3A**, for statistics, refer to **Supplementary Table S2**). In contrast, in correspondence with the NET staining, NE levels showed continuously increasing levels in the caudal (hindbrain) VZ/SVZ regions during development between E16.5 and P0 (**Figure 3B**, **Supplementary Table S3**). The pattern of catecholaminergic innervation was similar at P0 compared to the adult, even though the catecholamine levels in the adult brain were much higher compared to the developing brain (**Supplementary Figure S1**). We did not detect epinephrine/adrenaline (<1 ng/g brain tissue) in any VZ/SVZ region of the developing and adult mouse brain.

Correlations Between Catecholaminergic Innervation and Stem Cell Proliferation

We assessed potential associations of the periventricular proliferative capacity of MCM2$^+$ neural stem/progenitor cells within the VZ/SVZ with periventricular DA and NE levels, developmental stages, and periventricular brain regions (**Figure 4**). Pearson correlation tests revealed correlations with a magnitude greater than |0.5| of log-transformed MCM2$^+$ cell counts with NE levels (Pearson correlation coefficient $r = -0.932$; $p < 0.001$) and developmental stages ($r = -0.789$; $p < 0.001$). We found no correlations with a magnitude greater than |0.5| of log-transformed MCM2$^+$ cell counts with DA levels ($r = 0.440$; $p = 0.051$) and brain regions ($r = -0.328$; $p = 0.117$). Multiple linear regression model analysis revealed that log-transformed MCM2$^+$ cell counts were significantly associated only with NE levels (corrected $r^2 = 0.858$, $\beta = -0.701$, $p = 0.003$), but not with DA levels ($\beta = 0.045$, $p = 0.694$), developmental stage ($\beta = -0.264$, $p = 0.137$) or brain region ($\beta = -0.053$, $p = 0.674$). Hierarchical stepwise multiple regression analysis using sequences of F-tests confirmed that VZ/SVZ log-transformed MCM2$^+$ cell counts were significantly correlated with NE levels.

DISCUSSION

We investigated the specific catecholaminergic innervation of the proliferative zones (VZ/SVZ) in the developing mouse brain and its putative association with their respective proliferation capacities throughout the ventricular system. We thereby demonstrate an inverse logarithmic correlation of the proliferation capacity of the VZ/SVZ with the NE content of the corresponding area during brain development, but no correlation with their DA levels. Since the NE neurotransmitter system develops after E14.5 in the midbrain/hindbrain regions bordering the ventricular system and omits the striatum, it is of particular relevance for the caudal VZ/SVZ regions. **Figure 5** displays a graphical synopsis summarizing the association of the catecholaminergic neurotransmitter systems development with the proliferation capacity in the VZ/SVZ bordering the ventricular system from its rostral (forebrain $LV_{lateral}$) to the caudal parts within the midbrain/hindbrain (3V through 4V) during mouse brain development. These data imply that NE might be a putative humoral factor involved in the physiological decrease of neural stem/progenitor cell proliferation during prenatal development. Consistently, we recently detected a similar role of NE in the adult brain with inhibitory effects on the proliferative activity of adult

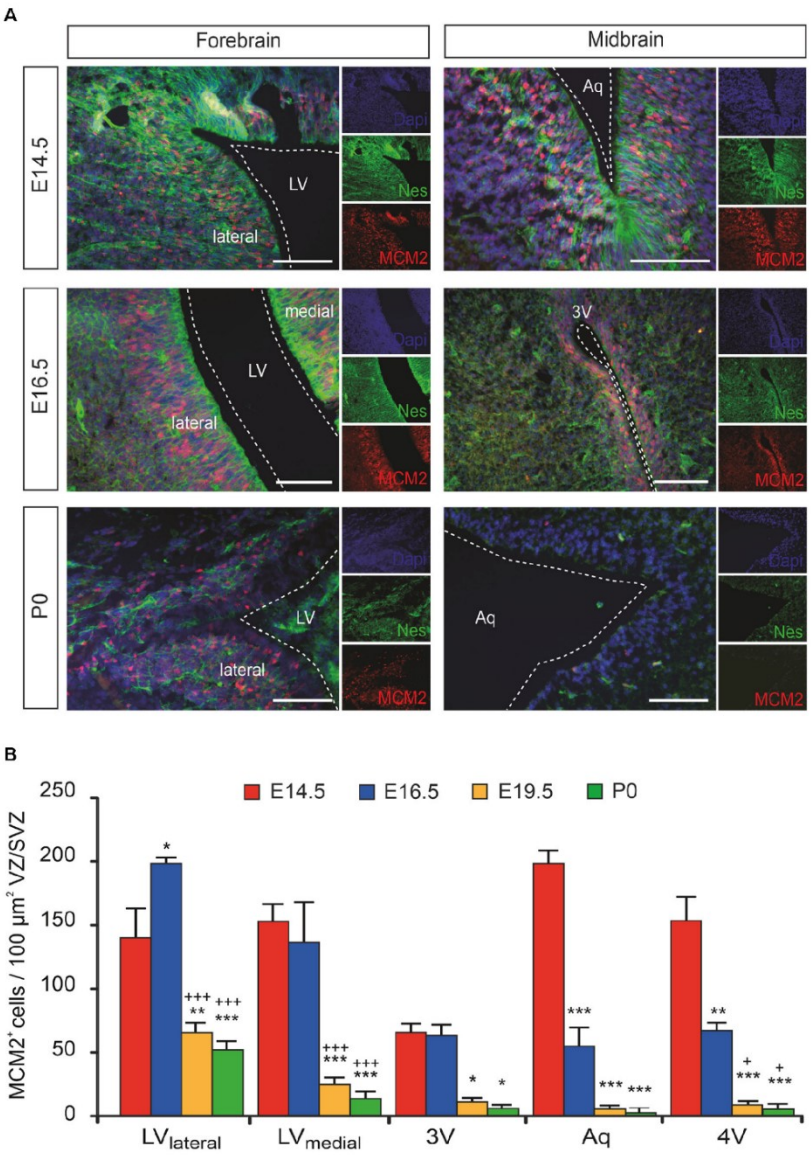

FIGURE 1 | The proliferation of ventricular/subventricular zone (VZ/SVZ) neural stem/progenitor cells (NPCs) within the developing mouse forebrain and midbrain at E14.5, E16.5, E19.5 (quantitative results only), and P0. **(A)** Proliferating stem/progenitor cells were co-stained with MCM2 (red) and Nestin (green) in VZ/SVZ. Cell nuclei are counterstained with 4,6-diamidino-2-phenylindole (DAPI). Scale bar: 50 µm. **(B)** Quantitative immunohistochemistry revealed a dramatic reduction to almost complete loss of proliferating ($MCM2^+$) cells during development within the VZ/SVZs except for the lateral VZ/SVZ of the lateral ventricles. Two-way ANOVA with *post hoc t*-test and Bonferroni adjustment with VZ/SVZ regions and developmental stages as fixed factors revealed that brain regions and embryonic stages had a significant interaction effect on $MCM2^+$ cells per 100 μm^2 ($P < 0.001$, F-value = 5.7) and significant differences among VZ/SVZ regions ($P < 0.001$, F-value = 17.1) and embryonic stages ($P < 0.001$, F-value = 95.0). P-values from *post hoc* tests with Bonferroni adjustment are $^*P < 0.05$, $^{**}P < 0.01$ and $^{***}P < 0.001$ when compared to E14.5 and $^+P < 0.05$ and $^{+++}P < 0.001$ when compared to E16.5 (only P-values among developmental stages are displayed for clarity; complete statistics in **Supplementary Tables S1A,B**). 3V, third ventricle; Aq, aqueduct; LV, lateral ventricle; $LV_{lateral}$, lateral wall of the lateral ventricles; LV_{medial}, medial wall of the lateral ventricles; MCM2, mini-chromosome maintenance protein 2; Nes, Nestin.

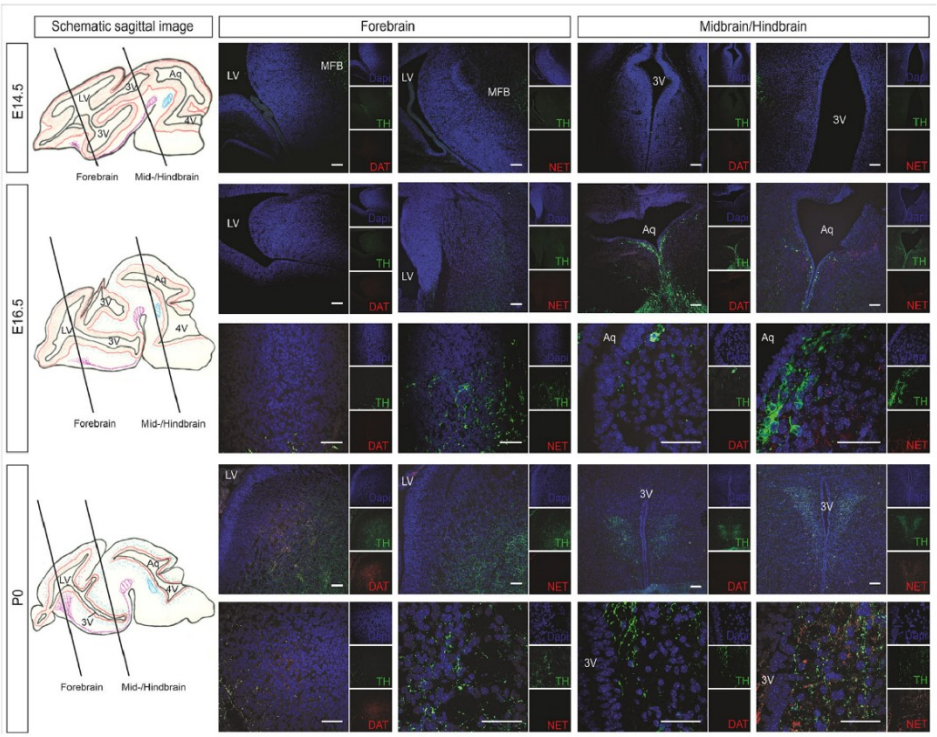

FIGURE 2 | Catecholaminergic innervation of the developing mouse brain (at developmental stages E14.5, E16.5, and P0) determined by immunostaining against the DAT and NET. The left panel shows schematic sagittal brain images illustrating the forebrain and midbrain/hindbrain sections. Representative immunohistological microphotographs of TH in green as a marker for catecholaminergic neurons as well as of DAT as a marker for dopaminergic cells and NET for norepinephrinergic cells. Lower panels in E16.5 and P0 represent individual images of forebrain or midbrain/hindbrain sections in higher magnification. Cell nuclei are counterstained with DAPI. Scale bars: 100 μm (E14.5, upper panels of E16.5 and P0) and 50 μm (lower panels of E16.5 and P0). 3V, third ventricle; Aq, aqueduct; DAT, dopamine transporter; LV, lateral ventricle; MFB, medial forebrain bundle; NET, norepinephrine transporter; TH, tyrosine hydroxylase.

neural stem cells in the consecutive neurogenic regions (Weselek et al., 2020). However, the physiological significance of our present findings needs to be determined by functional studies, for example by pharmacologic or genetic manipulation of DA and/or NE levels during the various development stages of the brain.

We used mini-chromosome maintenance protein 2 (MCM2) as a marker for proliferating cells because it is known to be directly involved in the cell cycle process through licensing DNA replication (Masai et al., 2010; Kuipers et al., 2011) and therefore marks proliferating regions (Maslov et al., 2007). Unlike other common markers, such as ph3 or Ki67, MCM2 is required for the initial cell cycling process (Stoeber et al., 2001). This allows the analysis of a broader spectrum of proliferating cells as compared to ph3 and gave a better signal than most Ki67 stainings. Regarding validity, MCM2 shows a good correlation with standard methods for *in vivo* proliferation analysis like thymidine analog labeling (Maslov et al., 2004) with the advantage of being independent of cell cycle length which may alternate during development and stem cell population (Calegari and Huttner, 2003; Calegari et al., 2005). MCM2 is expressed in adult as well as in embryonal neural stem cells *in vivo* (Berg et al., 2019). Together, MCM2 is—although not often used—a well-characterized and established marker for proliferation analysis in brain development (von Bohlen und Halbach, 2011).

A large body of research during the late 1980s and 1990s explored the development of the two major catecholaminergic neurotransmitter systems in the mammalian brain. All these studies looked at these systems as developing neurotransmitter systems, but could not focus on the regulation of neurogenesis or brain development, since the knowledge of such regulatory functions of neurotransmitters was rather limited at that time. Consequently, dopaminergic innervation was studied mainly in the nigrostriatal and mesolimbic systems, and

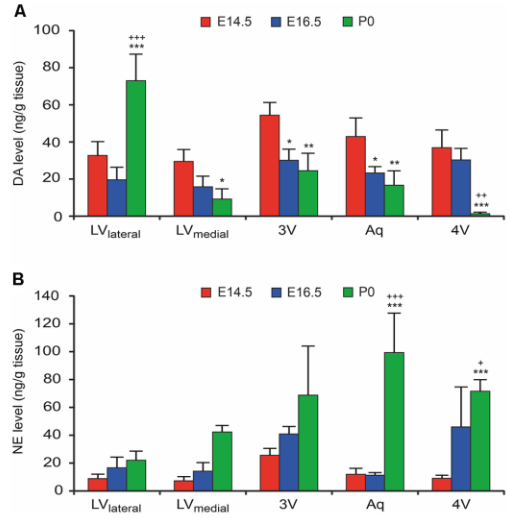

FIGURE 3 | Catecholamine levels in microdissected VZ/SVZ regions of the developing mouse brain (at developmental stages E14.5, E16.5. and P0). Catecholamine levels were measured in microdissected VZ/SVZ regions using an HPLC with electrochemical detection and normalized to tissue weight. **(A)** Dopamine (DA) levels were increasing in the VZ/SVZ of the LV lateral walls ($LV_{lateral}$), while they were continuously declining during development in the caudal VZ/SVZ regions. Two-way ANOVA with brain regions and developmental stages as fixed factors revealed that VZ/SVZ regions and stages had a significant interaction effect on DA levels ($P < 0.001$, F-value = 13.3) and significant differences among VZ/SVZ regions ($P < 0.001$, F-value = 10.3) and stages ($P < 0.001$, F-value = 14.1). **(B)** In contrast to DA, norepinephrine (NE) showed continuously increasing levels in the caudal (hindbrain) VZ/SVZ regions during development. Two-way ANOVA revealed that VZ/SVZ regions and stages had a significant interaction effect on NE levels ($P = 0.001$, F-value = 4.3) and significant differences among VZ/SVZ regions ($P = 0.003$, F-value = 5.3) and stages ($P < 0.001$, F-value = 32.4). P-values from *post hoc* tests with Bonferroni adjustment are $^{*}P < 0.05$, $^{**}P < 0.01$ and $^{***}P < 0.001$ when compared to E14.5 and $^{+}P < 0.05$, $^{++}P < 0.01$ and $^{+++}P < 0.001$ when compared to E16.5 (only P-values among developmental stages are displayed for clarity; complete statistics in **Supplementary Tables S2**, **S3**). 3V, third ventricle; 4V, fourth ventricle; Aq, aqueduct; $LV_{lateral}$, lateral wall of the lateral ventricles; LV_{medial}, medial wall of the lateral ventricles.

noradrenergic innervation was investigated mainly preferentially in cortical areas and the hypothalamus (Coyle and Molliver, 1977; Levitt and Moore, 1979; Berger and Verney, 1984), but no data on catecholaminergic innervation of the VZ/SVZ as the main proliferating zone of the developing brain are available. Even though the two systems develop in parallel with increasing innervation of the VZ/SVZ in perinatal stages (between E16.5 and P0), we found different innervation patterns of the periventricular regions mainly containing the VZ/SVZ by the two catecholamines largely reaching the adult patterns at birth (P0): While the dopaminergic innervation focusses on the VZ/SVZ of the $LV_{lateral}$ close to the striatum, the noradrenergic innervation omits the striatum and the adjacent periventricular region but instead reaches the midbrain/hindbrain periventricular regions. These results closely fit data from previous studies showing noradrenergic innervation in the diencephalon surrounding the 3rd ventricle and dopaminergic innervation in the striatum adjacent to the $LV_{lateral}$ between E13 and E15 (Olson and Seiger, 1972; Ribary et al., 1986; Tomasini et al., 1997). Of note, although the general patterns of catecholaminergic innervation levels match the adult situation already in the early postnatal period, brain catecholamine levels are much higher in the adult brain compared to perinatal stages due to further postnatal maturation of the two catecholaminergic systems (Berger and Verney, 1984; Ribary et al., 1986; Tomasini et al., 1997; Murrin et al., 2007).

The major catecholamines DA and NE are pleiotropic molecules and do not only play a pivotal role in synaptic neurotransmission but are also involved in brain maturation (Felten et al., 1982; Gustafson and Moore, 1987; Berger-Sweeney and Hohmann, 1997). Particularly NE is expressed during early embryonic development and regulates both the development of the respective neuronal population and the development of its various target areas including the cortex (Berger-Sweeney and Hohmann, 1997). Consistently, the NE system regulates the development of the Cajal-Retzius cells as the first cortical neurons and is thus considered to be involved in neuronal migration and laminar formation most likely *via* α2 adrenergic receptor signaling (Wang and Lidow, 1997; Naqui et al., 1999). All these studies applied lesions of the NE system during the early postnatal period and mainly addressed cortical development and in some cases also cerebellar development (for review see Berger-Sweeney and Hohmann, 1997; Saboory et al., 2020). A single study reporting the effects of severe prenatal lesioning of the NE system by the intrauterine 6-hydroxydopamine application at E17 revealed no major alterations in cortical morphology in adulthood but did not study other brain regions (Lidov and Molliver, 1982). Our data provide first morphological evidence to support putative pleiotropic effects of NE even during earlier stages of brain development mainly in the diencephalic region as one region with high periventricular NE innervation: we detected an inverse strong negative correlation of the proliferation capacity in the periventricular neurogenic regions with their NE levels ($r = -0.932$ for log-transformed counts of proliferating cells; $P < 0.001$), but not their DA levels. Though, a functionally relevant inhibitory effect of NE on stem cell proliferation within the periventricular regions during development still needs to be confirmed by future pharmacological and genetic studies. are warranted to show the functional importance of these findings, our data suggest potent inhibitory effects of NE on stem cell proliferation within the periventricular regions during development. Consistently, prenatal treatment of rats with β-adrenoceptor agonists at gestational days 17–20 results in decreased cell numbers in the fetal brain through cAMP production in target cells (Garofolo et al., 2003; Slotkin et al., 2003). This sensitive developmental stage closely corresponds to parallels the stage of increasing NE levels and decreasing cell proliferation within the mouse

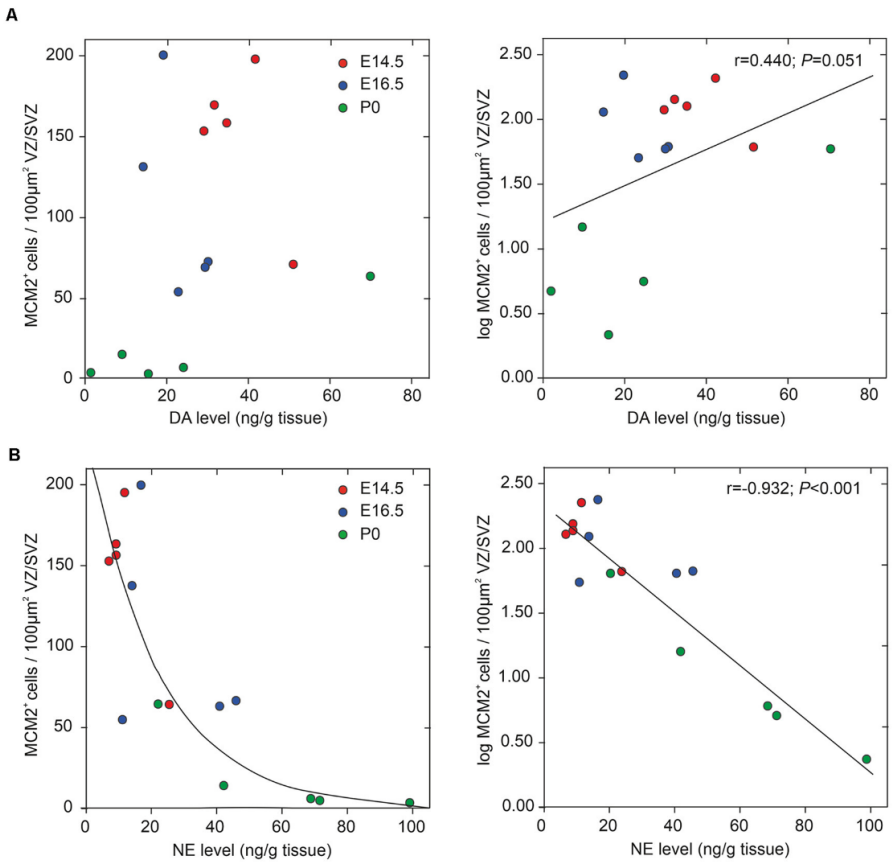

FIGURE 4 | Correlation between periventricular catecholamine levels and neural stem/progenitor cells (NPC) proliferation in VZ/SVZ regions (at developmental stages E14.5, E16.5, and P0). NPC proliferation rate was estimated by quantitative MCM2 immunohistochemistry and DA levels **(A)** and NE levels **(B)**, respectively, were measured in microdissected VZ/SVZ regions using HPLC with electrochemical detection. Pearson correlation tests revealed correlations with a magnitude greater than |0.5| of log-transformed MCM2$^+$ cell counts with NE levels, but not with DA levels ($r = 0.440$; $p = 0.051$). The Pearson correlation coefficients for the respective variables are displayed in the upper right part of the graphs. Multiple linear regression model analysis revealed that log-transformed MCM2$^+$ cell counts were significantly associated only with NE levels (corrected $r^2 = 0.858$, $\beta = -0.701$, $p = 0.003$), but not with DA levels ($\beta = 0.045$, $p = 0.694$), embryonic stage ($\beta = -0.264$, $p = 0.137$) or brain region ($\beta = -0.053$, $p = 0.674$).

VZ/SVZ at E16.5 to P0. Unfortunately, there are no detailed brain morphology studies in genetic NE depleted mice (DbH knockout mice) available, most likely due to the almost 100% early postnatal mortality without indirect NE substitution during development (Thomas et al., 1995; Jin et al., 2004). The lethal phenotype without NE supplementation during crucial developmental stages however makes it impossible to accurately study embryonic/fetal brain development under NE depletion in this model. Nevertheless, these data in the fetal brain are in strong agreement with the inhibitory effects of NE on neural stem/progenitor cell proliferation within the periventricular regions of the adult mouse brain most likely also mediated through direct stimulation of β-adrenoceptors (Weselek et al., 2020).

Together, the levels of the two major catecholamines DA and NE dramatically increased within the VZ/SVZ area of the developing brain between E16.5 and P0 with DA levels increasing in forebrain VZ/SVZs bordering the $LV_{lateral}$ and NE levels raising in midbrain/hindbrain VZ/SVZs bordering the third ventricle, the aqueduct, and the fourth ventricle. Conversely, the number of proliferating cells of the VZ/SVZ areas dropped between E16.5 and E19.5 with a special focus on all VZ/SVZs outside the lateral ventricles leading to an inverse strong negative correlation of the proliferation capacity in the

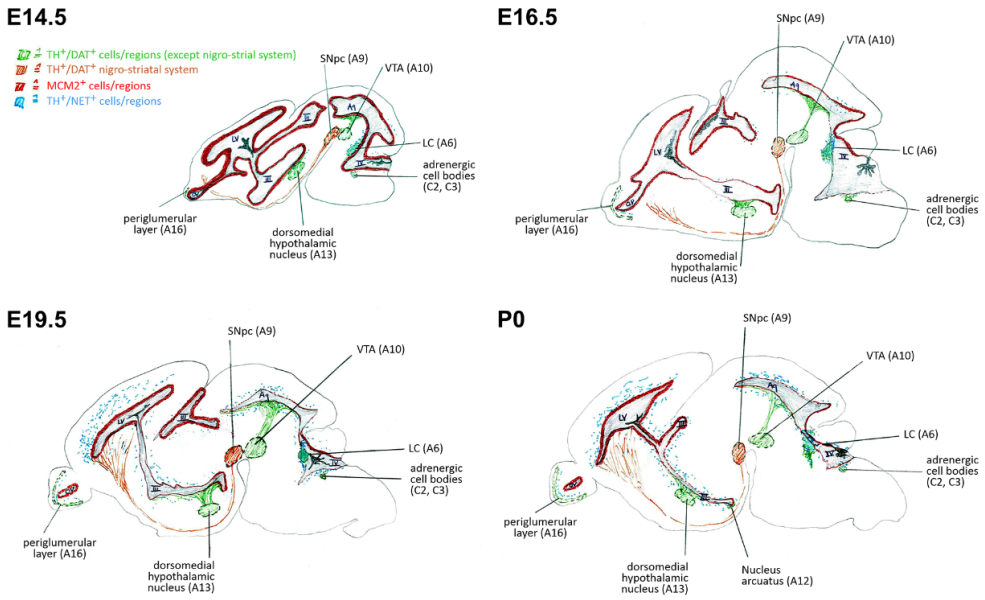

FIGURE 5 | Schematic representation of correlations of neural stem/progenitor cell proliferation and catecholaminergic innervation within VZ/SVZ regions at E14.5, E16.5, E19.5, and P0. III, third ventricle; IV, fourth ventricle; Aq, aqueduct; DAT, dopamine transporter; LC, *locus coeruleus*; LV, lateral ventricle; MCM2, mini-chromosome maintenance protein 2; NET, norepinephrine transporter; OV, olfactory ventricle; SNpc, *substantia nigra pars compacta*; TH, tyrosine hydroxylase; VTA, ventral tegmental area.

periventricular neurogenic regions with their NE levels. These results are backed by our recent findings of direct negative effects of NE on the proliferation of adult periventricular neural stem/progenitor cells (Weselek et al., 2020). Our data provide the first framework to further study the potential functional importance of catecholamines—particularly NE—in regulating neural stem and progenitor cell proliferation and differentiation during mammalian brain development.

DATA AVAILABILITY STATEMENT

The raw data supporting the conclusions of this article will be made available by the authors, without undue reservation.

ETHICS STATEMENT

The animal study was reviewed and approved by Animal Welfare Committee at the Technische Universität Dresden and Landesdirektion Sachsen (governmental authorities).

AUTHOR CONTRIBUTIONS

GW, AH and AS substantially contributed to the study concept and design, acquisition of data, analyzing of data, interpretation of data, drafting and finalizing the manuscript. MG and CH substantially contributed to the acquisition of data, analyzing of data and interpretation of data. MF and FM substantially contributed to the interpretation of data, drafting and finalizing the manuscript. All authors critically revised the final manuscript.

FUNDING

This work was supported by the Deutsche Forschungsgemeinschaft (DFG) through the Collaborative Research Centres CRC 655 "Cells into Tissue" (project A23). MF was supported by the CRC 1270 "Electrically Active Implants" (DFG; SFB 1270/1-299150580) through the rotation position program for clinician scientists. AH was supported by the Hermann and Lilly Schilling-Stiftung für medizinische Forschung im Stifterverband.

ACKNOWLEDGMENTS

We would like to thank Sylvia Kanzler, Andrea Kempe, and Cornelia May for their technical support.

SUPPLEMENTARY MATERIAL

The Supplementary Material for this article can be found online at: https://www.frontiersin.org/articles/10.3389/fnana.2020.558435/full#supplementary-material.

REFERENCES

Aroca, P., Lorente-Cánovas, B., Mateos, F. R., and Puelles, L. (2006). Locus coeruleus neurons originate in alar rhombomere 1 and migrate into the basal plate: studies in chick and mouse embryos. *J. Comp. Neurol.* 496, 802–818. doi: 10.1002/cne.20957

Aston-Jones, G., Shipley, M. T., and Grzanna, R. (1995). "The locus coeruleus, A5 and A7 noradrenergic cell groups," in *The Rat Nervous System*, ed. G. Paxinos, 2nd Edn (New York: Academic Press), 183–214.

Berg, D. A., Su, Y., Jimenez-Cyrus, D., Patel, A., Huang, N., Morizet, D., et al. (2019). A common embryonic origin of stem cells drives developmental and adult neurogenesis. *Cell* 177, 654.e15–668.e15. doi: 10.1016/j.cell.2019.02.010

Berger, B., and Verney, C. (1984). "Development of the catechoamine innervation in rat neocortex: morphological features," in *Monoamine Innervation of Cerebral Cortex*, eds L. Descarries, T. R. Reader, H. H. Jasper (New York, NY: Liss), 95–121.

Berger-Sweeney, J., and Hohmann, C. F. (1997). Behavioral consequences of abnormal cortical development: insights into developmental disabilities. *Behav. Brain Res.* 86, 121–142. doi: 10.1016/s0166-4328(96)02251-6

Calegari, F., Haubensak, W., Haffner, C., and Huttner, W. B. (2005). Selective lengthening of the cell cycle in the neurogenic subpopulation of neural progenitor cells during mouse brain development. *J. Neurosci.* 25, 6533–6538. doi: 10.1523/JNEUROSCI.0778-05.2005

Calegari, F., and Huttner, W. B. (2003). An inhibition of cyclin-dependent kinases that lengthens, but does not arrest, neuroepithelial cell cycle induces premature neurogenesis. *J. Cell Sci.* 116, 4947–4955. doi: 10.1242/jcs.00825

Coyle, J. T. (1977). Biochemical aspects of neurotransmission in the developing brain. *Int. Rev. Neurobiol.* 20, 65–103. doi: 10.1016/s0074-7742(08)60651-0

Coyle, J. T., and Molliver, M. E. (1977). Major innervation of newborn rat cortex by monoaminergic neurons. *Science* 196, 444–447. doi: 10.1126/science.850788

Erdtsieck-Ernste, B. H., Feenstra, M. G., and Boer, G. J. (1991). Pre- and postnatal developmental changes of adrenoceptor subtypes in rat brain. *J. Neurochem.* 57, 897–903. doi: 10.1111/j.1471-4159.1991.tb08235.x

Felten, D. L., Hallman, H., and Jonsson, G. (1982). Evidence for a neurotropic role of noradrenaline neurons in the postnatal development of rat cerebral cortex. *J. Neurocytol.* 11, 119–135. doi: 10.1007/bf01258008

Foote, S. L., Bloom, F. E., and Aston-Jones, G. (1983). Nucleus locus ceruleus: new evidence of anatomical and physiological specificity. *Physiol. Rev.* 63, 844–914. doi: 10.1152/physrev.1983.63.3.844

Garofolo, M. C., Seidler, F. J., Cousins, M. M., Tate, C. A., Qiao, D., and Slotkin, T. A. (2003). Developmental toxicity of terbutaline: critical periods for sex-selective effects on macromolecules and DNA synthesis in rat brain, heart and liver. *Brain Res. Bull.* 59, 319–329. doi: 10.1016/s0361-9230(02)00925-5

Gerlach, M., Gsell, W., Kornhuber, J., Jellinger, K., Krieger, V., Pantucek, F., et al. (1996). A post mortem study on neurochemical markers of dopaminergic, GABA-ergic and glutamatergic neurons in the motor circuit of basal ganglia in Parkinson's disease. *Brain Res.* 741, 142–152. doi: 10.1016/s0006-8993(96)00915-8

Gustafson, E. L., and Moore, R. Y. (1987). Noradrenaline neuron plasticity in developing rat brain: effects of neonatal 6-hydroxydopamine demonstrated by dopamine-beta-hydroxylase immunocytochemistry. *Brain Res.* 465, 143–155. doi: 10.1016/0165-3806(87)90236-7

Jin, S.-H., Kim, H. J. T., Harris, D. C., and Thomas, S. A. (2004). Postnatal development of the cerebellum and the CNS adrenergic system is independent of norepinephrine and epinephrine. *J. Comp. Neurol.* 477, 300–309. doi: 10.1002/cne.20263

Kohno, Y., Tanaka, M., Nakagawa, R., Ida, Y., Iimori, K., and Nagasaki, N. (1982). Postnatal development of noradrenaline and 3-methoxy-4-hydroxyphenylethyleneglycol sulphate levels in rat brain regions. *J. Neurochem.* 39, 878–881. doi: 10.1111/j.1471-4159.1982.tb07975.x

Kuhn, W., Müller, T., Gerlach, M., Sofic, E., Fuchs, G., Heye, N., et al. (1996). Depression in Parkinson's disease: biogenic amines in CSF of "*de novo*" patients. *J. Neural. Transm.* 103, 1441–1445. doi: 10.1007/bf01271258

Kuipers, M., Stasevich, T. J., Sasaki, T., Wilson, K. A., Hazelwood, K. L., McNally, J. G., et al. (2011). Highly stable loading of mcm proteins onto chromatin in living cells requires replication to unload. *J. Cell Biol.* 192, 29–41. doi: 10.1083/jcb.201007111

Lauder, J. M., and Bloom, F. E. (1974). Ontogeny of monoamine neurons in the locus coeruleus, raphe nuclei and substantia nigra of the rat. I. Cell differentiation. *J. Comp. Neurol.* 155, 469–481. doi: 10.1002/cne.901550407

Levitt, P., and Moore, R. Y. (1979). Development of the noradrenergic innervation of neocortex. *Brain Res.* 162, 243–259. doi: 10.1016/0006-8993(79)90287-7

Lidov, H. G., and Molliver, M. E. (1982). The structure of cerebral cortex in the rat following prenatal administration of 6-hydroxydopamine. *Dev. Brain Res.* 3, 81–108. doi: 10.1016/0165-3806(82)90077-3

Masai, H., Matsumoto, S., You, Z., Yoshizawa-Sugata, N., and Oda, M. (2010). Eukaryotic chromosome DNA replication: where, when and how? *Annu. Rev. Biochem.* 79, 89–130. doi: 10.1146/annurev.biochem.052308.103205

Maslov, A. Y., Bailey, K. J., Mielnicki, L. M., Freeland, A. L., Sun, X., Burhans, W. C., et al. (2007). Stem/progenitor cell-specific enhanced green fluorescent protein expression driven by the endogenous Mcm2 promoter. *Stem Cells* 25, 132–138. doi: 10.1634/stemcells.2006-0032

Murrin, L. C., Sanders, J. D., and Bylund, D. B. (2007). Comparison of the maturation of the adrenergic and serotonergic neurotransmitter systems in the brain: implications for differential drug effects on juveniles and adults. *Biochem. Pharmacol.* 73, 1225–1236. doi: 10.1016/j.bcp.2007.01.028

Naqui, S. Z., Harris, B. S., Thomaidou, D., and Parnavelas, J. G. (1999). The noradrenergic system influences the fate of cajal-retzius cells in the developing cerebral cortex. *Dev. Brain Res.* 113, 75–82. doi: 10.1016/s0165-3806(99)00003-6

Olson, L., and Seiger, A. (1972). Early prenatal ontogeny of central monoamine neurons in the rat: fluorescence histochemical observations. *Z. Anat. Entwicklungsgesch.* 137, 301–316. doi: 10.1007/bf00519099

Pattyn, A., Goridis, C., and Brunet, J. F. (2000). Specification of the central noradrenergic phenotype by the homeobox gene Phox2b. *Mol. Cell. Neurosci.* 15, 235–243. doi: 10.1006/mcne.1999.0826

Ribary, U., Schlumpf, M., and Lichtensteiger, W. (1986). Analysis by HPLC-EC of metabolites of monoamines in fetal and postnatal rat brain. *Neuropharmacology* 25, 981–986. doi: 10.1016/0028-3908(86)90191-7

Saboory, E., Ghasemi, M., and Mehranfard, N. (2020). Norepinephrine, neurodevelopment and behavior. *Neurochem. Int.* 135:104706. doi: 10.1016/j.neuint.2020.104706

Schambra, U. (2008). *Prenatal Mouse Brain Atlas*. Germany: Heidelberg.

Slotkin, T. A., Auman, J. T., and Seidler, F. J. (2003). Ontogenesis of beta-adrenoceptor signaling: implications for perinatal physiology and for fetal effects of tocolytic drugs. *J. Pharmacol. Exp. Ther.* 306, 1–7. doi: 10.1124/jpet.102.048421

Steindler, D. A., and Trosko, B. K. (1989). Two types of locus coeruleus neurons born on different embryonic days in the mouse. *Anat. Embryol.* 179, 423–434. doi: 10.1007/bf00319584

Stoeber, K., Tlsty, T. D., Happerfield, L., Thomas, G. A., Romanovm, S., Bobrowm, L., et al. (2001). DNA replication licensing and human cell proliferation. *J. Cell Sci.* 114, 2027–2041.

Thomas, S. A., Matsumoto, A. M., and Palmiter, R. D. (1995). Noradrenaline is essential for mouse fetal development. *Nature* 374, 643–646. doi: 10.1038/374643a0

Tomasini, R., Kema, I. P., Muskiet, F. A., Meiborg, G., Staal, M. J., and Go, K. G. (1997). Catecholaminergic development of fetal rat ventral mesencephalon: characterization by high-performance liquid chromatography with electrochemical detection and immunohistochemistry. *Exp. Neurol.* 145, 434–441. doi: 10.1006/exnr.1997.6461

von Bohlen und Halbach, O. (2011). Immunohistological markers for proliferative events, gliogenesis and neurogenesis within the adult hippocampus. *Cell Tissue Res.* 345, 1–19. doi: 10.1007/s00441-011-1196-4

Wagner, J., Vitali, P., Palfreyman, M. G., Zraika, M., and Huot, S. (1982). Simultaneous determination of 3,4-dihydroxyphenylalanine, 5-hydroxytryptophan, dopamine, 4-hydroxy-3-methoxyphenylalanine, norepinephrine, 3,4-dihydroxyphenylacetic acid, homovanillic acid,

serotonin and 5-hydroxyindoleacetic acid in rat cerebrospinal fluid and brain by high-performance liquid chromatography with electrochemical detection. *J. Neurochem.* 38, 1241–1254. doi: 10.1111/j.1471-4159.1982.tb07897.x

Wang, F., and Lidow, M. S. (1997). Alpha 2A-adrenergic receptors are expressed by diverse cell types in the fetal primate cerebral wall. *J. Comp. Neurol.* 378, 493–507.

Weselek, G., Keiner, S., Fauser, M., Wagenführ, L., Müller, L., Kaltschmidt, B., et al. (2020). Norepinephrine is a negative regulator of the adult periventricular neural stem cell niche. *Stem Cells* 38, 1188–1201. doi: 10.1002/stem.3232

Conflict of Interest: The authors declare that the research was conducted in the absence of any commercial or financial relationships that could be construed as a potential conflict of interest.

frontiers

Supplementary Material

1 Supplementary Figures

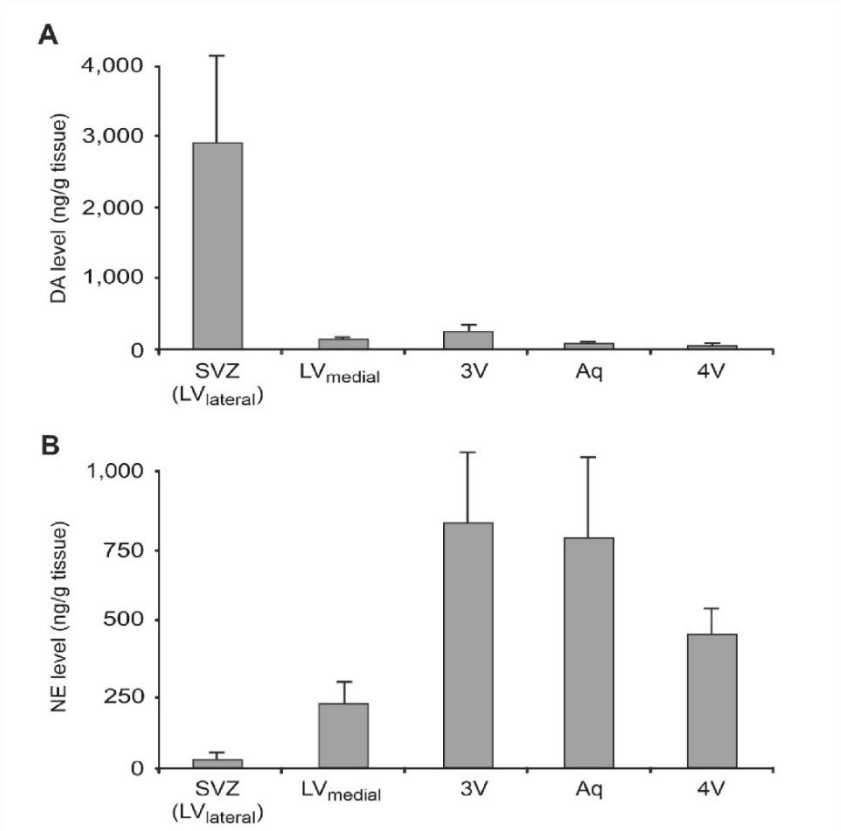

Supplementary Figure S1: Catecholamine levels in microdissected periventricular regions of the adult mouse brain (8 to 12 weeks). Catecholamine levels were measured in microdissected periventricular regions using a HPLC-based method and normalized to tissue weight. **(A)** Dopamine (DA) levels were high in the subventricular zone (SVZ) of the lateral walls of the lateral ventricles ($LV_{lateral}$), but low in medial wall of the LV (LV_{medial}) as well as the caudal periventricular regions bordering the 3rd ventricle (3V), the aqueduct and the 4th ventricle (4V) (n=4). **(B)** In contrast to DA, norepinephrine (NE) showed high levels only in the caudal (midbrain/hindbrain) periventricular regions (n=3-4). Data on NE levels from SVZ, 3V and Aq are from Weselek and co-workers (Weselek, Keiner et al. [2020]. Stem Cells, doi: 10.1002/stem.3232).

2 Supplementary Tables

Supplementary Table S1A,B: Statistics determined for the amount of proliferative cells within the VZ ($MCM2^+$ nuclei per $100\mu m^2$) in the different regions and developmental stages (**Figure 1**). Two-way ANOVA with *post-hoc* t-test and Bonferroni adjustment with VZ regions and developmental stages as fixed factors revealed that VZ regions and stages had a significant interaction effect on $MCM2^+$ cells per 100 μm^2 ($P<0.001$, F-value=5.7) and significant differences among VZ regions ($P<0.001$, F-value=17.1) and stages ($P<0.001$, F-value=95.0). Displayed are the Bonferroni-adjusted *P*-values. **(A)** Significances among the different VZ regions. **(B)** Significances among the developmental stages. Bold values indicate significant differences.

A

	E14.5	**E16.5**	**E19.5**	**P0**
LV lateral wall vs. LV medial wall	1.000	0.116	0.069	0.054
LV lateral wall vs. 3V	**0.004**	**<0.001**	**0.043**	**0.049**
LV lateral wall vs. Aqueduct	0.124	**<0.001**	**0.025**	**0.017**
LV lateral wall vs. 4V	1.000	**<0.001**	**0.036**	**0.046**
LV medial wall vs. 3V	**<0.001**	**0.025**	1.000	1.000
LV medial wall vs. Aqueduct	0.546	**0.009**	1.000	1.000
LV medial wall vs. 4V	1.000	**0.017**	1.000	1.000
3V vs. Aqueduct	**<0.001**	1.000	1.000	1.000
3V vs. 4V	**0.001**	1.000	1.000	1.000
Aqueduct vs. 4V	0.956	1.000	1.000	1.000

B

	LV lateral wall	LV medial wall	3V	Aqueduct	4V
E14.5 vs. E16.5	**0.043**	1.000	1.000	**<0.001**	**0.001**
E14.5 vs. E19.5	**0.003**	**<0.001**	**0.046**	**<0.001**	**<0.001**
E14.5 vs. P0	**<0.001**	**<0.001**	**0.025**	**<0.001**	**<0.001**
E16.5 vs. E19.5	**<0.001**	**<0.001**	0.122	0.148	**0.022**
E16.5 vs. P0	**<0.001**	**<0.001**	0.074	0.123	**0.017**
E19.5 vs. P0	1.000	1.000	1.000	1.000	1.000

3

Supplementary Material

Supplementary Table S2A,B: Statistics determined for the DA levels within the VZ in the different regions and developmental stages (**Figure 3A**). Two-way ANOVA with *post-hoc* t-test and Bonferroni adjustment with VZ regions and developmental stages as fixed factors revealed that VZ regions and stages had a significant interaction effect on DA levels ($P<0.001$, F-value=13.3) and significant differences among VZ regions ($P<0.001$, F-value=10.3) and stages ($P<0.001$, F-value=14.1). Displayed are the Bonferroni-adjusted *P*-values. **(A)** Significances among the different VZ regions. **(B)** Significances among the developmental stages. Bold values indicate significant differences.

A

	E14	**E16**	**P0**
LV lateral wall vs. LV medial wall	1.000	1.000	**<0.001**
LV lateral wall vs. 3V	**0.049**	1.000	**<0.001**
LV lateral wall vs. Aqueduct	1.000	1.000	**<0.001**
LV lateral wall vs. 4V	1.000	1.000	**<0.001**
LV medial wall vs. 3V	**0.028**	0.731	0.415
LV medial wall vs. Aqueduct	0.724	1.000	1.000
LV medial wall vs. 4V	1.000	0.699	1.000
3V vs. Aqueduct	1.000	1.000	1.000
3V vs. 4V	0.211	1.000	**0.028**
Aqueduct vs. 4V	1.000	1.000	0.412

4

B

	LV lateral wall	LV medial wall	3V	Aqueduct	4V
E14 vs. E16	0.239	0.256	**0.010**	**0.031**	1.000
E14 vs. P0	**<0.001**	**0.038**	**0.001**	**0.001**	**<0.001**
E16 vs. P0	**<0.001**	1.000	1.000	1.000	**0.002**

5

Supplementary Material

Supplementary Table S3A,B: Statistics determined for the NE levels within the VZ in the different regions and developmental stages (**Figure 3B**). Two-way ANOVA with *post-hoc* t-test and Bonferroni adjustment with VZ regions and developmental stages as fixed factors revealed that VZ regions and stages had a significant interaction effect on NE levels (P=0.001, F-value=4.3) and significant differences among VZ regions (P=0.003, F-value=5.3) and stages (P<0.001, F-value=32.4). Displayed are the Bonferroni-adjusted P-values. **(A)** Significances among the different VZ regions. **(B)** Significances among developmental stages. Bold values indicate significant differences.

A

	E14	**E16**	**P0**
LV lateral wall vs. LV medial wall	1.000	1.000	1.000
LV lateral wall vs. 3V	1.000	1.000	0.134
LV lateral wall vs. Aqueduct	1.000	1.000	**<0.001**
LV lateral wall vs. 4V	1.000	0.418	**0.003**
LV medial wall vs. 3V	1.000	1.000	1.000
LV medial wall vs. Aqueduct	1.000	1.000	**0.002**
LV medial wall vs. 4V	1.000	0.516	0.531
3V vs. Aqueduct	1.000	1.000	**0.006**
3V vs. 4V	1.000	1.000	1.000
Aqueduct vs. 4V	1.000	0.374	0.185

B

	LV lateral wall	**LV medial wall**	**3V**	**Aqueduct**	**4V**
E14 vs. E16	1.000	1.000	1.000	1.000	**0.036**
E14 vs. P0	1.000	0.067	0.110	**<0.001**	**<0.001**
E16 vs. P0	1.000	0.256	0.265	< 0.001	0.263

6

7

5 Diskussion

5.1 Kurzzeitige Sauerstoffapplikation führt zu beschleunigter Neurogenese

Die vorgelegten Daten zeigen, dass kurzzeitige maternale Hyperoxie die Neurogenese durch vermehrte Zellteilungen der neuronalen Vorläuferzellen beschleunigt sowie temporär zu einem vergrößerten Kortex führt (Markert and Storch 2022). Die Anwendung maternaler Hyperoxie über 48 h von Embryonalstadium (E) 14,5 bis E16,5 ist dabei von entscheidender Bedeutung, da die Applikationen >48 h, die Applikation zu früheren Zeitpunkten oder die chronische intermittierende Applikation zu gegenteiligen oder keinen Effekten führt (Wagenfuhr et al. 2015, Lange et al. 2016, Markert et al. 2020). Der aufgrund kurzzeitiger maternaler Hyperoxie vergrößerte Kortex ist spezifisch durch eine Zunahme an $Ctip2^+$ Schicht V-Neuronen charakterisiert, deren Anzahl im Postnatalstadium (P) jedoch normalisiert wird (siehe Abbildung 5). Die Normalisierung erfolgt durch Beteiligung aktiver Mikroglia, welche die überschüssigen, nicht-apoptotischen $Ctip2^+$ Neurone und apikal verbliebene überschüssige Vorläuferzellen phagozytieren und deren reguläre Zellzahl wiederherstellen. Daher stellen Mikroglia Schlüsselfaktoren zur Wiederherstellung einer normalen kortikalen Schichtung nach maternaler Hyperoxie dar, wobei sie diese Funktion möglicherweise auch im Rahmen der physiologischen Gehirnentwicklung erfüllen.

Zur Erforschung der Effekte von Sauerstoff auf die Neurogenese wurde das etablierte murine Modell mit maternaler Hyperoxie von E14,5 bis E16,5 zurande gezogen, welches spezifisch Zellen der subventrikulären Zone (SVZ) zu erhöhter Proliferation anregt (Wagenfuhr et al. 2015, Wagenfuhr et al. 2016). Trotz eines in diesem Modell vergrößerten Kortex, kann Hyperoxie in der Gehirnentwicklung zu neurologischen Beeinträchtigungen führen (Deulofeut et al. 2006, Gerstner et al. 2008, Porzionato et al. 2015, Ramani et al. 2018). Daher stellte sich zunächst die Frage, ob maternale Hyperoxie zur persistierenden Effekten führt, wobei gezeigt werden konnte, dass aktive Mikroglia kurz nach Geburt für eine Normalisierung der Anzahl an Neuronen in Schicht V des Kortex sorgen, sodass an P3,5 zwischen behandelten Tieren und den Kontrolltieren kein Unterschied mehr in der Morphologie des Gehirns feststellbar ist. Für Mikroglia ist zwar bekannt, dass auch nicht-apoptotische Vorläuferzellen und Neurone in der VZ und SVZ phagozytieren, bevor sie ab

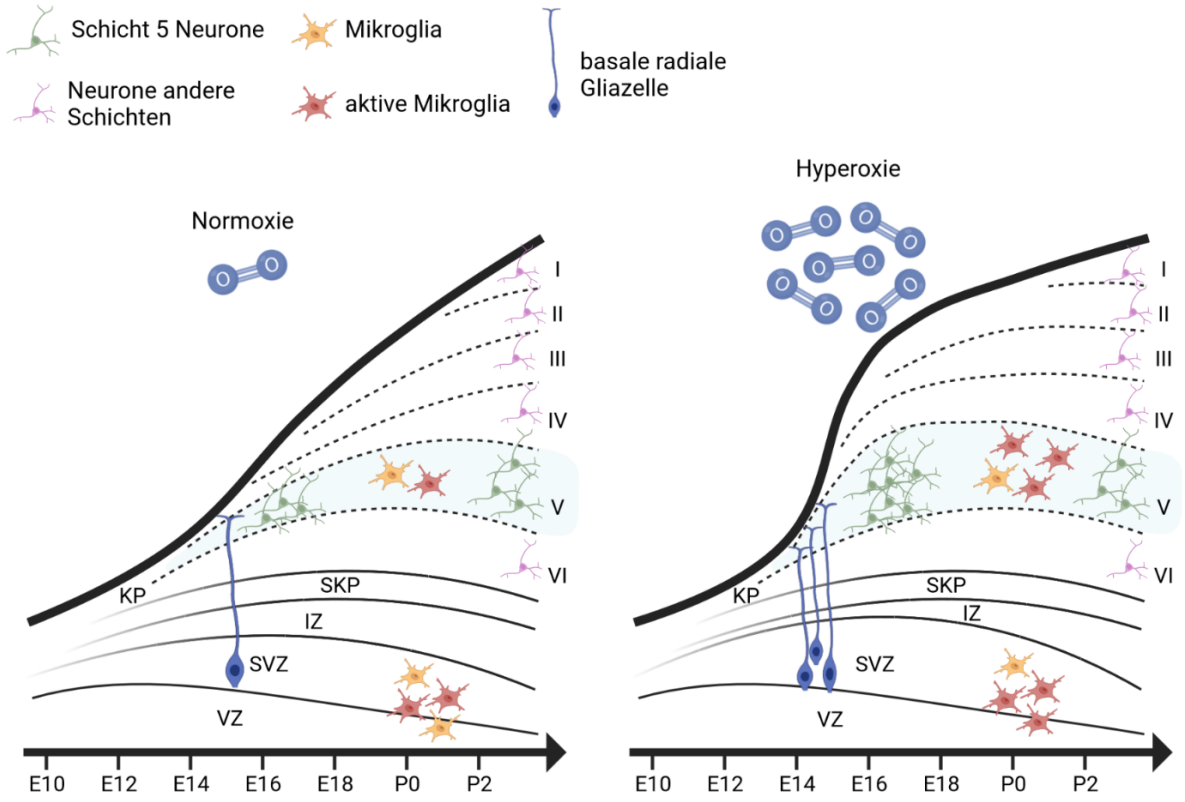

Abbildung 5: Schematische Darstellung der postnatalen Normalisierung des durch Sauerstoffbehandlung expandierten Mauskortex aufgrund vermehrter Aktivität von Mikroglia. E = Embryonalstadium; P = postnatales Stadium; VZ = ventrikuläre Zone; SVZ = subventrikuläre Zone; IZ = Intermediärzone; SKP = subkortikale Platte; KP = kortikale Platte; VI - I = kortikalen Schichten sechs bis eins. Erstellt mit BioRender.com.

E16 die kortikale Platte kolonisieren (Cunningham et al. 2013, Squarzoni et al. 2014), dass sie diese Funktion allerdings auch in der kortikalen Platte weiter ausfüllen und dabei physiologisch die Anzahl an Ctip2$^+$ Zellen und wahrscheinlich auch die Anzahl Satb2$^+$ Zellen regulieren ist bislang gänzlich unerforscht. Dazu passend konnte bereits gezeigt werden, dass Mikroglia im Kortex bis P3 ihren amöboiden aktiven Zustand beibehalten und erst nach P3 ihr typisches verzweigtes Aussehen bekommen sowie durch Ausschüttung trophischer Faktoren das Überleben von Schicht V Neuronen ermöglichen (Hristova et al. 2010, Ueno et al. 2013). Um diesen Mechanismus weiter aufzuklären, sind Folgestudien notwendig, in welchen Mikroglia gezielt ausgeschaltet werden und die Auswirkungen auf die Regulation der Neurogenese in den jeweiligen kortikalen Schichten untersucht wird. Ein entsprechender Zusammenhang könnte die Pathologie von entwicklungsbiologischen neurologischen Störungen erklären, bei denen sowohl Mikroglia als auch Schicht V Neurone beteiligt sind (Mi et al. 2019, Kolomeets and Uranova 2019, Uranova et al. 2020, Uranova, Vikhreva and Rakhmanova 2021). In diesem Kontext ist aktuell noch nicht

bekannt, ob und inwieweit diese neuropathologischen Alterationen auch mit messbaren Verhaltensänderungen/-auffälligkeiten assoziiert sind. Ein erstes Indiz dazu liefert die initiale immunhistochemische Analyse von VGlut2$^+$ Synapsen, welche ebenfalls von maternaler Hyperoxie betroffen sind und im Anschluss normalisiert werden (Nakamura et al. 2007). Ohne weitere Studien können Auswirkungen auf das Verhalten oder kognitive Störungen jedoch nicht ausgeschlossen werden. Sowohl das Verhalten bei physiologischer Entwicklung nach maternaler Hyperoxie, sowie das Verhalten und die Gehirnmorphologie bei fehlender Normalisierung, etwa durch Mikrogliadepletion, sollten Gegenstand zukünftiger Forschung sein.

Nachdem in einer initialen Studie sowie in Vorarbeiten der Arbeitsgruppe um Prof. Storch gezeigt werden konnte, dass maternale Hyperoxie nicht-invasiv die Gehirnentwicklung beeinflussen kann (Wagenfuhr et al. 2015, Markert and Storch 2022), wurde in einer Folgestudie untersucht, inwieweit dieser Effekt durch ein chronisches Applikationsschema ausgedehnt oder verändert werden kann (Markert et al. 2020). Dazu wurden trächtige C57BL/6J Mäuse von E5 bis E16 intermittierend unter Hyperoxie gehalten. Die Unterbrechung der maternalen Sauerstoffbehandlung diente dabei als Erholungsphase, da eine Hyperoxie von >72 h mit schweren Belastungen der Muttertiere einhergeht. Es wurde gezeigt, dass chronische intermittierende maternale Hyperoxie zu einer Reduktion von Pax6$^+$ neuronalen Vorläuferzellen und einer abnormalen kortikalen Schichtung führt, welche nicht durch Apoptose oder veränderte Angiogenese bedingt sind. Die Effekte sind dabei konträr zur kurzzeitigen maternalen Hyperoxie (48 h), ähneln aber einer maternalen Hyperoxie über 72 h, bei welcher ebenfalls eine Reduktion ventrikulärer Vorläuferzellen gezeigt werden konnte (Wagenfuhr et al. 2015, Lange et al. 2016, Markert and Storch 2022). Aus *in vitro* Studien ist bereits bekannt, dass chronisch hypoxischer bzw. physiologischer Sauerstoffpartialdruck um 5%, ähnlich wie auch in den neurogenen Nischen vorkommend, den Erhalt von Stammzellen fördern können, wohingegen normaler Sauerstoffpartialdruck um 20 % eher zu Differenzierung führt (Studer et al. 2000, Storch et al. 2001, Erecinska and Silver 2001, Santilli et al. 2010, Braunschweig et al. 2015). Die in den vorliegenden Studien unterschiedlichen Auswirkungen von Sauerstoff in Abhängigkeit von Intensität bzw. Dauer lassen jedoch einen dynamischen Prozess vermuten, in welchem eine kurzzeitige maternale Hyperoxie die Proliferation fördert, langfristig jedoch zu erhöhter Differenzierung führt. Entsprechend könnte die chronische intermittierende Sauerstoffbehandlung initial zu einer kurzfristigen Zunahme der Proliferation, über die Dauer der Behandlung hinweg jedoch zur Zunahme der

Differenzierung geführt haben, sodass zum Analysezeitpunkt insgesamt weniger $Pax6^+$ Zellen und verringerter Mitoseaktivität nachgewiesen werden konnten. Wie in Markert et al. 2020 gezeigt, wäre der resultierende Kortex in seiner Dicke unverändert, würde jedoch aufgrund des Mangels an $Pax6^+$ Zellen eine abnormale Schichtung aufweisen (Tuoc et al. 2009, Georgala, Manuel and Price 2011). Passend dazu befinden sich mehr Zellen in den chronologisch frühen Schichten des Kortex ($Tbr1^+$ Zellen in inneren Schicht VI), dafür weniger in den darauffolgenden Schichten ($Satb2^+$ Zellen in den äußeren Schichten). Andererseits können spezifische Effekte ausgelöst durch das intermittierende Applikationsschema oder eingeschränkte Migration der Neurone nicht ausgeschlossen werden (Talamillo et al. 2003, Tsai et al. 2005, Nishimura et al. 2010). Zudem ist nicht klar, ob die morphologischen Veränderungen zu späteren kognitiven Beeinträchtigungen führen. So konnten in einer klinischen Pilotstudie bezüglich chronischer intermittierender maternaler Applikation von Sauerstoff zur Therapie des hypoplastischen Linksherzsyndrom bei Kindern im Alter von 6 Monaten zwar ein verringerter Kopfumfang, jedoch keine kognitive Beeinträchtigung festgestellt werden (Edwards et al. 2018). Zur Untersuchung, inwieweit regulatorische Effekte wie in Markert&Storch (2022) auch hier zu einer späteren Normalisierung führen, müssen weitere Studien durchgeführt werden.

5.2 Regulation der fetalen Neurogenese durch Noradrenalin

Zur Untersuchung der Effekte von Noradrenalin (NA) und Dopamin (DA) auf die ventrikuläre und subventrikuläre Zonen (VZ/SVZ) im sich entwickelnden Gehirn wurden der Katecholamingehalt und die Anzahl an proliferierenden Zellen zu definierten Zeitpunkten ermittelt. Der NA Gehalt steigt dabei im Verlauf der Entwicklung in allen untersuchten Hirnregionen an und korreliert invers mit der Anzahl an proliferierenden Zellen. DA hingegen zeigt ein differenziertes Bild im Verlauf der Gehirnentwicklung und korreliert nicht mit der Anzahl an proliferierenden Zellen entlang der Ventrikel. Die Studie postuliert daher eine physiologische Funktion von Noradrenalin als Hemmstoff für die Proliferation von Stammzellen während der Gehirnentwicklung. Eine experimentelle Evidenz für diesen Effekt steht allerdings noch aus.

Diese Daten sind konsistent mit einer vorherigen Studie an adulten Tieren, in welcher der NA-Gehalt im Gehirn pharmakologisch beeinflusst wurde und ebenfalls zu einer Hemmung der adulten Neurogenese entlang der Ventrikel führte (Weselek et al. 2020). Im Detail konnte gezeigt werden, dass die Degeneration der NA produzierenden LC Neurone

zu vermehrter Proliferation von Zellen entlang der Ventrikelachse führt und dieser Effekt durch exogene Zugabe von NA reversibel ist. Zudem führte die exogene NA Zugabe in der SVZ adulter Tiere, welche physiologischerweise wenig NA beinhaltet, zu einer Hemmung der adulten Neurogenese. Ergänzend hierzu konnte in der aktuellen Studie gezeigt werden, dass die Hemmung der periventrikulären Neurogenese nicht auf die adulte Situation begrenzt ist, sondern bereits physiologisch die Gehirnentwicklung beeinflusst. Durch Nutzung des Stammzellmarkers MCM2 (*Mini-chromosom maintenance protein 2*), einem etablierten Proliferationsmarker *in vivo*, konnten wir die perinatal anhaltende Neurogenese über den Zeitverlauf E14,5, E16,5, E19,5 und P0 analysieren (Stoeber et al. 2001, von Bohlen und Halbach 2011). Da MCM2 beinahe über den gesamten Zellzyklus hinweg exprimiert wird, ist er unabhängig von der sich während der Gehirnentwicklung ändernden Zellzykluslänge (Calegari and Huttner 2003, Calegari et al. 2005). Die erhaltenen Daten sind daher robust, um eine Aussage über die generelle Neurogenese zu treffen.

Zur Korrelation der Neurogenese mit dem Gehalt an Katecholaminen wurde der NA- und DA-Gehalt mit Hochleistungsflüssigkeitschromatographie (HPLC) analysiert, dem Goldstandard für quantitative Katecholaminmessungen. Beide Katecholamine sind seit Jahrzehnten in ihrer Rolle als Neurotransmitter detailliert beschrieben (Berridge and Waterhouse 2003, Greengard, Allen and Nairn 1999, Ruitenberg et al. 2021, Cools et al. 2022). Weniger erforscht sind dagegen die Effekte von NA und DA auf die Regulation der Neurogenese bzw. der Gehirnentwicklung (Felten, Hallman and Jonsson 1982, Gustafson and Moore 1987). Bislang ist bekannt, dass NA die adulte hippokampale Neurogenese via β_2-Adrenorezeptoren anregt (Bortolotto et al. 2019), während die Migration und Schichtung des Kortex via α_2-Adrenorezeptoren, welche pränatal im Bereich der VZ stark exprimiert werden, sowie des Kleinhirns über andere Rezeptoren beeinflusst werden und unter pathologischen Bedingungen zu späteren Verhaltensstörungen führen (Naqui et al. 1999, Djatchkova-Podkletnova and Alho 2005, Wang and Lidow 1997, Lidow and Rakic 1994, Wang et al. 2002). Die meisten funktionellen Studien wurden jedoch mittels Läsion des dopaminergen bzw- noradrenergen Systems durch 6-Hydroxydopamin und maßgeblich in postnatalen Entwicklungstadien durchgeführt, sodass konkrete Aussagen der Katecholamineffekte auf die zeitige Neurogenese aufgrund der Toxizität des Agens nicht möglich waren (Bear and Singer 1986, Osterheld-Haas, Van der Loos and Hornung 1994). Ansätze mit transgenen Mäuse, in welchen die NA synthetisierende Dopamin-β-Hydroxylase ausgeschaltet wurde, waren ebenso wenig geeignet, da NA Mangel während der Entwicklung letal ist und die Tiere mit NA-Vorläufersubstanzen substituiert werden

mussten (Thomas, Matsumoto and Palmiter 1995, Shepard et al. 2015). Die Daten aus (Fauser et al. 2020) zeigen daher zum ersten Mal einen Zusammenhang zwischen NA und der periventrikulären embryonalen Neurogenese in Form einer starken inversen Korrelation. DA hingegen scheint keine Einfluss auf selbige zu haben. Ein ähnlicher Effekt konnte in einem Mausmodell mit Noradrenalinüberschuss gezeigt werden, in welchem weniger Neurone während der Entwicklung auftraten, obgleich verschiedenen Limitationen wie Begrenzung der Analyse auf nur eine Neuronenart und zusätzlich Serotoninüberschuss den Vergleich limitieren (Pronina et al. 2007). Auch Untersuchungen, in denen die Wirkung von NA mittels Injektion von β-Adrenorezeptoragonisten in Ratten (E17 bis E20) nachgeahmt wurde, zeigen eine Reduktion des DNA-Gehalts und somit der Zellzahl im Gehirn und reflektieren dabei nahezu das gleiche Stadium der Gehirnentwicklung wie in den von uns gezeigten Daten (Garofolo et al. 2003). Dennoch sind weitere funktionelle Untersuchungen hinsichtlich etwaiger späterer Verhaltensänderungen sowie insbesondere detailliertere Analysen der Beteiligung der verschiedenen Rezeptorsubtypen notwendig, um den Mechanismus von insbesondere NA auf die Gehirnentwicklung besser zu verstehen (Dygalo, Shishkina and Milova 1993, Dygalo et al. 2000). Trotz dieser Limitationen legen die Daten zum Einfluss von NA auf die fetale Hirnentwicklung nahe, dass NA eine inhibitorische Wirkung auf die Proliferation neuronaler Stammzellen in VZ/SVZ aufweist und diese eine entscheidende Rolle sowohl während des Verlaufs der Gehirnentwicklung, als auch bei der adulten Neurogenese spielt.

6 Zusammenfassung

Die Entstehung des Gehirns ist ein streng regulierter und komplexer Prozess, welcher sowohl unter physiologischen, als auch pathologischen Bedingungen bis dato nur ansatzweise verstanden ist. Um dieses grundlegende Wissen zu erweitern, wurden in der vorliegenden Arbeit zwei Parameter untersucht: Sauerstoff, als ein wichtiger Signalfaktor innerhalb der Entwicklung und Katecholamine, welche neben ihrer Funktion als Neurotransmitter als trophische Faktoren die Neurogenese mit regulieren. Als Modellorganismen dienten zeitlich exakt verpaarte C57BL/6 Mäuse, welche zur Untersuchungen des Effektes von erhöhtem Sauerstoffpartialdruck von Embryonalstadium (E) 14,5 bis E16,5 in 75 % Sauerstoff oder von E5,5 bis E16,5 im 24 Stundenintervall (24 h 75 % Sauerstoff / 24 h Normalluft) gehalten wurden. Zu jeweils verschiedenen Zeitpunkten der Entwicklung erfolgte die Präparation der fetalen Gehirne und Analyse dieser mittels immunhistochemischer Färbungen bzw. HPLC der Katecholamine. Der Einflussfaktor Sauerstoff zeigte dabei ein differenziertes Bild: während die zeitige intervallartige Sauerstoffbehandlung zu verringerter Zellteilung führt, ruft die kurzeitige Sauerstoffbehandlung über 48 h vermehrte Zellteilung und größere Kortizes aufgrund einer vergrößerten neokortikalen Schicht V hervor. Spannenderweise sorgen kurz nach Geburt aktive Mikroglia dafür, dass diese Schicht V wieder auf das Level unbehandelter Tiere normalisiert wird. Die kurzzeitige Sauerstoffbehandlung stellt daher eine leicht applizierbare, nicht-invasive Behandlungsmöglichkeit dar, um möglicherweise fetalen kortikalen Unterentwicklungen entgegenzuwirken, ohne einen persistierenden Überschuss an Neuronen hervorzurufen. Die Analyse der zeitlich parallel ablaufenden dopaminergen und noradrenergen Innervation der neurogenen Nischen im fetalen Mausgehirn ergab, dass Noradrenalin, nicht jedoch Dopamin invers mit der fetalen Neurogenese bzw. invers mit der Anzahl an proliferierenden Zellen korreliert. Noradrenalin ist daher ein potentieller Inhibitor der Neurogenese, wie es im adulten Mausgehirn beschrieben wurde. Experimentell muss dieser Effekt jedoch noch bestätigt werden. Sowohl Sauerstoff als auch Noradrenalin scheinen grundlegende physiologische Faktoren darzustellen, welche die Neurogenese durch direkte Beeinflussung der Proliferation neuronaler Stammzellen steuern. Diese Erkenntnis dient als Basis dafür, die Rolle beider Parameter unter pathologischen Bedingungen zu untersuchen sowie durch therapeutische Manipulation eine adäquate Entwicklung des Gehirns unter pathologischen Bedingungen zu ermöglichen.

Summary

Brain development is a tightly regulated and complex process, which is only partially understood to date, both under physiological and pathological conditions. In order to expand this basic knowledge, two parameters were investigated in the present study: oxygen representing an important signaling factor during development and catecholamines, which, in addition to their function as neurotransmitters, are also associated with neurogenesis as trophic factors. The model organisms were C57BL/6 mice mated exactly in time. They were kept either in 75 % oxygen from embryonic stage (E) 14.5 to E16.5 or in a 24 h interval (24 h 75 % oxygen / 24 h normal air) from E5.5 to E16.5 to investigate the effect of elevated oxygen levels. At different time points of development, fetal brains were prepared and analyzed by immunohistochemical stainings or HPLC of the catecholamines. The parameter oxygen showed a differentiated picture: while the temporal interval-like oxygen treatment leads to reduced cell division, the short-term oxygen treatment over 48 h causes increased cell division and larger cortices due to an enlarged layer 5. Excitingly, shortly after birth, active microglia ensure that this layer 5 is normalized back to the level of untreated animals. Short-term oxygen treatment is therefore an easy-to-apply, non-invasive treatment option to potentially counteract fetal cortical underdevelopment without causing a persistent excess of neurons. Analysis of temporally parallel dopaminergic and noradrenergic innervation of the neurogenic niches in the fetal mouse brain revealed that noradrenaline, but not dopamine, inversely correlates with fetal neurogenesis or inversely correlates with the number of proliferating cells. Norepinephrine is therefore a potential inhibitor of neurogenesis, as has been described in the adult mouse brain. Experimentally, however, this effect remains to be confirmed.

Together, both oxygen and noradrenaline seems to represent fundamental physiological factors that control neurogenesis by directly influencing the proliferation of neural stem cells. Knowledge of this provides the basis for investigating the role of both parameters under pathological conditions as well as for enabling adequate brain development during pathological conditions through therapeutic manipulation.

7 Literatur

Alliot, F., I. Godin & B. Pessac (1999) Microglia derive from progenitors, originating from the yolk sac, and which proliferate in the brain. *Brain Res Dev Brain Res,* 117.

Alsiö, J., B. Tarchini, M. Cayouette & F. Livesey (2013) Ikaros promotes early-born neuronal fates in the cerebral cortex. *Proceedings of the National Academy of Sciences of the United States of America,* 110.

Antony, J., A. Paquin, S. Nutt, D. Kaplan & F. Miller (2011) Endogenous microglia regulate development of embryonic cortical precursor cells. *J Neurosci Res,* 89.

Arnold, S., G. Huang, A. Cheung, T. Era, S. Nishikawa, E. Bikoff, Z. Molnár, E. Robertson & M. Groszer (2008) The T-box transcription factor Eomes/Tbr2 regulates neurogenesis in the cortical subventricular zone. *Genes Dev,* 22.

Arnò, B., F. Grassivaro, C. Rossi, A. Bergamaschi, V. Castiglioni, R. Furlan, M. Greter, R. Favaro, G. Comi, B. Becher, G. Martino & L. Muzio (2014) Neural progenitor cells orchestrate microglia migration and positioning into the developing cortex. *Nat Commun,* 5**,** 5605 - 5611.

Bayer, S., K. Wills, L. Triarhou & B. Ghetti (1995) Time of neuron origin and gradients of neurogenesis in midbrain dopaminergic neurons in the mouse. *Exp Brain Res,* 105.

Bear, M. & W. Singer (1986) Modulation of visual cortical plasticity by acetylcholine and noradrenaline. *Nature,* 320.

Berger, B., C. Verney, C. Alvarez, A. Vigny & K. Helle (1985) New dopaminergic terminal fields in the motor, visual (area 18b) and retrosplenial cortex in the young and adult rat. Immunocytochemical and catecholamine histochemical analyses. *Neuroscience,* 15.

Berger, B., C. Verney, M. Gay & A. Vigny (1983) Immunocytochemical characterization of the dopaminergic and noradrenergic innervation of the rat neocortex during early ontogeny. *Prog Brain Res,* 58.

Berger-Sweeney, J. & C. Hohmann (1997) Behavioral consequences of abnormal cortical development: insights into developmental disabilities. *Behav Brain Res,* 86.

Berridge, C. & B. Waterhouse (2003) The locus coeruleus-noradrenergic system: modulation of behavioral state and state-dependent cognitive processes. *Brain Res Brain Res Rev,* 42.

Blackard, K., K. Krahn, R. Andris, D. Lake & K. Fairchild (2021) Autism risk in neonatal intensive care unit patients associated with novel heart rate patterns. *Pediatr Res,* 90.

Bortolotto, V., H. Bondi, B. Cuccurazzu, M. Rinaldi, P. Canonico & M. Grilli (2019) Salmeterol, a β2 Adrenergic Agonist, Promotes Adult Hippocampal Neurogenesis in a Region-Specific Manner. *Front Pharmacol,* 10.

Braunschweig, L., A. Meyer, L. Wagenfuhr & A. Storch (2015) Oxygen regulates proliferation of neural stem cells through Wnt/beta-catenin signalling. *Mol Cell Neurosci,* 67**,** 84-92.

Bye, C., L. Thompson & C. Parish (2012) Birth dating of midbrain dopamine neurons identifies A9 enriched tissue for transplantation into parkinsonian mice. *Exp Neurol,* 236.

Calegari, F., W. Haubensak, C. Haffner & W. Huttner (2005) Selective Lengthening of the Cell Cycle in the Neurogenic Subpopulation of Neural Progenitor Cells During Mouse Brain Development. *The Journal of neuroscience : the official journal of the Society for Neuroscience,* 25.

Calegari, F. & W. Huttner (2003) An Inhibition of Cyclin-Dependent Kinases That Lengthens, but Does Not Arrest, Neuroepithelial Cell Cycle Induces Premature Neurogenesis. *Journal of cell science,* 116.

Carpentier, P., U. Haditsch, A. Braun, A. Cantu, H. Moon, R. Price, M. Anderson, V. Saravanapandian, K. Ismail, M. Rivera, J. Weimann & T. Palmer (2013) Stereotypical alterations in cortical patterning are associated with maternal illness-induced placental dysfunction. *J Neurosci,* 33.

Caviness, V., T. Takahashi & R. Nowakowski (1995) Numbers, time and neocortical neuronogenesis: a general developmental and evolutionary model. *Trends Neurosci,* 18.

Chen, V., J. Morrison, M. Southwell, J. Foley, B. Bolon & S. Elmore (2017) Histology Atlas of the Developing Prenatal and Postnatal Mouse Central Nervous System, with Emphasis on Prenatal Days E7.5 to E18.5. *Toxicol Pathol,* 45.

Cools, R., J. Tichelaar, R. Helmich, B. Bloem, R. Esselink, K. Smulders & M. Timmer (2022) Role of dopamine and clinical heterogeneity in cognitive dysfunction in Parkinson's disease. *Prog Brain Res,* 269.

Covello, K., J. Kehler, H. Yu, J. Gordan, A. Arsham, C. Hu, P. Labosky, M. Simon & B. Keith (2006) HIF-2alpha regulates Oct-4: effects of hypoxia on stem cell function, embryonic development, and tumor growth. *Genes Dev,* 20**,** 557-70.

Coyle, J. (1977) Biochemical aspects of neurotransmission in the developing brain. *Int Rev Neurobiol,* 20.

Coyle, J. & M. Kuhar (1974) Subcellular localization of dopamine beta-hydroxylase and endogenous norepinephrine in the rat hypothalamus. *Brain Res,* 65.

Cunningham, C., V. Martínez-Cerdeño & S. Noctor (2013) Microglia regulate the number of neural precursor cells in the developing cerebral cortex. *J Neurosci,* 33**,** 4216-4233.

Deulofeut, R., A. Critz, I. Adams-Chapman & A. Sola (2006) Avoiding hyperoxia in infants. *J Perinatol,* 26.

Di Bella, D., E. Habibi, R. Stickels, G. Scalia, J. Brown, P. Yadollahpour, S. Yang, C. Abbate, T. Biancalani, E. Macosko, F. Chen, A. Regev & P. Arlotta (2021) Molecular logic of cellular diversification in the mouse cerebral cortex. *Nature,* 595.

Djatchkova-Podkletnova, I. & H. Alho (2005) Alterations in the development of rat cerebellum and impaired behavior of juvenile rats after neonatal 6-OHDA treatment. *Neurochem Res,* 30.

Dygalo, N., A. Iushkova, T. Kalinina, N. Surnina, L. Mel'nikova & G. Shishkina (2000) The ontogenetic correlations of noradrenaline level and adrenergic receptor density in the rat brain. *Ontogenez,* 31.

Dygalo, N., G. Shishkina & A. Milova (1993) The beta-adrenoreceptors of the cerebral cortex in rat pups after exposures altering the noradrenaline level. *Ontogenez,* 24.

Edwards, L., D. Lara, M. Sanz Cortes, J. Hunter, S. Andreas, M. Nguyen, L. Schoppe, J. Zhang, E. Smith, S. Maskatia, S. Sexson-Tejtel, K. Lopez, E. Lawrence, Y. Wang, M. Challman, N. Ayres, C. Altman, K. Aagaard, J. Becker & S. Morris (2018) Chronic Maternal Hyperoxygenation and Effect on Cerebral and Placental Vasoregulation and Neurodevelopment in Fetuses with Left Heart Hypoplasia. *Fetal Diagn Ther***,** 1-13.

Englund, C., A. Fink, C. Lau, D. Pham, R. A. Daza, A. Bulfone, T. Kowalczyk & R. F. Hevner (2005) Pax6, Tbr2, and Tbr1 are expressed sequentially by radial glia, intermediate progenitor cells, and postmitotic neurons in developing neocortex. *J Neurosci,* 25**,** 247-51.

Erecinska, M. & I. Silver (2001) Tissue oxygen tension and brain sensitivity to hypoxia. *Respir Physiol,* 128**,** 263-76.

Fauser, M., G. Weselek, C. Hauptmann, F. Markert, M. Gerlach, A. Hermann & a. Storch (2020) Catecholaminergic Innervation of Periventricular Neurogenic Regions of the Developing Mouse Brain | Frontiers in Neuroanatomy.

Felderhoff-Mueser, U., P. Bittigau, M. Sifringer, B. Jarosz, E. Korobowicz, L. Mahler, T. Piening, A. Moysich, T. Grune, F. Thor, R. Heumann, C. Bührer & C. Ikonomidou (2004) Oxygen causes cell death in the developing brain. *Neurobiology of disease,* 17.

Felten, D., H. Hallman & G. Jonsson (1982) Evidence for a neurotropic role of noradrenaline neurons in the postnatal development of rat cerebral cortex. *J Neurocytol,* 11.

Fietz, S., I. Kelava, J. Vogt, M. Wilsch-Bräuninger, D. Stenzel, J. Fish, D. Corbeil, A. Riehn, W. Distler, R. Nitsch & W. Huttner (2010) OSVZ progenitors of human and ferret neocortex are epithelial-like and expand by integrin signaling. *Nat Neurosci,* 13.

Florio, M., M. Albert, E. Taverna, T. Namba, H. Brandl, E. Lewitus, C. Haffner, A. Sykes, F. Wong, J. Peters, E. Guhr, S. Klemroth, K. Prüfer, J. Kelso, R. Naumann, I. Nüsslein, A. Dahl, R. Lachmann, S. Pääbo & W. Huttner (2015) Human-specific gene ARHGAP11B promotes basal progenitor amplification and neocortex expansion. *Science,* 347.

Forristal, C., K. Wright, N. Hanley, R. Oreffo & F. Houghton (2010) Hypoxia inducible factors regulate pluripotency and proliferation in human embryonic stem cells cultured at reduced oxygen tensions. *Reproduction.,* 139**,** 85–97.

Fricker, M., J. J. Neher, J. W. Zhao, C. Thery, A. M. Tolkovsky & G. C. Brown (2012) MFG-E8 mediates primary phagocytosis of viable neurons during neuroinflammation. *J Neurosci,* 32**,** 2657-66.

Garofolo, M., F. Seidler, M. Cousins, C. Tate, D. Qiao & T. Slotkin (2003) Developmental toxicity of terbutaline: critical periods for sex-selective effects on macromolecules and DNA synthesis in rat brain, heart, and liver. *Brain Res Bull,* 59.

Gaspar, P., B. Berger, C. Alvarez, A. Vigny & J. Henry (1985) Catecholaminergic innervation of the septal area in man: immunocytochemical study using TH and DBH antibodies. *J Comp Neurol,* 241.

Gaspar, P., B. Berger, A. Febvret, A. Vigny & J. Henry (1989) Catecholamine innervation of the human cerebral cortex as revealed by comparative immunohistochemistry of tyrosine hydroxylase and dopamine-beta-hydroxylase. *J Comp Neurol,* 279.

Georgala, P., M. Manuel & D. Price (2011) The generation of superficial cortical layers is regulated by levels of the transcription factor Pax6. *Cereb Cortex,* 21**,** 81-94.

Gerstner, B., T. DeSilva, K. Genz, A. Armstrong, F. Brehmer, R. Neve, U. Felderhoff-Mueser, J. Volpe & P. Rosenberg (2008) Hyperoxia causes maturation-dependent cell death in the developing white matter. *J Neurosci,* 28**,** 1236-1245.

Ghiani, C., A. Eisen, X. Yuan, R. DePinho, C. McBain & V. Gallo (1999) Neurotransmitter receptor activation triggers p27(Kip1)and p21(CIP1) accumulation and G1 cell cycle arrest in oligodendrocyte progenitors. *Development,* 126.

Greengard, P., P. Allen & A. Nairn (1999) Beyond the dopamine receptor: the DARPP-32/protein phosphatase-1 cascade. *Neuron,* 23.

Gustafson, E. & R. Moore (1987) Noradrenaline neuron plasticity in developing rat brain: effects of neonatal 6-hydroxydopamine demonstrated by dopamine-beta-hydroxylase immunocytochemistry. *Brain Res,* 465.

Hansen, D., J. Lui, P. Parker & A. Kriegstein (2010) Neurogenic radial glia in the outer subventricular zone of human neocortex. *Nature,* 464.

Harb, K., E. Magrinelli, C. Nicolas, N. Lukianets, L. Frangeul, M. Pietri, T. Sun, G. Sandoz, F. Grammont, D. Jabaudon, M. Studer & C. Alfano (2016) Area-specific development of distinct projection neuron subclasses is regulated by postnatal epigenetic modifications. *eLife,* 5.

Hassani, O., V. Rymar, K. Nguyen, L. Huo, J. Cloutier, F. Miller & A. Sadikot (2020) The noradrenergic system is necessary for survival of vulnerable midbrain dopaminergic neurons: implications for development and Parkinson's disease. *Neurobiol Aging,* 85.

Haubensak, W., A. Attardo, W. Denk & W. B. Huttner (2004) Neurons arise in the basal neuroepithelium of the early mammalian telencephalon: a major site of neurogenesis. *Proc Natl Acad Sci U S A,* 101**,** 3196-201.

Herrera, E. & A. González-Candia (2021) Gestational Hypoxia and Blood-Brain Barrier Permeability: Early Origins of Cerebrovascular Dysfunction Induced by Epigenetic Mechanisms. *Front Physiol,* 12.

Hoshiko, M., I. Arnoux, E. Avignone, N. Yamamoto & E. Audinat (2012) Deficiency of the microglial receptor CX3CR1 impairs postnatal functional development of thalamocortical synapses in the barrel cortex. *The Journal of neuroscience : the official journal of the Society for Neuroscience,* 32.

Hristova, M., D. Cuthill, V. Zbarsky, A. Acosta-Saltos, A. Wallace, K. Blight, S. Buckley, D. Peebles, H. Heuer, S. Waddington & G. Raivich (2010) Activation and deactivation of periventricular white matter phagocytes during postnatal mouse development. *Glia,* 58**,** 11-28.

Jhaveri, D., I. Nanavaty, B. Prosper, S. Marathe, B. Husain, S. Kernie, P. Bartlett & V. Vaidya (2014) Opposing effects of α2- and β-adrenergic receptor stimulation on quiescent neural precursor cell activity and adult hippocampal neurogenesis. *PloS one,* 9.

Kalsbeek, A., M. Matthijssen & H. Uylings (1989) Morphometric analysis of prefrontal cortical development following neonatal lesioning of the dopaminergic mesocortical projection. *Exp Brain Res,* 78.

Kolomeets, N. & N. Uranova (2019) Reduced oligodendrocyte density in layer 5 of the prefrontal cortex in schizophrenia. *Eur Arch Psychiatry Clin Neurosci,* 269**,** 379-386.

Kulkarni, V., S. Jha & V. Vaidya (2002) Depletion of norepinephrine decreases the proliferation, but does not influence the survival and differentiation, of granule cell progenitors in the adult rat hippocampus. *The European journal of neuroscience,* 16.

Lange, C., M. Turrero Garcia, I. Decimo, F. Bifari, G. Eelen, A. Quaegebeur, R. Boon, H. Zhao, B. Boeckx, J. Chang, C. Wu, F. Le Noble, D. Lambrechts, M. Dewerchin, C. Kuo, W. Huttner & P. Carmeliet (2016) Relief of hypoxia by angiogenesis promotes neural stem cell differentiation by targeting glycolysis. *Embo j,* 35**,** 924-41.

Lara, D., S. Morris, S. Maskatia, M. Challman, M. Nguyen, D. Feagin, L. Schoppe, J. Zhang, A. Bhatt, S. Sexson-Tejtel, K. Lopez, E. Lawrence, S. Andreas, Y. Wang, M. Belfort, R. Ruano, N. Ayres, C. Altman, K. Aagaard & J. Becker (2016) Pilot study of chronic maternal hyperoxygenation and effect on aortic and mitral valve annular dimensions in fetuses with left heart hypoplasia. *Ultrasound Obstet Gynecol,* 48**,** 365-72.

Lidov, H. & M. Molliver (1982) The structure of cerebral cortex in the rat following prenatal administration of 6-hydroxydopamine. *Brain Res,* 255.

Lidow, M. & P. Rakic (1994) Unique profiles of the alpha 1-, alpha 2-, and beta-adrenergic receptors in the developing cortical plate and transient embryonic zones of the rhesus monkey. *J Neurosci,* 14.

Malberg, J., A. Eisch, E. Nestler & R. Duman (2000) Chronic antidepressant treatment increases neurogenesis in adult rat hippocampus. *J Neurosci,* 20.

Markert, F., L. Müller, K. Badstübner-Meeske & A. Storch (2020) Early Chronic Intermittent Maternal Hyperoxygenation Impairs Cortical Development by Inhibition of Pax6-Positive Apical Progenitor Cell Proliferation. *J Neuropathol Exp Neurol,* 79**,** 1223-1232.

Markert, F. & A. Storch (2022) Hyperoxygenation During Mid-Neurogenesis Accelerates Cortical Development in the Fetal Mouse Brain. *Front Cell Dev Biol,* 10.

Masuda, T., S. Nakagawa, S. Boku, H. Nishikawa, N. Takamura, A. Kato, T. Inoue & T. Koyama (2012) Noradrenaline increases neural precursor cells derived from adult rat dentate gyrus through β2 receptor. *Prog Neuropsychopharmacol Biol Psychiatry,* 36.

Maxwell, P., C. Pugh & P. Ratcliffe (1993) Inducible operation of the erythropoietin 3' enhancer in multiple cell lines: evidence for a widespread oxygen-sensing mechanism. *Proc Natl Acad Sci U S A,* 90.

McKenna, W. L., J. Betancourt, K. A. Larkin, B. Abrams, C. Guo, J. L. Rubenstein & B. Chen (2011) Tbr1 and Fezf2 regulate alternate corticofugal neuronal identities during neocortical development. *J Neurosci,* 31**,** 549-564.

Mi, Z., J. Yang, Q. He, X. Zhang, Y. Xiao & Y. Shu (2019) Alterations of Electrophysiological Properties and Ion Channel Expression in Prefrontal Cortex of a Mouse Model of Schizophrenia. *Front Cell Neurosci,* 13**,** 1-8.

Milosevic, J., I. Adler, A. Manaenko, S. Schwarz, G. Walkinshaw, M. Arend, L. Flippin, A. Storch & J. Schwarz (2009) Non-hypoxic stabilization of hypoxia-inducible factor alpha (HIF-alpha): relevance in neural progenitor/stem cells. *Neurotox Res,* 15**,** 367-80.

Miyata, T., A. Kawaguchi, K. Saito, M. Kawano, T. Muto & M. Ogawa (2004) Asymmetric production of surface-dividing and non-surface-dividing cortical progenitor cells. *Development,* 131.

Murrin, L., J. Sanders & D. Bylund (2007) Comparison of the maturation of the adrenergic and serotonergic neurotransmitter systems in the brain: implications for differential drug effects on juveniles and adults. *Biochem Pharmacol,* 73.

Murtha, S., B. Pappas & S. Raman (1990) Neonatal and adult forebrain norepinephrine depletion and the behavioral and cortical thickening effects of enriched/impoverished environment. *Behav Brain Res,* 39.

Nakamura, K., A. Watakabe, H. Hioki, F. Fujiyama, Y. Tanaka, T. Yamamori & T. Kaneko (2007) Transiently increased colocalization of vesicular glutamate transporters 1 and 2 at single axon terminals during postnatal development of mouse neocortex: a quantitative analysis with correlation coefficient. *Eur J Neurosci,* 26.

Naqui, S., B. Harris, D. Thomaidou & J. Parnavelas (1999) The noradrenergic system influences the fate of Cajal-Retzius cells in the developing cerebral cortex. *Brain Res Dev Brain Res,* 113.

Nishimura, Y., K. Sekine, K. Chihama, K. Nakajima, M. Hoshino, Y. Nabeshima & T. Kawauchi (2010) Dissecting the factors involved in the locomotion mode of neuronal migration in the developing cerebral cortex. *J Biol Chem,* 285**,** 5878-87.

Noctor, S. C., V. Martinez-Cerdeno, L. Ivic & A. R. Kriegstein (2004) Cortical neurons arise in symmetric and asymmetric division zones and migrate through specific phases. *Nat Neurosci,* 7**,** 136-44.

Nonaka-Kinoshita, M., I. Reillo, B. Artegiani, M. Martínez-Martínez, M. Nelson, V. Borrell & F. Calegari (2013) Regulation of cerebral cortex size and folding by expansion of basal progenitors. *EMBO J,* 32.

Ohh, M., C. Park, M. Ivan, M. Hoffman, T. Kim, L. Huang, N. Pavletich, V. Chau & W. Kaelin (2000) Ubiquitination of hypoxia-inducible factor requires direct binding to the beta-domain of the von Hippel-Lindau protein. *Nat Cell Biol,* 2.

Osterheld-Haas, M., H. Van der Loos & J. Hornung (1994) Monoaminergic afferents to cortex modulate structural plasticity in the barrelfield of the mouse. *Brain Res Dev Brain Res,* 77.

Padilla, N., C. Falcón, M. Sanz-Cortés, F. Figueras, N. Bargallo, F. Crispi, E. Eixarch, A. Arranz, F. Botet & E. Gratacós (2011) Differential effects of intrauterine growth restriction on brain structure and development in preterm infants: a magnetic resonance imaging study. *Brain Res,* 1382.

Paolicelli, R., G. Bolasco, F. Pagani, L. Maggi, M. Scianni, P. Panzanelli, M. Giustetto, T. Ferreira, E. Guiducci, L. Dumas, D. Ragozzino & C. Gross (2011) Synaptic pruning by microglia is necessary for normal brain development. *Science,* 333.

Pierce, E. (1973) Time of origin of neurons in the brain stem of the mouse. *Prog Brain Res,* 40.

Pilz, G., A. Shitamukai, I. Reillo, E. Pacary, J. Schwausch, R. Stahl, J. Ninkovic, H. Snippert, C. H, L. Godinho, F. Guillemot, V. Borrell, F. Matsuzaki & M. Götz (2013) Amplification of progenitors in the mammalian telencephalon includes a new radial glial cell type. *Nat Commun,* 4.

Pla, L., M. Illa, C. Loreiro, M. Lopez, P. Vázquez-Aristizabal, B. Kühne, M. Barenys, E. Eixarch & E. Gratacós (2020) Structural Brain Changes during the Neonatal Period in a Rabbit Model of Intrauterine Growth Restriction. *Dev Neurosci,* 42.

Porzionato, A., V. Macchi, P. Zaramella, G. Sarasin, D. Grisafi, A. Dedja, L. Chiandetti & R. De Caro (2015) Effects of postnatal hyperoxia exposure on the rat dentate gyrus and subventricular zone. *Brain Struct Funct,* 220**,** 229-47.

Pronina, T., A. Calas, I. Seyf, S. Voronova, A. Nanaev & M. Ugriumov (2007) [Migration and differentiation of neurons producing gonadotropin-releasing hormone under conditions of serotonin excess in the brain of mouse embryos]. *Zh Evol Biokhim Fiziol,* 43.

Ramani, M., R. Kumar, B. Halloran, C. Lal, N. Ambalavanan & L. McMahon (2018) Supraphysiological Levels of Oxygen Exposure During the Neonatal Period Impairs Signaling Pathways Required for Learning and Memory. *Sci Rep,* 8**,** 9914.

Ruitenberg, M., N. van Wouwe, S. Wylie & E. Abrahamse (2021) The role of dopamine in action control: Insights from medication effects in Parkinson's disease. *Neurosci Biobehav Rev,* 127.

Santilli, G., G. Lamorte, L. Carlessi, D. Ferrari, N. Rota, L, E. Binda, D. Delia, A. Vescovi & L. De Filippis (2010) Mild hypoxia enhances proliferation and multipotency of human neural stem cells. *PLoS One,* 5**,** 1-12.

Saurat, N., T. Andersson, N. Vasistha, Z. Molnár & F. Livesey (2013) Dicer is required for neural stem cell multipotency and lineage progression during cerebral cortex development. *Neural development,* 8.

Schafer, D., E. Lehrman, A. Kautzman, R. Koyama, A. Mardinly, R. Yamasaki, R. Ransohoff, M. Greenberg, B. Barres & B. Stevens (2012) Microglia sculpt postnatal neural circuits in an activity and complement-dependent manner. *Neuron,* 74.

Schneider, C., G. Krischke, W. Rascher, M. Gassmann & R. Trollmann (2012) Systemic hypoxia differentially affects neurogenesis during early mouse brain maturation. *Brain Dev,* 34**,** 261-73.

Schulz, C., E. Gomez Perdiguero, L. Chorro, H. Szabo-Rogers, N. Cagnard, K. Kierdorf, M. Prinz, B. Wu, S. Jacobsen, J. Pollard, J. Frampton, K. Liu & F. Geissmann (2012) A lineage of myeloid cells independent of Myb and hematopoietic stem cells. *Science,* 336.

Semenza, G. & G. Wang (1992) A nuclear factor induced by hypoxia via de novo protein synthesis binds to the human erythropoietin gene enhancer at a site required for transcriptional activation. *Mol Cell Biol.,* 12**,** 5447–5454.

Shepard, K., L. Liles, D. Weinshenker & R. Liu (2015) Norepinephrine is necessary for experience-dependent plasticity in the developing mouse auditory cortex. *J Neurosci,* 35.

Shigemoto-Mogami, Y., K. Hoshikawa, J. Goldman, Y. Sekino & K. Sato (2014) Microglia enhance neurogenesis and oligodendrogenesis in the early postnatal subventricular zone. *The Journal of neuroscience : the official journal of the Society for Neuroscience,* 34.

Sola, A., S. Golombek, M. Montes Bueno, L. Lemus-Varela, C. Zuluaga, F. Dominguez, H. Baquero, A. Young Sarmiento, D. Natta, J. Rodriguez Perez, R. Deulofeut, A. Quiroga, G. Flores, M. Morgues, A. Perez, B. Van Overmeire & F. van Bel (2014) Safe oxygen saturation targeting and monitoring in preterm infants: can we avoid hypoxia and hyperoxia? *Acta Paediatr,* 103**,** 1009-18.

Squarzoni, P., G. Oller, G. Hoeffel, L. Pont-Lezica, P. Rostaing, D. Low, A. Bessis, F. Ginhoux & S. Garel (2014) Microglia modulate wiring of the embryonic forebrain. *Cell Rep,* 8**,** 1271-9.

Steindler, D. & B. Trosko (1989) Two types of locus coeruleus neurons born on different embryonic days in the mouse. *Anat Embryol,* 179.

Stepien, B., R. Naumann, A. Holtz, J. Helppi, W. Huttner & S. Vaid (2020) Lengthening Neurogenic Period during Neocortical Development Causes a Hallmark of Neocortex Expansion. *Curr Biol,* 30.

Stoeber, K., T. Tlsty, L. Happerfield, G. Thomas, S. Romanov, L. Bobrow, E. Williams & G. Williams (2001) DNA Replication Licensing and Human Cell Proliferation. *Journal of cell science,* 114.

Storch, A., G. Paul, M. Csete, B. Boehm, P. Carvey, A. Kupsch & J. Schwarz (2001) Long-term proliferation and dopaminergic differentiation of human mesencephalic neural precursor cells. *Exp Neurol.,* 170**,** 317–325.

Studer, L., M. Csete, S. Lee, N. Kabbani, J. Walikonis, B. Wold & R. McKay (2000) Enhanced Proliferation, Survival, and Dopaminergic Differentiation of CNS Precursors in Lowered Oxygen. *J Neurosci.,* 20**,** 7377–7383.

Stuhlmiller, T. & M. García-Castro (2012) Current perspectives of the signaling pathways directing neural crest induction. *Cell Mol Life Sci,* 69.

Swinnen, N., S. Smolders, A. Avila, K. Notelaers, R. Paesen, M. Ameloot, B. Brône, P. Legendre & J. Rigo (2013) Complex invasion pattern of the cerebral cortex bymicroglial cells during development of the mouse embryo. *Glia,* 61.

Talamillo, A., J. Quinn, J. Collinson, D. Caric, D. Price, J. West & R. Hill (2003) Pax6 regulates regional development and neuronal migration in the cerebral cortex. *Dev Biol,* 255**,** 151-63.

Thomas, S., A. Matsumoto & R. Palmiter (1995) Noradrenaline is essential for mouse fetal development. *Nature,* 374.

Tomita, S., M. Ueno, M. Sakamoto, Y. Kitahama, M. Ueki, N. Maekawa, H. Sakamoto, M. Gassmann, R. Kageyama, N. Ueda, F. Gonzalez & Y. Takahama. 2003. Defective Brain Development in Mice Lacking the Hif-1α Gene in Neural Cells. In *Mol Cell Biol*, 6739-49.

Tronnes, A. A., J. Koschnitzky, R. Daza, J. Hitti, J. M. Ramirez & R. Hevner (2016) Effects of Lipopolysaccharide and Progesterone Exposures on Embryonic Cerebral Cortex Development in Mice. *Reprod Sci,* 23**,** 771-8.

Tsai, J., Y. Chen, A. Kriegstein & R. Vallee (2005) LIS1 RNA interference blocks neural stem cell division, morphogenesis, and motility at multiple stages. *J Cell Biol,* 170**,** 935-45.

Tuoc, T., K. Radyushkin, A. Tonchev, M. Pinon, R. Ashery-Padan, Z. Molnar, M. Davidoff & A. Stoykova (2009) Selective cortical layering abnormalities and behavioral deficits in cortex-specific Pax6 knock-out mice. *J Neurosci,* 29**,** 8335-49.

Ueno, M., Y. Fujita, T. Tanaka, Y. Nakamura, J. Kikuta, M. Ishii & T. Yamashita (2013) Layer V cortical neurons require microglial support for survival during postnatal development. *Nat Neurosci,* 16**,** 543-51.

Uranova, N., O. Vikhreva & V. Rakhmanova (2021) Abnormal microglial reactivity in gray matter of the prefrontal cortex in schizophrenia. *Asian journal of psychiatry,* 63.

Uranova, N., O. Vikhreva, V. Rakhmanova & D. Orlovskaya (2020) Dystrophy of Oligodendrocytes and Adjacent Microglia in Prefrontal Gray Matter in Schizophrenia. *Frontiers in psychiatry,* 11.

Vaucher, Y., M. Peralta-Carcelen, N. Finer, W. Carlo, M. Gantz, M. Walsh, A. Laptook, B. Yoder, R. Faix, A. Das, K. Schibler, W. Rich, N. Newman, B. Vohr, K. Yolton, R. Heyne, D. Wilson-Costello, P. Evans, R. Goldstein, M. Acarregui, I. Adams-Chapman, A. Pappas, S. Hintz, B. Poindexter, A. Dusick, E. McGowan, R. Ehrenkranz, A. Bodnar, C. Bauer, J. Fuller, T. O'Shea, G. Myers, R. Higgins & SUPPORT Study Group of the Eunice Kennedy Shriver NICHD Neonatal Research Network (2012) Neurodevelopmental outcomes in the early CPAP and pulse oximetry trial. *N Engl J Med,* 367.

Verney, C., B. Berger, M. Baulac, K. Helle & C. Alvarez (1984) Dopamine-β-hydroxylase-like immunoreactivity in the fetal cerebral cortex of the rat: Noradrenergic ascending pathways and terminal fields. *Int J Dev Neurosci,* 2.

Verney, C., M. Molliver & R. Grzanna (1982) Noradrenergic innervation of rat neocortex during development: immunocytochemical evidence using anti-dopamine-beta-hydroxylase antibodies. *C R Seances Acad Sci III,* 294.

von Bohlen und Halbach, O. (2011) Immunohistological markers for proliferative events, gliogenesis, and neurogenesis within the adult hippocampus. *Cell Tissue Res,* 345.

Wagenfuhr, L., A. Meyer, L. Braunschweig, L. Marrone & A. Storch (2015) Brain oxygen tension controls the expansion of outer subventricular zone-like basal progenitors in the developing mouse brain. *Development,* 142**,** 2904-15.

Wagenfuhr, L., A. Meyer, L. Marrone & A. Storch (2016) Oxygen Tension Within the Neurogenic Niche Regulates Dopaminergic Neurogenesis in the Developing Midbrain. *Stem Cells Dev,* 25**,** 227-38.

Wang, B., H. Zeng, J. Liu & M. Sun (2021) Effects of Prenatal Hypoxia on Nervous System Development and Related Diseases. *Front Neurosci,* 15.

Wang, F. & M. Lidow (1997) Alpha 2A-adrenergic receptors are expressed by diverse cell types in the fetal primate cerebral wall. *J Comp Neurol,* 378.

Wang, G., N. Chang, S. Wu & A. Chang (2002) Regulated expression of alpha2B adrenoceptor during development. *Dev Dyn,* 225.

Wang, G. & G. Semenza (1993) Characterization of hypoxia-inducible factor 1 and regulation of DNA binding activity by hypoxia. *J Biol Chem,* 268**,** 21513-8.

Weselek, G., S. Keiner, M. Fauser, L. Wagenführ, J. Müller, B. Kaltschmidt, M. Brandt, M. Gerlach, C. Redecker, A. Hermann & A. Storch (2020) Norepinephrine is a

negative regulator of the adult periventricular neural stem cell niche. *Stem cells (Dayton, Ohio),* 38.

Winkler-Schwartz, A., J. Garfinkle & M. Shevell (2014) Autism spectrum disorder in a term birth neonatal intensive care unit population. *Pediatr Neurol,* 51.

Wu, S., S. Goebbels, K. Nakamura, K. Nakamura, K. Kometani, N. Minato, T. Kaneko, K. Nave & N. Tamamaki (2005) Pyramidal neurons of upper cortical layers generated by NEX-positive progenitor cells in the subventricular zone. *Proc Natl Acad Sci U S A,* 102.

Yang, Y., C. Lin, C. Yang, Y. Lai, P. Wu & S. Yang (2013) Neurogenesis recovery induced by granulocyte-colony stimulating factor in neonatal rat brain after perinatal hypoxia. *Pediatr Neonatol,* 54.

Zgraggen, E., M. Boitard, I. Roman, M. Kanemitsu, G. Potter, P. Salmon, L. Vutskits, A. Dayer & J. Kiss (2012) Early postnatal migration and development of layer II pyramidal neurons in the rodent cingulate/retrosplenial cortex. *Cereb Cortex,* 22.

8 Abkürzungen

BrdU	Bromdesoxyuridin
brGZ	basale radiale Gliazelle
DA	Dopamin
E	Embryonalstadium
EdU	Ethynyldesoxyuridin
HIF	Hypoxie induzierender Faktor
HPLC	Hochleistungs-Flüssigkeitschromatographie; *High-Performance Liquid Chromatography*
iVZ	Intermediäre Vorläuferzelle
LC	Locus coeruleus
P	Postnatalstadium
rGZ	Radiale Gliazelle
RRID	Identifikatoren für Forschungsressourcen; *Research Resource Identification*
SN	Substantia nigra
SVZ	Subventrikuläre Zone
TBST	Tris gepufferte Salzlösung mit TWEEN 20; Tris buffered saline with TWEEN 20
VGlut2	Vesikulärer Glutamattransporter 2
VTA	Ventrales tegmentales Areal
VZ	Ventrikuläre Zone

9 Abbildungsverzeichnis

10 Tabellenverzeichnis

11 Appendix

Danksagung

Mein herzlicher Dank gilt allen voran Prof. Dr. Storch für die exzellente Betreuung, für die wann immer nötige Unterstützung und für die vielen Erfahrungen und Ratschläge, die Sie mit mir sowie der Arbeitsgruppe teilen. Die vielen wissenschaftlichen – sowie auch nicht-wissenschaftlichen – Gespräche waren stets Inspiration zu neuen Zielen und haben mich in der Wissenschaft wie auch menschlich weitergebracht.
Auch möchte ich mich bei Prof. Dr. Dr. Hermann, Dr. Francia Molina, Dr. Kathrin Badstübner-Meeske, sowie Dr. Grit Weselek bedanken, durch deren jeweilige Leitung des Labors ich perfekte Bedingungen für meine Experimente und die Anfertigung meiner Promotionsschrift vorgefunden habe.
Ein sehr großer Teil des Dankes gilt dem gesamten Laborteam des FEN, sowie auch dem AKOS, für die stets tolle Stimmung. Die gemeinsamen Mittagessen, Ausflüge und Feiern waren immer Highlights. Insbesondere seien dabei Uta Naumann für ihre unglaubliche Hilfe bei allen denkbaren Angelegenheiten und besonders für ihr sonniges Gemüt, Dr. Mareike Fauser für die vielen Tipps, Ratschläge, Hilfestellungen und Diskussionen und Jennifer Lanto für die tolle Stimmung im Büro und die wunderbare Freundschaft erwähnt. Besonders dankbar bin ich Anna-Maria Pielka für all die gemeinsame Zeit, egal ob Leid oder Freude, egal ob Dresden, Malta oder Rostock, mit und dank dir hat die ganze Arbeit viel mehr Spaß gemacht und all die Experimente die nicht geklappt haben waren nur halb so schlimm. Auch wenn wir nicht mehr zusammen arbeiten kann ich heute wie auch damals zwei Wochen nach Beginn unserer Promotion sagen: „ich bin echt froh, dass ich dich als Kollegin habe“!
Nicht zuletzt danke ich auch meiner Familie, welche mich trotz meiner häufigen Abwesenheit jederzeit unterstützt hat. Von Schule, Bund, Studium bis zur Promotion, ihr seid im Zweifel immer für mich da. Dank euch war dies alles möglich und ich bin jedes Mal froh, wenn ich mal wieder ein Wochenende zuhause bin.

Selbstständigkeitserklärung zur Promotionsschrift

Ich versichere hiermit, dass ich die vorliegende Arbeit mit dem Thema „Einfluss von Sauerstoff und Katecholaminen auf die fetale kortikale Entwicklung der Maus“ selbstständig verfasst und keine anderen Hilfsmittel als die angegebenen benutzt habe. Die Stellen, die anderen Werken dem Wortlaut oder dem Sinn nach entnommen sind, habe ich in jedem einzelnen Fall durch Angabe der Quelle kenntlich gemacht.
Meine Anteile an den in die Promotionsschrift eingegangenen Veröffentlichungen sind im Folgenden aufgelistet:

- Hyperoxygenation during mid-neurogenesis accelerates cortical development in the fetal mouse brain
    - Planung und Durchführung der Versuche
    - Erhebung, Auswertung und Interpretation aller Daten
    - Erstellung, Finalisierung und Revision des Manuskripts

- Chronic maternal hyperoxygenation impairs cortical development by inhibition of $Pax6^+$ apical progenitor cell proliferation
    - Planung und Durchführung der Versuche
    - Erhebung aller Daten, außer:
        - immunhistochemische Färbung NeuN
        - Messung kortikale Dicke
    - Auswertung und Interpretation aller Daten
    - Erstellung, Finalisierung und Revision des Manuskripts

- Catecholaminergic Innervation of Periventricular Neurogenic Regions of the Developing Mouse Brain
    - Interpretation aller Daten
    - Finalisierung und Revision des Manuskripts

Ich erkläre hiermit weiterhin, dass ich meine wissenschaftlichen Arbeiten nach den Prinzipien der guten wissenschaftlichen Praxis gemäß der gültigen „Regeln zur Sicherung guter wissenschaftlicher Praxis und zur Vermeidung wissenschaftlichen Fehlverhaltens“ an der Universitätsmedizin Rostock angefertigt habe.

Datum: Unterschrift

_____ _____

Lebenslauf

Franz Markert

Forschungslabor Experimentelle Neurologie
Klinik und Poliklinik für Neurologie
Universitätsmedizin Rostock
Gehlsheimer Straße 20
18147 Rostock

Persönliche Daten

Geburtsdatum / -ort:	22.02.1989, Großenhain
Staatsangehörigkeit:	Deutsch
Familienstand:	Ledig

Forschungsschwerpunkte

Fetale kortikale Neurogenese
Effekte von Sauerstoff auf die Neurogenese
Tiefe Hirnstimulation im Kleintiermodell

Ausbildung und akademische Grade

Promotion	Avisierte Einreichung der Dissertation 2022
Master of Science	Medizinische Biotechnologie, 2014, Universität Rostock, Gesamtnote: 1,6 Thema der Masterarbeit: „Effekte des M1-Proteins von *Streptococcus pyogenes* auf humane mesenchymale Stammzellen“ Note: 1,0
Bachelor of Science	Molekulare Biotechnologie, 2012, Hochschule für angewandte Wissenschaften Zittau/Görlitz, Gesamtnote: 1,8 Thema der Bachelorarbeit: „Untersuchungen zur Wirkung der Bioresonanztherapie auf Zellkulturen“ Note: 1,3
Abitur	2007, Werner-von-Siemens-Gymnasium Großenhain, Gesamtnote: 2,3

Berufserfahrung

seit 2022	Bestelltes Mitglied des Tierschutzausschusses, Universitätsmedizin Rostock
seit 2021	Labormanager, Forschungslabor Experimentelle Neurologie, Klinik und Poliklinik für Neurologie, Universitätsmedizin Rostock
seit 2020	Stellvertretende Leitung der Tierhaltung, Klinik und Poliklinik für Neurologie, Universitätsmedizin Rostock
seit 2016	Wiss. Mitarbeiter im Forschungslabor Experimentelle Neurologie, Klinik und Poliklinik für Neurologie, Universitätsmedizin Rostock
2014 - 2015	Wiss. Mitarbeiter im Institut für Zellbiologie, Universitätsmedizin Rostock
2011 - 2012	Wiss. Mitarbeiter am Fraunhofer-Institut für Organische Elektronik, Elektronenstrahl- und Plasmatechnik in Dresden

Tagungen

2021	„Research Day of the Department of Neurology", Universitätsmedizin Rostock, Klinik und Poliklinik für Neurologie. **Vortrag:** „Oxygen as a regulator of brain development"
2018	Symposium „The many faces of Parkinson's disease - motor and non-motor symptoms from prodromal to advanced disease stages", Universitätsmedizin Rostock, Klinik und Poliklinik für Neurologie **Poster:** „Prolonged maternal hyperoxygenation affects proliferation in the developing mouse brain"

Forschungsförderung

2021 - GfN-MV	**Antrag auf der Forschungsförderung** durch die Gesellschaft für Nervenheilkunde M/V zum Thema „Physiologische Entwicklung des Gehirns durch aktive Mikroglia" (bewilligt)

2020 - FORUN	**FORUN-Antrag** auf Forschungsförderung durch die Universitätsmedizin Rostock (abgelehnt: fehlende Promotion)
2019 - DFG	Maßgebliche Beteiligung am DFG Großgeräteantrag: **Konfokales Laser Scanning Mikroskop** LSM 900 mit AiryScan (bewilligt)
2018 - EFRE	Maßgebliche Beteiligung am Wissenschaftliche-Geräte-Antrag für eine **Glove-Box** sowie für ein **Kryomikrotom** des Europäischen Fonds für regionale Entwicklung (beide bewilligt)

Veröffentlichungen

Markert, F. & A. Storch: Hyperoxygenation During Mid-Neurogenesis Accelerates Cortical Development in the Fetal Mouse Brain. Frontiers in Cell and Developmental Biology 2022 Mar;10:732682 DOI: 10.3389/fcell.2022.732682

Fauser M, … **Markert F**, … & A Storch: Subthalamic nucleus deep brain stimulation induces sustained neurorestoration in the mesolimbic dopaminergic system in a Parkinson's disease model; Neurobiology of Disease 2021 Aug;156:105404; DOI: 10.1016/j.nbd.2021.105404

Markert F, … & A Storch: Early Chronic Intermittent Maternal Hyperoxygenation Impairs Cortical Development by Inhibition of Pax6-Positive Apical Progenitor Cell Proliferation;
Journal of Neuropathology & Experimental Neurology 2020 Nov 1;79(11):1223-1232; DOI: 10.1093/jnen/nlaa072

Fauser M, … **Markert F**, … & A Storch: Catecholaminergic Innervation of Periventricular Neurogenic Regions of the Developing Mouse Brain;
Frontiers in Neuroanatomy 2020 Sep 23;14:558435; DOI: 10.3389/fnana.2020.558435